Tkáňové kultury

Šimon Cipro[1], Tomáš Groh[2]

[1]Ústav patologie a molekulární medicíny 2. LF UK a FN Motol, Praha
[2]Klinika dětské hematologie a onkologie 2. LF UK a FN Motol, Praha

SOUHRN

Buněčné či tkáňové kultury (oba termíny jsou prakticky zaměnitelné) představují způsob, jak in vitro kultivovat eukaryotní buňky mimo jejich přirozené podmínky. Jejich využití zdaleka nespadá pouze do akademické sféry, neboť buněčné kultury představují nejvýznamnější způsob produkce monoklonálních protilátek využívaných jak diagnosticky, tak terapeuticky. Vedle toho se uplatňují jako „kultivační médium" ve virologii a jako prostředek pro získání proliferujících buněk v cytogenetické diagnostice. Své nezastupitelné místo mají i na poli výzkumu, kde poskytují finančně i technicky relativně snadno dostupný model. Mimo to jsou neocenitelným zdrojem materiálu v podobě nukleových kyselin či proteinů pro řadu molekulárně biologických metod. Článek ve stručnosti shrnuje význam buněčných kultur, metodiku a úskalí jejich kultivace a nové trendy na tomto poli.

Klíčová slova: buněčné kultury – tkáňové kultury – protilátky - patologie

Cell cultures

SUMMARY

Cell or tissue cultures (both terms are interchangeable) represent a complex process by which eukaryotic cells are maintained in vitro outside their natural environment. They have a broad usage covering not only scientific field but also diagnostic one since they represent the most important way of monoclonal antibodies production which are used for both diagnostic and therapeutic purposes. Cell cultures are also used as a "cultivation medium" in virology and for establishing proliferating cells in cytodiagnostics. They are well-established and easy-to-handle models in the area of research, e.g. as a precious source of nucleic acids or proteins. This paper briefly summarizes their importance and methods as well as the pitfalls of the cultivation and new trends in this field.

Keywords: cell cultures – tissue culture – antibodies – pathology

Cesk Patol 2014; 50(1): 30-32

Tkáňové nebo také buněčné kultury (oba termíny jsou prakticky zaměnitelné) reprezentují způsob, jakým lze eukaryotní buňky udržovat mimo jejich přirozené podmínky. Rozsah jejich současného využití je enormní. Buněčné kultury opustily v posledních 50 letech laboratoře základního výzkumu a široce se uplatňují i na poli diagnostiky a farmaceutického průmyslu a jakkoliv se to může zdát málo pravděpodobné, setkává se s jejich existencí, byť nepřímo, i každý diagnostikující patolog.

VÝZNAM BUNĚČNÝCH KULTUR

Existuje několik oblastí využití savčích buněčných kultur. Na poli diagnostiky se jedná převážně o produkci monoklonálních protilátek, kterou buněčné kultury umožňují v odpovídajícím množství a čistotě. V minulosti se k produkci protilátek využívaly tzv. hybridomy, tedy buněčné linie vzniklé fůzí nádorových buněk myelomu s nenádorovými B-lymfocyty, které byly před fůzí imunizované antigenem, proti kterému měla být zamýšlená protilátka namířena. Myelomové buňky poskytovaly takto vzniklé kultuře „nesmrtelnost" a lymfocyty antigenní specifitu. V současné době se však stále více používají rekombinatní technologie, kdy se do speciálně upravených savčích buněk (nejčastěji buněk morčecích ovárií) vnese uměle připravená genetická informace kódující konkrétní monoklonální protilátku. Touto technologií se vyrábí jak diagnosticky, tak i terapeuticky využívané protilátky. Za všechny uveďme například rituximab (anti-CD20) nebo trastuzumab (anti-HER2/neu) (1).

Buněčné kultury se široce uplatňují i v oblasti výzkumu, kde slouží jako snadno dostupný a v porovnání s použitím živých zvířat i poměrně levný model *in vivo* podmínek. Rozsah jejich využití na tomto poli má široký záběr a sahá od hájemství základního výzkumu nádorové biologie po zcela rutinní aplikace při preklinickém testování nových protinádorových léčiv, kterému jsme se věnovali i v naší laboratoři (2). Tím však možnosti použití buněčných kultur zdaleka nekončí; hojně se využívají při produkci složitých proteinů (například vakcín), ve virologické diagnostice, kde se slouží jako kultivační médium pro pomnožení viru a v cytogenetice pro přípravu dělících se buněk pro karyotypování.

PŮVOD BUNĚČNÝCH KULTUR

Získání buněčné kultury je principiálně jednoduchý proces, při kterém se z organismů explantuje tkáň obsahující buňky našeho zájmu. Tu následně podrobíme šetrnému enzymatickému či mechanickému rozvolnění za účelem získání buněčné suspenze, kterou je již možné smíchat s kultivačním médiem (viz níže). Tímto způsobem získaná buněčná kultura se označuje jako primární. Pochází-li buňky z jiné než nádorové tkáně, je je-

✉ ***Adresa pro korespondenci***
MUDr. Šimon Cipro
Ústav patologie a molekulární medicíny 2. LF UK a FN Motol, Praha
V Úvalu 84, Praha 5, Motol, 150 06
tel.: +420 602 439 413
e-mail: simon.cipro@gmail.com

jich životaschopnost a tím i délka, po kterou je můžeme in vitro kultivovat, značně omezena. Naproti tomu u buněk pocházejících z maligních nádorů, je toto období prakticky neomezené a mluvíme o *tzv. buněčných liniích*.

Příprava buněčných kultur, ať už z nádorové či nenádorové tkáně, však přináší řadu technických obtíží, je časově nákladná a výsledek je nejistý. Většina zavedených a široce používaných linií je proto dostupná i komerčně.

V praxi se můžeme čas od času setkat s požadavkem na založení kultury fibroblastů a to např. při pitvách pacientů s podezřením na vrozenou metabolickou vadu. Takový proces obnáší pouze odebrání malého vzorku kůže a jeho vložení do kultivačního média, které nám zpravidla poskytne specializovaná laboratoř metabolických vad, která se rovněž postará o následné zpracování kultury. Jediný požadavek kladený na patologa je absolutní sterilita odběru, neboť i malá kontaminace může celý odběr znehodnotit (viz níže).

TECHNIKA PRÁCE S BUNĚČNÝMI KULTURAMI

Ať už buňky získáme nákupem nebo „vlastní výrobou", udržují se v uzavřených nádobách v kultivačním médiu, které je směsí všech základních nutričních látek, růstových faktorů a pH pufrů. Kultivačních médií je celá řada, liší se složením, přítomností krevního séra i dalšími parametry. Volbu určitého typu média pak určují potřeby konkrétní buněčné linie, např. pro kultivaci kmenových buněk se často využívají bezsérová média.

Nezbytným nástrojem pro práci s buněčnými kulturami je laminární box, ve kterém se odehrává veškerá přímá manipulace s buňkami. Tento přístroj o velikosti průměrné šatní skříně je možné jednak pravidelně sterilizovat UV zářením, jednak vytváří takové proudění vzduchu, které zamezí nežádoucí kontaminaci kultury z okolního prostředí (viz níže).

Nádoby s buněčnými kulturami se uchovávají v inkubátorech, které udržují stálou teplotu 37°C a vysokou vlhkost atmosféry, která zamezuje vysychání kultivačního média.

Průběh kultivace se pravidelně sleduje pomocí inverzního mikroskopu, což je běžný optický mikroskop, jehož objektivy jsou však umístěny pod posuvným stolem a zdroj světla se nachází nad pozorovaným objektem. To nám umožní sledovat průběh kultivačního procesu, morfologii buněk a potřebu výměny média. Buňky se prohlíží nativně, zpravidla ve fázovém kontrastu (obr. 1). Inverzní mikroskopy existují i ve fluroscenčním nebo konfokálním provedení (obr. 2).

Každá buněčná kultura prochází pravidelně se opakujícím cyklem (graf). Bezprostředně po založení kultury se buňky po-

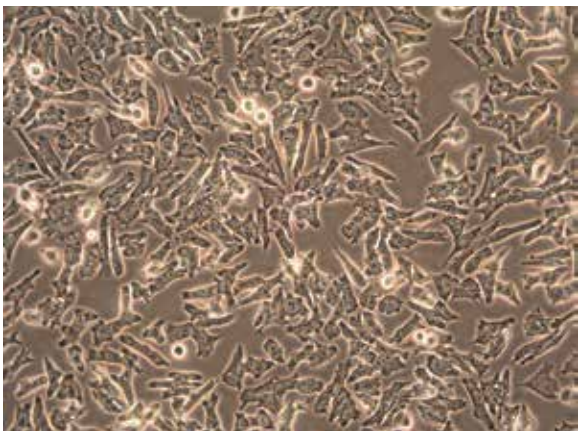

Obr. 1. Obrázek z inverzního mikroskopu pořízený ve fázovém kontrastu v průběhu kultivace neuroblastomové buněčné linie UKF-NB-4 (originální zvětšení 200x).

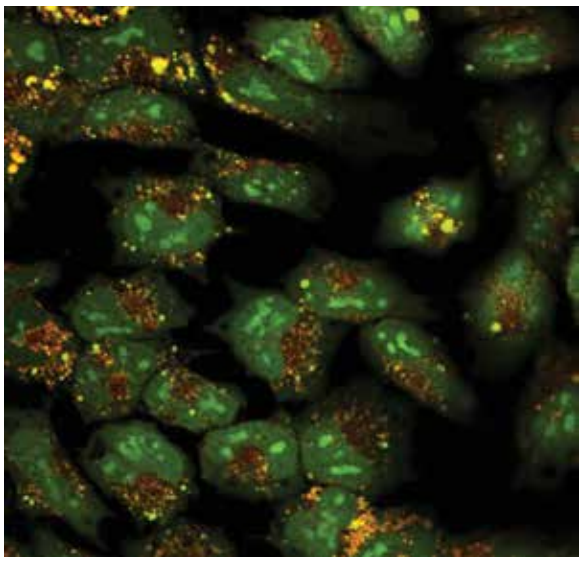

Obr. 2. Fotografie z konfokálního inverzního mikroskopu zobrazující neuroblastomovou buněčnou linii UKF-NB-4. Cytostatikum ellipticin zelený signál, lysozomy červený signál, žlutá barva pak značí jejich kolokalizaci (originální zvětšení 400x).

stupně adaptují na nové prostředí a celkový počet buněk v kultuře je zhruba konstantní nebo mírně poklesne. Buňky, které fázi adaptace přežijí, se začnou záhy intenzivně dělit a následuje období exponenciálního růstu. Během toho dochází nejen k rychlé konzumpci živin, kterých je v uzavřeném prostředí kultivační nádoby jen omezené množství, ale i k rychlému snižování pH. Oba faktory způsobí zpomalení až úplnou zástavu proliferace a přechod celé kultury do plató fáze.

Kultury, které se do této fáze dostanou, jsou vystaveny značnému nutričnímu a metabolickému stresu, který nevyhnutelně vede k aktivaci alternativních metabolických drah. V plató fázi se tedy buněčná kultura, která je už z podstaty pouze experimentálním modelem, ještě více odlučuje od reálných podmínek in vivo. Navíc dochází k akumulaci celé řady odpadových produktů metabolismu, které mohou významně ovlivňovat následující experimenty (např. PCR) a vnášet do výsledků značnou míru nejistoty. Výsledky experimentů provedených na buňkách pohybujících se na hranici přežití jsou z uvedených důvodů zcela nereprodukovatelné.

Ve snaze zabránit přechodu z exponenciální fáze do fáze plató se buňky tzv. pasážují. Jedná se o postup, kdy se v kultivační nádobě ponechá jen malá část z celkového množství buněk a ostatní se odstraní. Zároveň s tím se staré kultivační médium, které je již zcela prosté živin a obsahuje vysokou koncentraci nežádoucích metabolitů, vymění za čerstvé. Tím se kultura „restartuje" a celý cyklus jejího růstu začíná od začátku.

Proces pasážování buněk, nejedná-li se o permanentní nádorovou linii, však není možné opakovat donekonečna. Mohou za to především při každém cyklu se zkracující telomery, jejichž zmenšení pod kritickou hranici způsobí, že buňka v lepším případě do dalšího replikačního cyklu nevstoupí, v tom horším se indukuje apoptóza a buňka zahyne (3).

Vlastní kultivace buněk je však pouze prostředkem nikoliv cílem a hlavní část práce zpravidla přichází až po ní. Buňky je možné zpracovat jako jakoukoliv jinou tkáň. Z mnoha možností patří mezi ty nejčastější příprava suspenze pro průtokovou cytometrii nebo izolace nukleových kyselin či proteinů, které se stávají materiálem pro další metody (např. PCR nebo Western blot). Izolace proteinů i nukleových kyselin začíná rozrušením – chemickým či mechanickým – buněčných membrán a následnou extrakcí DNA, RNA či proteinů za pomoci jakékoliv z mnoha dostupných metod.

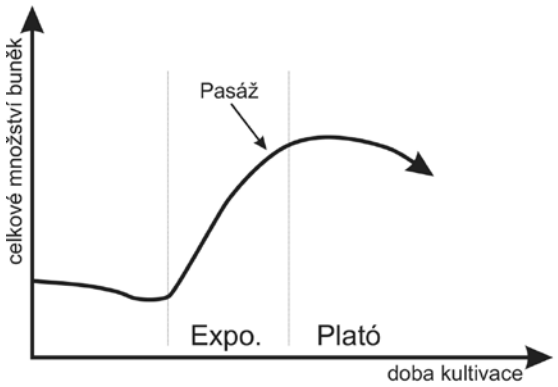

Graf 1. Graf růstového cyklu buněčné kultury. Expo. - exponenciální fáze. Šipka ukazuje vhodnou dobu pro pasážování buněk (viz text).

Jedná-li se o buňky určené pro produkci protilátek, pak se tyto izolují přímo z kultivačního média. Buňky je však možné zpracovat i pro patologa obvyklým způsobem a to jejich zalitím do parafínového cytobloku s možností následných morfologických nebo imunohistochemických vyšetření.

ÚSKALÍ KULTIVACE

Jedním z největších problémů, který techniku kultivace buněk provází, je kontaminace kultur plísněmi a bakteriemi (4). Kontaminace v lepším případě znamená znehodnocení právě probíhajícího experimentu, v horším případě přijde laboratoř o cennou buněčnou kulturu. Z toho důvodu je nezbytné dodržovat při manipulaci s buňkami sterilní podmínky, případně obohacovat kultivační médium o antibiotika, která nežádoucí kontaminaci eliminují hned v počátku.

Plošné a trvalé používání antibiotika má však i své stinné stránky. Jednak bakteriální kmeny vyskytující se v té které laboratoři získají (dříve či později) rezistenci na používaná antibiotika a vedle toho vstupují antibiotika do experimentálního modelu jako další faktor potenciálně ovlivňující konečný výsledek experimentu (5).

Mimo mikroskopicky dobře detekovatelných agens je však možná, a naneštěstí poměrně častá, i kontaminace mykoplasmaty. Ta při rutinním prohlížení buněčné kultury v inverzním mikroskopu unikají detekci a mohou tak být po dlouhou dobu „černým pasažérem". Udává se, že 5 - 35 % buněčných kultur je kontaminováno mykoplasmaty (6). Takto postižené kultury nevykazují na první pohled žádné nápadné známky infekce, nicméně výsledky na nich provedených experimentů lze považovat za zcela nevypovídající a nereprodukovatelné. Je proto nezbytné buněčné kultury na přítomnost mykoplasmat pravidelně testovat (dnes nejčastěji pomocí PCR) a případnou kontaminaci řešit antibiotiky či lépe postiženou kulturu zničit (7).

V laboratorní praxi je třeba většinu experimentů opakovat a často se k nim i v budoucnu vracet, a to ideálně za použití stejných buněk jako v experimentech původních. Jinými slovy, je třeba mít buňky „stejné šarže", aby byly výsledky relevantní a reprodukovatelné. Z toho důvodu se nepostradatelným pomocníkem všech laboratoří pracujících s buněčnými kulturami stala metoda kryoprezervace. Při ní se buňky ve speciálním médiu zabraňujícím tvorbě vodních krystalů zamrazí v tekutém dusíku, ve kterém potom mohou být několik měsíců až let uchovávány a být připraveny pro další použití, aniž by došlo k výrazné změně jejich vlastností oproti době před zamražením.

BUDOUCNOST TKÁŇOVÝCH KULTUR

Práce s buněčnými kulturami je ve své podstatě velice jednoduchá a tato vlastnost je vítána všude tam, kde se buněčné kultury používají k rutinním diagnostickým účelům nebo k produkci protilátek. Naproti tomu tam, kde mají být buňky výzkumným modelem a věrně simulovat reálné podmínky živých organismů, je jejich jednoduchost na škodu. Z pohledu solidních nádorů, které *in vivo* představují složitý trojrozměrný systém, jsou totiž buněčné kultury až příliš nedokonalým modelem (8).

Již více než tři dekády se proto setkáváme se snahou vyvinout trojrozměrnou buněčnou kulturu, která by svým prostorovým uspořádáním a složením více odrážela realitu živých organismů. Jeden z prvních trojrozměrných modelů, který je dodnes široce používán, představila Hynda Kleinmanová se svým týmem už v roce 1982 (9) a dnes je znám pod pojmem *Matrigel*. Jedná se o směs izolovanou z extracelulární matrix myšího nádoru, která je v teplotách nižších než 4°C kapalná a při zahřívání se proměňuje v gel. Tato substance obsahuje celou řadu strukturálních proteinů, růstových faktorů a sloučenin, které simulují podmínky *in vivo* a umožňují buňkám trojrozměrný růst. Tento model má však celou řadu omezení, jejichž popis přesahuje rámec tohoto sdělení.

Nové možnosti na poli trojrozměrných buněčných kultur otevřel nedávný rozmach nanotechnologií, s jejichž pomocí je dnes možné vyrábět trojrozměrné „sítě", po kterých se studované buňky šíří obdobně jako po strukturálních proteinech extracelulární matrix. Do těchto sítí jsou navíc zabudovány růstové faktory a další přesně definované látky, které věrně napodobují původní složení studované tkáně.

Takové technologie otevírají nové možnosti výzkumu, žel svou metodickou i finanční náročností jsou v rámci tkáňových kultur spíše okrajovou záležitostí a podobně jako je tomu se světelnou mikroskopií v molekulární éře patologie, zůstávají standardní buněčné kultury pro většinu aplikací dobře čitelnou a robustní metodou a jejich odchod ze scény v nejbližších letech zcela jistě nehrozí.

PODĚKOVÁNÍ

Podpořeno MZ ČR – RVO, FN v Motole 00064203.

LITERATURA

1. **Li F, Vijayasankaran N, Shen A, Kiss R, Amanullah A.** Cell culture processes for monoclonal antibody production. *mAbs* 2010; 2(5): 466-479.
2. **Cipro Š, Hřebačková J, Hraběta J, Poljaková J, Eckschlager T.** Valproic acid overcomes hypoxia-induced resistance to apoptosis. *Oncol Rep* 2012; 27(4): 1219-1226.
3. **Hayflick L, Moorhead PS.** The serial cultivation of human diploid cell strains. *Exp Cell Res* 1961; 25: 585-621.
4. **Uphoff CC, Denkmann S-A, Drexler HG.** Treatment of Mycoplasma contamination in cell cultures with plasmocin. *J Biomed Biotechnol* 2012; 2012 (1): 267678.
5. **Lincoln CK, Gabridge MG.** Cell culture contamination: sources, consequences, prevention, and elimination. *Methods Cell Biol* 1998; 57: 49-65.
6. **Young L, Sung J, Stacey G, Masters JR.** Detection of Mycoplasma in cell cultures. *Nat Protoc* 2010; 5(5): 929-934.
7. **Volokhov DV, Graham LJ, Brorson KA, Chizhikov VE.** Mycoplasma testing of cell substrates and biologics: Review of alternative non-microbiological techniques. *Mol Cell Probes* 2011; 25(2-3): 69-77.
8. **Abbott A.** Biology´s new dimension. *Nature* 2003; 424: 870-872.
9. **Kleinman HK, McGarvey ML, Liotta LA, et al.** Isolation and characterization of type IV procollagen, laminin, and heparan sulfate proteoglycan from the EHS sarcoma. *Biochemistry* 1982; 21(24): 6188-6193.

Impact of histone deacetylase inhibitor valproic acid on the anticancer effect of etoposide on neuroblastoma cells

Tomas Groh [1,2], Jan Hrabeta [2], Jitka Poljakova [1], Tomas Eckschlager [2], Marie Stiborova [1]

1 Department of Biochemistry, Faculty of Science, Charles University, Prague, Czech Republic
2 Department of Pediatric Hematology and Oncology, Charles University and University Hospital Motol, Prague, Czech Republic

Correspondence to: Prof. RNDr. Marie Stiborova, DSc.
Department of Biochemistry, Faculty of Science, Charles University in Prague, Albertov 2030, 128 40 Prague 2, Czech Republic.
TEL: +420-221951285; FAX: +420-221951283; E-MAIL: stiborov@natur.cuni.cz

Submitted: 2012-09-01 Accepted: 2011-11-15 Published online: 2012-00-00

Key words: **etoposide; valproic acid; neuroblastoma; cytotoxicity; cell cycle**

Neuroendocrinol Lett 2012; **33**(Suppl.3):101–109 **PMID:** ----- NEL330912AXX

Abstract

OBJECTIVES: Etoposide (Vepesid, VP-16), an inhibitor of topoisomerase II, is a chemotherapeutic drug commonly used for treatment of different types of malignant diseases. By inhibiting the topoisomerase II enzyme activity in cancer cells, this drug leads to DNA damage and subsequently to cell death. In this study, we investigated the effect of this anticancer drug alone and in combination with a histone deacetylase (HDAC) inhibitor, valproic acid (VPA), on a human UKF-NB-4 neuroblastoma cell line. **METHODS:** The effects of etoposide and VPA on UKF-NB-4 cells were tested under the normoxic and also the hypoxic (1% O_2) cultivation conditions. The cytotoxicity of etoposide and VPA to a UKF-NB-4 neuroblastoma cell line was evaluated with MTT assay. Apoptosis of the cells was analyzed by flow cytometry using an Annexin V and propidium iodide binding method. The effect of etoposide and VPA on the cell cycle distribution was determined by flow cytometric analysis using propidium iodide staining. **RESULTS:** The results of the study demonstrate that UKF-NB-4 neuroblastoma cells are sensitive both to etoposide and to VPA. They also indicate that the impact of VPA on cytotoxicity of etoposide in these tumor cells varies depending on the sequence of cultivation of the cells with the drugs. As a suitable sequence of cultivation, with a high rate of suppression of neuroblastoma cell growth was found the preincubation of the cells with etoposide, which was followed by their cultivation with VPA. In contrast, the reversed combination (preincubation of the cells with VPA before their treating with etoposide) did not give any increase in etoposide cytotoxicity. The effect of such combined treatment can be explained by measuring the cell cycle distribution, which shows that both etoposide and VPA change the cell cycle phase distribution. **CONCLUSION:** Etoposide and VPA were found as cycle phase specific drugs that are cytotoxic to human UKF-NB-4 neuroblastoma cells used either as single drugs or both together. However, whereas VPA might sensitize the cells to etoposide, inappropriate sequence of cultivation of the cells with VPA can decrease the etoposide cytotoxic efficacy. The results found here warrant further studies of combined treatment of neuroblastoma cells with etoposide with HDAC inhibitors and may help in the design of new protocols geared to the treatment of high risk neuroblastomas.

ORIGINAL ARTICLE

Abbreviations:

AP-1	- activating protein-1
ATM	- ataxia telangiectasia mutated
ATR	- ataxia telangiectasia and Rad3-related protein
CYP3A4	- cytochrome P450 3A4
ERK	- extracellular-regulated kinase
GSK-3beta	- glycogen synthase kinase-3beta
HDAC	- histone deacetylase
HR	- homologous recombination
CHK	- Csk homologous kinase
IC_{50}	- half maximal inhibitory concentration
IMDM	- Iscove´s modified Dulbecco´s medium
MDR	- multidrug resistance
MTT	- 3-(4,5-dimethylthiazol-2-yl)-2,5 diphenyltetrazolium bromide
NHEJ	- non-homologous end-joining
PKC	- protein kinase C
PPAR	- peroxisome proliferator-activated receptor
VPA	- valproic acid

INTRODUCTION

Etoposide (Vepesid, VP-16) belongs to a component of basic anticancer regimens used in modern oncology. It is a standard part of treatment with highly significant clinical activity against a wide variety of neoplasms (e.g. Small cell lung cancer, Testicular cancer). Etoposide is a semisynthetic derivate of the natural product podophyllotoxin. Of the natural products, podophyllotoxins belong to an important class of compounds extracted from roots and rhizomes of the plants genus Podophyllum (Imbert 1998). Two important compounds were synthesized and selected for clinical trials – etoposide and teniposide (Li *et al.* 2012). Etoposide prevents cells from entering into mitosis, accumulates cells in a G2 phase and is a phase specific cytotoxic drug (Krishan *et al.* 1975). The first significant breakthrough in understanding of a mechanism of etoposide action was realized in 1976, when Loike and Horwitz suggested that etoposide induces single-strand breaks in DNA of HeLa cells and showed that these cells can repair such breaks within 150 minutes (Loike & Horwitz 1976). After this finding, it was also demonstrated that etoposide generates not only single-strand breaks, but the double-strand DNA breaks, too. Furthermore, it was found that DNA breakage can be detected in isolated nuclei, but such DNA damage was not induced in purified DNA (Wozniak & Ross 1983). Therefore, some nuclear enzymes should be involved in generation of breaks in DNA. These observations led to exploring a detailed mechanism of action of etoposide and identifying the main cell target of this drug, topoisomerase II (Chen *et al.* 1984).

DNA topoisomerases solve the topological problems associated with DNA replication, transcription, recombination and chromatin remodeling by introducing temporary single- or double-strand breaks in the DNA in an ATP-dependent reaction (Champoux 2001). The topoisomerase II enzyme changes its conformation particularly due to a binding of ATP, then allows the separation of the two strands of DNA and the passage of a second helix through the enzyme-bound DNA in the produced break. Finally, topoisomerase II religates the cleaved strands *via* the transesterification reaction, followed by a DNA release (Meresse *et al.* 2004). Topoisomerase II is a well established target in cancer therapy and its inhibition by etoposide leads to formation of DNA double-strand breaks and subsequently to cell death (Walker & Nitiss 2002). Besides etoposide, certain other antitumor agents acting as inhibitors of this enzyme are widely used for treatment of neoplasms (e.g. amsacrine, mitoxantrone, doxorubicin) (Nelson *et al.* 1984; Tewey *et al.* 1984; van der Graaf & de Vries 1990). They are targeting topoisomerase II, covalently attach it and increase double-strand breaks in DNA. The exact mechanism resulting from double-strand break formation to cell death is still a matter of debate. Cells react to DNA damage *via* cell cycle arrest, DNA repair or trigger apoptosis. Two processing pathways leading to double-strand break repair have, however, been described recently: non-homologous end-joining (NHEJ) and homologous recombination (HR) (Schonn *et al.* 2010). Etoposide can activate also two important initiators of cell cycle arrest (ataxia telangiectasia mutated – ATM and ataxia telangiectasia and Rad3-related protein – ATR) *via* phosphorylation of Csk homologous kinase (CHK) proteins that can inhibit DNA replication (Agner *et al.* 2005; Tanaka *et al.* 2007). As Schonn and co-workers (Schonn *et al.* 2010) showed in their study, 10 μM etoposide cause massive block in G2/M phase of cell cycle. It was also found that etoposide is approximately threefold more toxic when added to cells in late S and G2 phases than when added in G1 phase (Stacey *et al.* 2000). Another study demonstrated that cells with S-phase DNA content showed about 2–3 times less DNA damage caused by etoposide than cells with G1- or G2/M-phase DNA content (Olive & Banath 1993). Another study detected resistance to etoposide in G1 phase cells (Obata *et al.* 1990).

As it is the case for the most anticancer drug regimens used for treatment of tumor cells, the resistance to etoposide, a major obstacle to the clinical use of etoposide, may develop (Meresse *et al.* 2004). Two main mechanisms of resistance have been identified yet: multidrug resistance (MDR) and specific resistance to topoisomerase II inhibitors by alteration of this enzyme (Robert & Larsen 1998; Schroeder *et al.* 2003). In addition, several mechanisms are based on metabolism of etoposide, which can generate the inactive forms of this drug. One of its major metabolic pathways involves *O*-demethylation to etoposide catechol (etoposide-OH) that is catalyzed by cytochrome P450 3A4 (CYP3A4) (Zheng *et al.* 2006). The data found in *in-vitro* studies utilizing human liver microsomes suggest that CYP3A4 predominantly catalyzes the metabolism of etoposide and also another topoisomerase II inhibitor, ellipticine, thereby dictating their anticancer effects in humans (Zhao *et al.* 1998; Stiborova *et al.* 2010, 2011).

Etoposide is used in monotherapy, but mostly combined with other antitumor agents such as carboplatin, cisplatin or cyclophosphamide (Belani *et al.* 1994).

Recently, a promising chance to combine clinically used drugs with selected inhibitors of histone deacetylase (HDAC) has been found. HDAC inhibitors may contribute to recurrence of the tumor cells by affecting the chromatin structure, thereby increasing the expression of critical tumor suppressor genes [for a summary, see (Stiborova *et al.* 2012)]. Cancer cells have often hypoacetylated histones, due to overexpression of HDACs (Santini *et al.* 2007).

Valproic acid (VPA) has been extensively studied in the last decades because of its potential to inhibit HDACs [for a summary, see (Hrebackova *et al.* 2010)]. VPA can be taken orally and is commonly used for epilepsy treatment. This inhibitor of HDACs increases acetylation of histones H3 and H4, both under the normoxic and the hypoxic conditions (Hrebackova *et al.* 2010). An exact mechanism of anticancer effect of VPA is however still unclear. VPA not only suppresses tumor growth and metastatic processes, but it also induces tumor differentiation and apoptosis. Several mechanisms might be relevant for the biological activity of VPA: VPA increases the DNA binding of activating protein-1 (AP-1) transcription factor, and the expression of genes regulated by the extracellular-regulated kinase (ERK)-AP-1 pathway; VPA downregulates protein kinase C (PKC) activity; it inhibits glycogen synthase kinase-3beta (GSK-3beta), a negative regulator of the Wnt signaling pathway; and it also activates the peroxisome proliferator-activated receptors PPARgamma and delta (Blaheta & Cinatl 2002; Hrebackova *et al.* 2010; Stiborova *et al.* 2012).

Inhibitors of HDACs can also increase the cytotoxicity of topoisomerase II inhibitors (Marchion *et al.* 2004; Marchion *et al.* 2005; Stiborova *et al.* 2012). This phenomenon is not well understood and it seems to be dependent on many factors, being also dependent on a sequence of cultivation of cells with used drugs. The example of the different effects of combination of topoisomerase II inhibitor (etoposide) with an inhibitor of HDACs (VPA) was shown by Das and co-workers (Das *et al.* 2010). These authors used two different neuroblastoma cell lines and different times of their cultivation with the drugs. The influence of another HDAC inhibitor, karenitecin, to increase the effect of inhibitor of topoisomerase I was also found, in the work of Daud *et al.* (2009). The increased effect of treatment of cells with combined regimens containing inhibitors of topoisomerases could be connected with possible changes in levels of topoisomerase I and II mRNA by the HDAC inhibitors. The enhanced expression of genes of DNA topoisomerase II can be associated with increased etoposide sensitivity (Uesaka *et al.* 2007).

Neuroblastoma is the most common extracranial solid tumor in infancy. It originates from undifferentiated cells of the sympaticus nervous system and it is very biologically heterogeneous. Neuroblastomas are ranged to low risk neuroblastoma tumors, which can spontaneously regress, and to high risk neuroblastomas, which are typical with early metastasis and poor prognosis (Brodeur 2003). Despite of a great progress in modern oncology, some forms of neuroblastoma disease are still found very difficult to treat (Brodeur 2003; Poljakova *et al.* 2011). In this study, we investigated the effect of etoposide and VPA and their combination, on a human UKF-NB-4 neuroblastoma cell line.

MATERIAL AND METHODS

Cell cultures and chemicals

The UKF-NB-4 cell line, established from bone marrow metastases of high risk neuroblastoma, was a gift of Prof. J. Cinatl, Jr. (J. W. Goethe University, Frankfurt, Germany). This neuroblastoma cell line was derived from recurrent disease. VPA and etoposide were purchased from Sigma Chemical Co. (MO, USA). All other chemicals used in experiment were of analytical purity or better. Cells were grown at 37 °C and 5% CO_2, cultivated in Iscove´s modified Dulbecco´s medium (IMDM) with 10% fetal bovine serum. For hypoxia experiments, cells were maintained in modular incubator chamber (Billups-Rothenberg Inc., CA, USA) flushed with 1% O_2, 5% CO_2 and balance N_2 at 37 °C (hereafter referred to as hypoxia).

MTT assay

The cytotoxicity of etoposide and valproic acid to UKF-NB-4 cells in exponential growth was determined in a 96-well plate. For a dose-response curve, cells in exponential growth were seeded in 100 µl of medium with 10^4 cells per well. To investigate the effect of etoposide, VPA and their combination on UKF-NB-4 cells, the cells were treated with 0.125–64 µM or 0.125–32 µM for etoposide and 0.25–128 mM VPA. In experiments where both drugs were applied, the preincubation medium containing one of the drugs was removed and replaced with a fresh medium containing both drugs. Tumor cell viability was evaluated by MTT test as previously described (Cinatl *et al.* 1997; Poljakova *et al.* 2011). Briefly, after 72 hours incubation at 37 °C in 5% CO_2 the MTT solution (2 mg/ml PBS) was added, the plates were incubated for 3 hours and cells lysed in solution containing 20% of SDS and 50% *N,N*-dimethylformamide pH 4.5. The absorbance at 570 nm was measured for each well by multiwell ELISA reader Versamax (Molecular Devices, CA, USA). The IC_{50} values were calculated from at least 3 independent experiments using the linear regression of the dose-log response curves by SOFTmaxPro.

Annexin V/propidium iodide labeling

To determine apoptosis, 1.6×10^6 cells were plated in 100 mm dishes and treated with individual drugs or their combinations (using 1 mM VPA and 8 µM etoposide). For detection of apoptosis Annexin V-FITC Apoptosis Detection kit (Biovision, CA, USA) was used according to manufacturer´s instructions and samples

were analyzed using flow cytometry (FACSCalibur BD, San Jose, CA, USA).

Cell cycle analysis

To determine cell cycle distribution, 7×10^5 cells were plated in 60 mm dishes and treated with individual drugs or their combinations for various incubation periods. In experiments where both drugs were applied, the preincubation medium containing one of the drugs was removed and replaced with a fresh medium containing both drugs. After treatment, the cells were collected by trypsinization, washed in PBS, stained using DNA PREP Reagents kit (Beckman Coulter Inc., CA, USA), incubated in the dark for 30 min at room temperature, measured by flow cytometry (FACSCalibur BD, San Jose, CA, USA) and the data were analyzed using ModFit LT software (Verity Software House, ME, USA).

Determination of doubling time

Defined amounts of neuroblastoma cells were cultivated with 1 mM VPA and after three days of cultivation they were collected and counted. Cells were counted using a Bürker chamber. Values of doubling time for control cells and cells cultivated with VPA were determined using a freeware program Doubling time (http://www.doubling-time.com/download.php).

Tab. 1. IC_{50} values for UKF-NB-4 neuroblastoma cells treated with etoposide or VPA.

	IC_{50} for etoposide (μM)		IC_{50} for VPA (mM)	
	Normoxia	Hypoxia	Normoxia	Hypoxia
Exp. I	1.8	3.0	1.7	1.1
Exp. II	3.1	3.7	1.6	1.4
Exp. III	2.1	3.0	1.3	1.1
Mean value	2.33	3.23	1.53	1.20
Stand. dev.	0.56	0.33	0.17	0.14

RESULTS

The effect of etoposide on UKF-NB-4 human neuroblastoma cells

The effects of etoposide on UKF-NB-4 cells were evaluated by MTT test after treating these cells with different concentrations of etoposide for 72 hours under the normoxic (aerobic) and the hypoxic conditions. IC_{50} values for the used neuroblastoma cell line determined in three independent experiments are shown in Table 1. Hypoxic culture conditions (1% O_2) reduced etoposide toxicity to this tumor cell line, increasing the IC_{50} values of etoposide from 2.33±0.56 μM to 3.23±0.33 μM (Table 1).

To investigate the mechanism explaining the cytotoxicity of etoposide to neuroblastoma cells, we evaluated the effect of this drug on induction of apoptosis in the cells. Etoposide is capable of inducing apoptosis in UKF-NB-4 cells in time- and concentration-dependent manner. Etoposide-mediated apoptosis in UKF-NB-4 cells was measured using Annexin V and propidium iodid staining at 3, 6, 12, 24 and 48 hours, after addition of 2–8 μM etoposide. The increased levels of apoptotic cells were found after 24 hours of the cells growth in the medium containing 8 μM etoposide and after the 48 hours cell growth in the presence of all used concentrations of etoposide (data not shown).

Cultivation of UKF-NB-4 cells with 8 μM etoposide for 48 hours changed their morphology as compared with that of the control, untreated cells (Figure 1). Cells treated with etoposide, which did not undergo apoptosis, were flatter than normal (untreated) cells and contained an increased amount of vacuoles.

We investigated the effect of etoposide treatment on the cell cycle distribution of UKF-NB-4 neuroblastoma cells. Compared to controls, treatment of cells with various concentration of etoposide resulted in an appreciable arrest of the cells in G2/M and/or S phases of cell cycle with a concomitant decrease in G0/G1 phase (Fig-

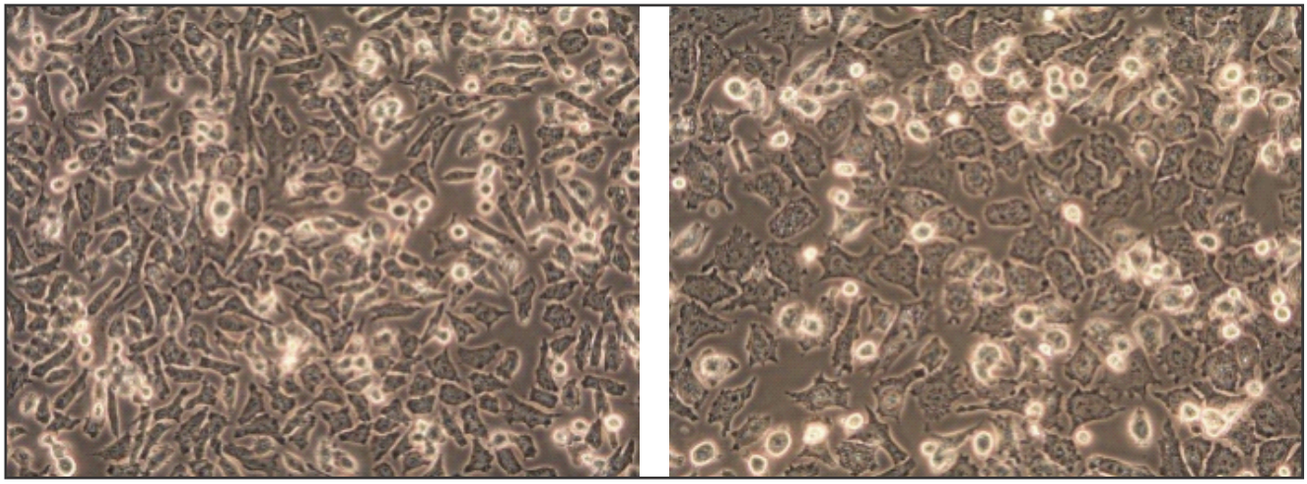

Fig. 1. Neuroblastoma cell line UKF-NB-4 (200 fold magnification) (A) and this cell line treated with 8 μM etoposide for 48 hours (B). Flatter and bigger cells with an increased amount of vacuoles can be seen in UKF-NB-4 cells treated with etoposide (200 fold magnification).

ures 2 and 3). These changes in cell cycle were time-dependent, early after adding of etoposide increased percentage of S phase and later it was replaced by increasing of G2/M phase (Figure 3).

The effect of valproic acid on UKF-NB-4 human neuroblastoma cells

The effects of VPA on UKF-NB-4 human neuroblastoma cells were evaluated by MTT test after treating these cells with different concentrations of VPA for 72 hours under the normoxic (aerobic) and the hypoxic conditions. The analyzed neuroblastoma cells were sensitive to VPA. IC_{50} values for the UKF-NB-4 neuroblastoma cell line determined in three independent experiments are shown in Table 1. Hypoxic culture conditions (1% O_2) had essentially no effect on cytotoxicity of VPA to these cells (see the IC_{50} values shown in Table 1).

To determine whether 1 mM VPA induces apoptosis in UKF-NB-4 cells, flow cytometry using Annexin V and propidium iodide staining was used in further experiments. Exposure of the cells to 1 mM VPA for 3–48 hours had practically no effects on viability of the cells (data not shown). However, treatment of UKF-NB-4 neuroblastoma cells resulted in changes of the cell cycle distribution of these cells. Compared to controls, treatment of cells with 1 mM VPA for various time periods resulted in an appreciable arrest of the cells in G2/M phase of cell cycle, mainly after more than 12 hour incubations (Figure 4).

Exposure of UKF-NB-4 cells to 1 mM VPA also led to a ~1.4-fold increase in a doubling time of the cells (data not shown). These results correspond to changes in cell cycle of the cells treated with 1 mM VPA.

The combined effect of etoposide and valproic acid on UKF-NB-4 human neuroblastoma cells

Because VPA is known to modulate response of several tumor cells to chemotherapy using different anticancer drugs, we investigated the ability of this HDAC inhibitor to alter response of UKF-NB-4 neuroblastoma cells to etoposide. The UKF-NB-4 neuroblastoma cells were treated with various concentrations of etoposide and constant concentration of VPA for 72 hours after their 24 hour pretreatment with the drugs under their various combinations. For evaluation of the effect of etoposide combined with VPA on UKF-NB-4 cells, the MTT assay was again used. Several combinations of treating the UKF-NB-4 neuroblastoma cells with the drugs were used: i) the cells were preincubated with 1 mM VPA for 24 hours and then treated with various concentrations of etoposide for 72 hours (combination assigned as V/E), ii) the cells were preincubated with various concentrations of etoposide for 24 hours and then with 1 mM VPA for 72 hours (combination assigned as E/V), iii) the cells were preincubated with various concentrations of etoposide for 24 hours and after that with various concentrations of etoposide in the presence of 1 mM VPA for 72 hours (combination assigned as E/V,E), iv) the cells were preincubated for 24 hours with 1 mM VPA and then treated with various concentrations of etoposide in the presence of 1 mM VPA for 72 hours (combination assigned as V/V,E), v) the cells were treated with medium without any drug added for 24 hours and then treated with various concentrations of etoposide in the presence of 1 mM VPA for 72 hours (combination assigned as 0/V,E) and vi) the cells were treated with medium without any drug added for 24 hours and then treated with various concentrations of etoposide for 72 hours (control incubations with etoposide only) (assigned as 0/E). IC_{50} values for the cells in the presence of etoposide alone or etoposide and VPA under the various incubation combinations with the drugs are shown in Figure 5.

The results found in these experiments indicate that in most cases VPA decreases the value of IC_{50}, thereby increasing the toxic effects of etoposide as compared with the effect of etoposide used for treating the cells

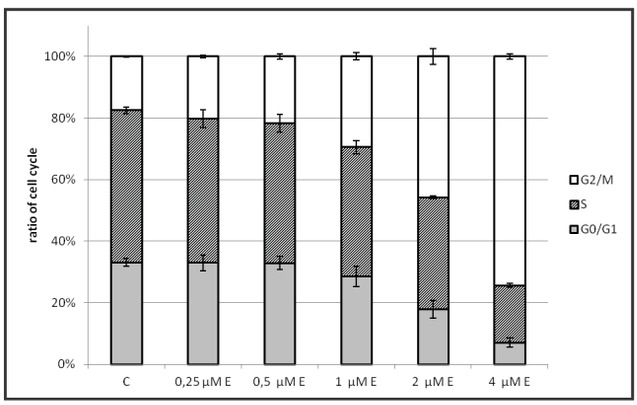

Fig. 2. Effect of various concentrations of etoposide (E) on cell cycle distribution in human UKF-NB-4 neuroblastoma cells after 48 hours etoposide treatment. C – control cells treated with medium without any drug added. The results shown in this figure are means and standard deviations of three experiments.

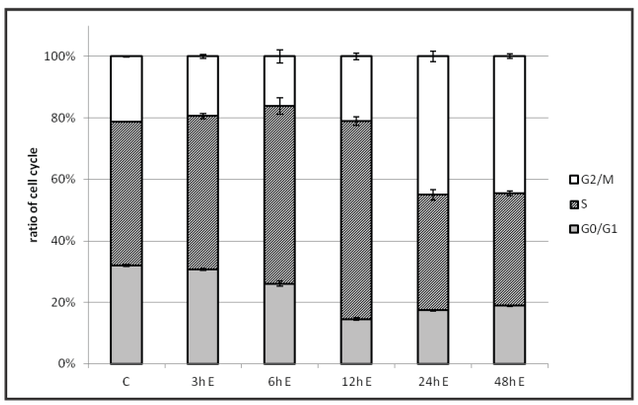

Fig. 3. Effect of 2 µM etoposide (E) on cell cycle distribution in human UKF-NB-4 neuroblastoma cells after 3 - 48 hours etoposide treatment. C – control cells treated with medium without any drug added. The results shown in this figure are means and standard deviations of three experiments.

for 72 hours alone (0/E). These results suggest that VPA sensitized cells to etoposide. However, in the case of pre-incubation of the cells with 1 mM VPA followed by their treating with etoposide (V/E), an increase in the IC_{50} value for etoposide was found (Figure 5). This finding suggests that VPA antagonizes the effect of etoposide on UKF-NB-4 cells at early time points of incubation. Even though we can only speculate how to explain this phenomenon, this sequence of cell incubations seems to slow cell cycle of the cells, thereby decreasing their sensitivity to etoposide.

The effect of combined treatment of UKF-NB-4 neuroblastoma cells with etoposide and VPA under the various combinations of treatment of these cells on their viability was also investigated using the Annexin V and propidium iodide staining. As shown in Figure 6, the most effective combination of the drug treatment to decrease viability of neuroblastoma cells was the combined treatment of cells with etoposide and VPA (cells pretreated with 8 μM etoposide for 24 hours and then treated with 1 mM VPA for 48 hours). These results indicate the synergistic effect of this combined treatment (see E/V in Figure 6).

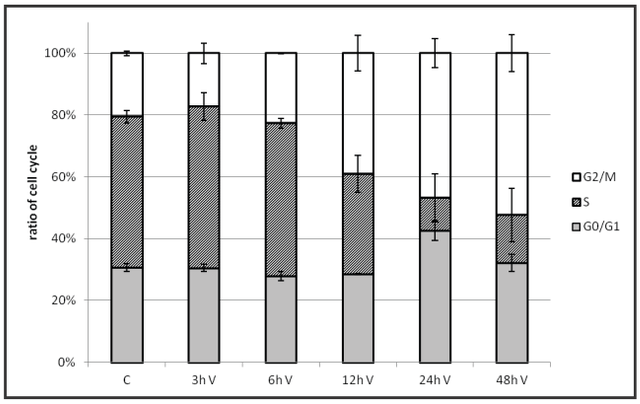

Fig. 4. Effect of 1 mM VPA (V) on cell cycle distribution in human UKF-NB-4 neuroblastoma cells after 3 - 48 hours VPA treatment. C – control cells treated with medium without any drug added. The results shown in this figure are means and standard deviations of three experiments.

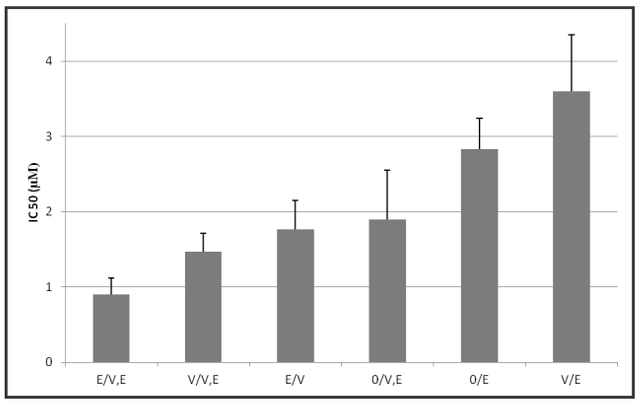

Fig. 5. Cytotoxicity of etoposide (E), VPA (V) and their combinations to human UKF-NB-4 cells expressed as IC_{50} values and standard deviations of three independent experiments determined by the MTT assay. The following combinations of treating the UKF-NB-4 neuroblastoma cells with the drugs were used: i) the cells were preincubated with 1 mM VPA for 24 hours and then treated with various concentrations of etoposide for 72 hours (V/E), ii) the cells were preincubated with various concentrations of etoposide for 24 hours and then with 1 mM VPA for 72 hours (E/V), iii) the cells were preincubated with various concentrations of etoposide for 24 hours and after that with various concentrations of etoposide in the presence of 1 mM VPA for 72 hours (E/V,E), iv) the cells were preincubated for 24 hours with 1 mM VPA and then treated with various concentrations of etoposide in the presence of 1 mM VPA for 72 hours (V/V,E), v) the cells were treated with medium without any drug added for 24 hours and then treated with various concentrations of etoposide in the presence of 1 mM VPA for 72 hours (0/V,E) and vi) the cells were treated with medium without any drug added for 24 hours and then treated with various concentrations of etoposide for 72 hours (control incubations with etoposide only) (0/E).

DISCUSSION

The poor response of high risk children neuroblastoma cancer to current treatment protocols indicates that novel therapeutical strategies are needed to be developed. Therefore, in this study, we investigated whether treatment of human UKF-NB-4 neuroblastoma cells with etoposide combined with the HDAC inhibitor, VPA, will increase the cytotoxicity of these drugs. Utilizing etoposide combined with VPA can, depending on the treatment regimens, both increased cytotoxicity of these drugs and decrease their effects on the treated cells (Das *et al.* 2010). Therefore, we also investigated various treatment regimens of these drugs in combination on UKF-NB-4 cells.

Etoposide, used as one of drugs in the study alone covalently binds to topoisomerase II enzyme stabilizing a cleavage complex, which subsequently leads to generation of double-strand breaks and cell death (Baldwin

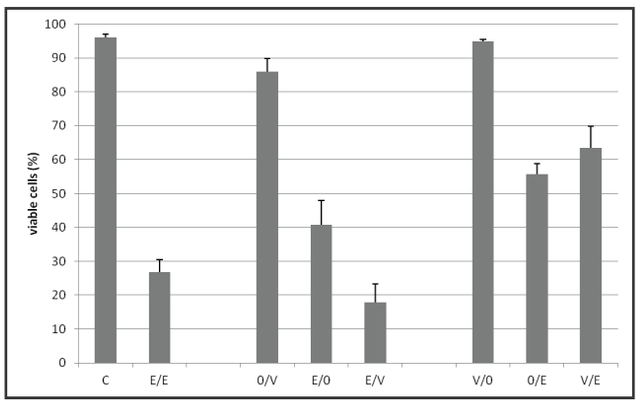

Fig. 6. Viability of neuroblastoma cells expressed as % of viability. C – cells treated with medium without any drug added, after combined treatment with 8 μM etoposide (E) and 1 mM VPA (V). Cells were pretreated for 24 hours either with medium without the drug (0) or with etoposide (E) or VPA (V) and then treated with the compounds for 48 hours. The results shown in this figure are means and standard deviations of three experiments.

& Osheroff 2005). Here, we demonstrate that this drug, when used at therapeutically relevant concentrations (~10 μM), modifies morphology of the UKF-NB-4 neuroblastoma cells. The cells also contain higher amounts of vacuoles. This finding is consistent with results found by Pérez *et al.* (1994), who found similar effects of etoposide on U-937 human promonocytic leukemia cells. This phenomenon can be caused by cell cycle arrest induced by etoposide in the cells, before they undergo apoptosis.

Etoposide kills UKF-NB-4 neuroblastoma cells in a time- and concentration-dependent manner. A high degree of apoptosis is produced by this drug after 48 hours of cultivation of these cells. This anticancer drug also causes an appreciable arrest of the cells in G2/M and/or S phases of cell cycle with a concomitant decrease in G0/G1 phase in UKF-NB-4 cells.

The second drug used in this study, the inhibitor of HDAC, VPA, is known to sensitize several cancer cells to chemotherapeutic agents (Hajji *et al.* 2010; Stiborova *et al.* 2012). This compound increases acetylation of specific lysine residues of chromatin-associated histones H3 and H4, and decreases chromatin compaction thus making DNA more accessible to DNA damaging agents (Stiborova *et al.* 2012). VPA can also influence the levels of DNA repair proteins, induce DNA damage or induce cell cycle arrest (Catalano *et al.* 2005; Kaiser *et al.* 2006; Lee *et al.* 2010; Hrebackova *et al.* 2010; Stiborova *et al.* 2012). As we found in this study, VPA used at the well clinically tolerated concentrations (1 mM) (Hrebackova *et al.* 2010), is cytotoxic to UKF-NB-4 neuroblastoma cells and causes an arrest of the cells in G2/M and later in G0/G1 phase.

In the case of the use of both drugs in combination examined in this study, we found that VPA can influence cytotoxicity of etoposide to a human UKF-NB-4 cell line, when VPA is used in a pre-incubation, co-incubation and post-incubation treatment manner. The preincubation of the cells with etoposide, which was followed by their cultivation with VPA, was found to be a suitable sequence of cultivation producing a high degree of suppression of neuroblastoma cell growth. In contrast, the reversed combination (preincubation of the cells with VPA before their treating with etoposide) did not give any increase in etoposide cytotoxicity. The effect of such combined treatment can be explained by changes of the cell cycle distribution because etoposide is more effective in proliferating S-phase cells. In addition both VPA and etoposide assessed in combination treatments are metabolized by biotransformation enzymes that might influence their cytotoxicity. Moreover, expression levels of transporters that mediate drug efflux can protect cancer cells against both damaging agents. Recently, it has been found that the activities of these enzymes and transporters and their expression can be changed by several HDAC inhibitors (Stiborova *et al.* 2012). Indeed, VPA, is an inducer of CYP3A4 (Cerveny *et al.* 2007; Poljakova *et al.* 2011), which metabolizes etoposide (Kawashiro *et al.* 1998; Zheng *et al.* 2006), and CYP24, the enzyme important in vitamin D homeostasis (Vrzal *et al.* 2011). Likewise, one transporter protein that mediates drug elimination from cells, P-glycoprotein (encoded by MDR gene), is induced by VPA (Eyal *et al.* 2006; Cerveny 2007; Poljakova *et al.* 2011).

The effects of VPA combined with etoposide on other types of human neuroblastoma cells, SK-N-AS and SK-N-SH cells, was investigated by Das *et al.* (2010). The effect of this combined treatment was also dependent on exposure regimens. Although the combination of drugs modestly enhanced cell-death in SK-N-SH cells at longer incubation periods (72 and 96 hours), it caused a decline in etoposide-mediated cell killing at shorter exposure times (48 hours). In contrast, VPA synergistically increased the cytotoxicity of etoposide in SK-N-AS cells. The modest increase in topoisomerase-II β expression upon VPA treatment was suggested by Das *et al.* (2010) to potentially explain the additive increase in cell-death in SK-N-SH cells in the presence of both agents.

In summary, the combination of etoposide and VPA increases their anti-tumor effects on human UKF-NB-4 neuroblastoma cells. The results found suggest that impact of VPA on anticancer effect of etoposide on these cells depends on a variety of factors, mainly on the sequence of cultivation of the cells with these drugs. Nevertheless, because the combination of both drugs at the clinically relevant doses and in suitable sequence regimens increases their toxic effects on human neuroblastoma UKF-NB-4 cells, such combination regimens might be utilized for treatment of patients suffering from high risk neuroblastomas.

ACKNOWLEDGEMENTS

This study was supported by GACR (grant P301/10/0356), Charles University (grants 635712/2012 and UNCE 204025/2012) and by the project for conceptual development of research organization 00064203. We thank to Prof. J. Cinatl, Jr. (J. W. Goethe University, Frankfurt, Germany) for providing cell lines.

REFERENCES

1 Agner J, Falck J, Lukas J and Bartek J (2005) Differential impact of diverse anticancer chemotherapeutics on the Cdc25A-degradation checkpoint pathway. Exp Cell Res **302**: 162–169.
2 Baldwin EL and Osheroff N (2005) Etoposide, topoisomerase II and cancer. Curr Med Chem Anticancer Agents **5**: 363–372.
3 Belani CP, Doyle LA and Aisner J (1994) Etoposide: current status and future perspectives in the management of malignant neoplasms. Cancer Chemother Pharmacol **34** Suppl: S118–126.
4 Blaheta RA and Cinatl J, Jr. (2002) Anti-tumor mechanisms of valproate: a novel role for an old drug. Med Res Rev **22**: 492–511.
5 Brodeur GM (2003) Neuroblastoma: biological insights into a clinical enigma. Nat Rev Cancer **3**: 203–216.

6 Catalano MG, Fortunati N, Pugliese M, Costantino L, Poli R, Bosco O et al. (2005) Valproic acid induces apoptosis and cell cycle arrest in poorly differentiated thyroid cancer cells. J Clin Endocrinol Metab **90**: 1383–1389.

7 Cerveny L, Svecova L, Anzenbacherova E, Vrzal R, Staud F, Dvorak Z, et al. (2007) Valproic acid induces CYP3A4 and MDR1 gene expression by activation of constitutive androstane receptor and pregnane X receptor pathways. Drug Metab Dispos **35**: 1032–1041.

8 Cinatl J, Jr., Cinatl J, Driever PH, Kotchetkov R, Pouckova P, Kornhuber B et al. (1997) Sodium valproate inhibits in vivo growth of human neuroblastoma cells. Anticancer Drugs **8**: 958–963.

9 Champoux JJ (2001) DNA topoisomerases: structure, function, and mechanism. Annu Rev Biochem **70**: 369–413.

10 Chen GL, Yang L, Rowe TC, Halligan BD, Tewey KM and Liu LF (1984) Nonintercalative antitumor drugs interfere with the breakage-reunion reaction of mammalian DNA topoisomerase II. J Biol Chem **259**: 13560–13566.

11 Das CM, Zage PE, Taylor P, Aguilera D, Wolff JE, Lee D et al. (2010) Chromatin remodelling at the topoisomerase II-beta promoter is associated with enhanced sensitivity to etoposide in human neuroblastoma cell lines. Eur J Cancer **46**: 2771–2780.

12 Eyal S, Lamb JG, Smith-Yockman M, Yagen B, Fibach E and Altschuler Y (2006) White HS, Bialer M. The antiepileptic and anticancer agent, valproic acid, induces P-glycoprotein in human tumour cell lines and in rat liver. Br J Pharmacol **149**: 250–260.

13 Daud AI, Dawson J, Deconti RC, Bicaku E, Marchion D, Bastien S et al. (2009) Potentiation of a topoisomerase I inhibitor, karenitecin, by the histone deacetylase inhibitor valproic acid in melanoma: translational and phase I/II clinical trial. Clin Cancer Res **15**: 2479–2487.

14 Hajji N, Wallenborg K, Vlachos P, Fullgrabe J, Hermanson O and Joseph B (2010) Opposing effects of hMOF and SIRT1 on H4K16 acetylation and the sensitivity to the topoisomerase II inhibitor etoposide. Oncogene **29**: 2192–2204.

15 Hrebackova J, Hrabeta J and Eckschlager T (2010) Valproic acid in the complex therapy of malignant tumors. Curr Drug Targets **11**: 361–379.

16 Imbert TF (1998) Discovery of podophyllotoxins. Biochimie **80**: 207–222.

17 Kaiser M, Zavrski I, Sterz J, Jakob C, Fleissner C, Kloetzel PM et al. (2006) The effects of the histone deacetylase inhibitor valproic acid on cell cycle, growth suppression and apoptosis in multiple myeloma. Haematologica **91**: 248–251.

18 Kawashiro T, Yamashita K, Zhao XJ, Koyama E, Tani M, Chiba K, et al. (1998) A study on the metabolism of etoposide and possible interactions with antitumor or supporting agents by human liver microsomes. J Pharmacol Exp Ther **286**: 1294–1300.

19 Krishan A, Paika K and Frei E, 3rd (1975) Cytofluorometric studies on the action of podophyllotoxin and epipodophyllotoxins (VM-26, VP-16-213) on the cell cycle traverse of human lymphoblasts. J Cell Biol **66**: 521–530.

20 Lee JH, Choy ML, Ngo L, Foster SS and Marks PA (2010) Histone deacetylase inhibitor induces DNA damage, which normal but not transformed cells can repair. Proc Natl Acad Sci U S A **107**: 14639–14644.

21 Li J, Hua HM, Tang YB, Zhang S, Ohkoshi E, Lee KH et al. (2012) Synthesis and evaluation of novel podophyllotoxin analogs. Bioorg Med Chem Lett **22**: 4293–4295.

22 Loike JD and Horwitz SB (1976) Effect of VP-16-213 on the intracellular degradation of DNA in HeLa cells. Biochemistry **15**: 5443–5448.

23 Marchion DC, Bicaku E, Daud AI, Sullivan DM and Munster PN (2005) In vivo synergy between topoisomerase II and histone deacetylase inhibitors: predictive correlates. Mol Cancer Ther **4**: 1993–2000.

24 Marchion DC, Bicaku E, Daud AI, Richon V, Sullivan DM and Munster PN (2004) Sequence-specific potentiation of topoisomerase II inhibitors by the histone deacetylase inhibitor suberoylanilide hydroxamic acid. J Cell Biochem **92**: 223–237.

25 Meresse P, Dechaux E, Monneret C and Bertounesque E (2004) Etoposide: discovery and medicinal chemistry. Curr Med Chem **11**: 2443–2466.

26 Nelson EM, Tewey KM and Liu LF (1984) Mechanism of antitumor drug action: poisoning of mammalian DNA topoisomerase II on DNA by 4'-(9-acridinylamino)-methanesulfon-m-anisidide. Proc Natl Acad Sci U S A **81**: 1361–1365

27 Obata S, Yamaguchi Y and Miyamoto T (1990) Effects of etoposide (VP-16) on the survival and progression of cultured HeLa S3 cells through the cell cycle. Nihon Gan Chiryo Gakkai Shi **25**: 2484–2491.

28 Olive PL and Banath JP (1993) Detection of DNA double-strand breaks through the cell cycle after exposure to X-rays, bleomycin, etoposide and 125IdUrd. Int J Radiat Biol **64**: 349–358.

29 Perez C, Pelayo F, Vilaboa NE and Aller P (1994) Caffeine attenuates the action of amsacrine and etoposide in U-937 cells by mechanisms which involve inhibition of RNA synthesis. Int J Cancer **57**: 889–893.

30 Poljakova J, Hrebackova J, Dvorakova M, Moserova M, Eckschlager T, Hrabeta J et al. (2011) Anticancer agent ellipticine combined with histone deacetylase inhibitors, valproic acid and trichostatin A, is an effective DNA damage strategy in human neuroblastoma. Neuro Endocrinol Lett **32** (Suppl 1): 101–116.

31 Robert J and Larsen AK (1998) Drug resistance to topoisomerase II inhibitors. Biochimie **80**: 247–254.

32 Santini V, Gozzini A and Ferrari G (2007) Histone deacetylase inhibitors: molecular and biological activity as a premise to clinical application. Curr Drug Metab **8**: 383–393.

33 Schonn I, Hennesen J and Dartsch DC (2010) Cellular responses to etoposide: cell death despite cell cycle arrest and repair of DNA damage. Apoptosis **15**: 162–172.

34 Schroeder U, Bernt KM, Lange B, Wenkel J, Jikai J, Shabat D et al. (2003) Hydrolytically activated etoposide prodrugs inhibit MDR-1 function and eradicate established MDR-1 multidrug-resistant T-cell leukemia. Blood **102**: 246–253.

35 Stacey DW, Hitomi M and Chen G (2000) Influence of cell cycle and oncogene activity upon topoisomerase IIalpha expression and drug toxicity. Mol Cell Biol **20**: 9127–9137.

36 Stiborova M, Eckschlager T, Poljakova J, Hrabeta J, Adam V, Kizek R et al. (2012) The synergistic effects of DNA-targeted chemotherapeutics and histone deacetylase inhibitors as therapeutic strategies for cancer treatment. Curr Med Chem **19**: 4218–4238.

37 Stiborova M, Moserova M, Mrazova B, Kotrbova V and Frei E (2010) Role of cytochromes P450 and peroxidases in metabolism of the anticancer drug ellipticine: additional evidence of their contribution to ellipticine activation in rat liver, lung and kidney. Neuro Endocrinol Lett **31** (Suppl. 2): 26–35.

38 Stiborova M, Rupertova M, and Frei E (2011) Cytochrome P450- and peroxidase-mediated oxidation of anticancer alkaloid ellipticine dictates its anti-tumor efficiency. Biochim Biophys Acta **1814**: 175–185.

39 Tanaka T, Halicka HD, Traganos F, Seiter K and Darzynkiewicz Z (2007) Induction of ATM activation, histone H2AX phosphorylation and apoptosis by etoposide: relation to cell cycle phase. Cell Cycle **6**: 371–376.

40 Tewey KM, Rowe TC, Yang L, Halligan BD and Liu LF (1984) Adriamycin-induced DNA damage mediated by mammalian DNA topoisomerase II. Science **226**: 466–468.

41 Uesaka T, Shono T, Kuga D, Suzuki SO, Niiro H, Miyamoto K et al. (2007) Enhanced expression of DNA topoisomerase II genes in human medulloblastoma and its possible association with etoposide sensitivity. J Neurooncol **84**: 119–129.

42 Van Der Graaf WT and De Vries EG (1990) Mitoxantrone: bluebeard for malignancies. Anticancer Drugs **1**: 109–125.

43 Vrzal R Doricakova A, Novotna A, Bachleda P, Bitman M, Pavek P, et al. (2011) Valproic acid augments vitamin D receptor-mediated induction of CYP24 by vitamin D3: a possible cause of valproic acid-induced osteomalacia? Toxicol Lett **200**:146–153.

44 Walker JV and Nitiss JL (2002) DNA topoisomerase II as a target for cancer chemotherapy. Cancer Invest **20**: 570–589.

45 Wozniak AJ and Ross WE (1983) DNA damage as a basis for 4'-demethylepipodophyllotoxin-9-(4,6-O-ethylidene-beta-D-glucopyranoside) (etoposide) cytotoxicity. Cancer Res **43**: 120–124.

46 Zhao XJ, Kawashiro T and Ishizaki T (1998) Mutual inhibition between quinine and etoposide by human liver microsomes. Evidence for cytochrome P4503A4 involvement in their major metabolic pathways. Drug Metab Dispos **26**: 188–191.

47 Zheng N, Pang S, Oe T, Felix CA, Wehrli S and Blair IA (2006) Characterization of an etoposide-glutathione conjugate derived from metabolic activation by human cytochrome p450. Curr Drug Metab **7**: 897–911.

Hypoxia-mediated histone acetylation and expression of *N*-myc transcription factor dictate aggressiveness of neuroblastoma cells

JITKA POLJAKOVÁ[1], TOMÁŠ GROH[1], ŽANETA OMANA GUDINO[1], JAN HRABĚTA[2], LUCIE BOŘEK-DOHALSKÁ[1], RENÉ KIZEK[3,4], HELENA DOKTOROVÁ[2], TOMÁŠ ECKSCHLAGER[2] and MARIE STIBOROVÁ[1]

[1]Department of Biochemistry, Faculty of Science, Charles University, 128 40 Prague 2; [2]Department of Pediatric Hematology and Oncology, 2nd Medical School, Charles University and University Hospital Motol, 150 06 Prague 5; [3]Department of Chemistry and Biochemistry, Faculty of Agronomy, Mendel University in Brno, 613 00 Brno; [4]Central European Institute of Technology, Brno University of Technology, 616 00 Brno, Czech Republic

Received November 26, 2013; Accepted December 23, 2013

DOI: 10.3892/or.2014.2999

Abstract. Cells of solid malignancies generally adapt to entire lack of oxygen. Hypoxia induces the expression of several genes, which allows the cells to survive. For DNA transcription, it is necessary that DNA structure is loosened. In addition to structural characteristics of DNA, its epigenetic alterations influence a proper DNA transcription. Since histones play a key role in epigenetics, changes in expression levels of acetylated histones H3 and H4 as well as of hypoxia-inducible factor-1α (HIF-1α) in human neuroblastoma cell lines cultivated under standard or hypoxic conditions (1% O_2) were investigated. Moreover, the effect of hypoxia on the expression of two transcription factors, *c*-Myc and *N*-myc, was studied. Hypoxic stress increased levels of acetylated histones H3 and H4 in UKF-NB-3 and UKF-NB-4 neuroblastoma cells with *N-myc* amplification, whereas almost no changes in acetylation of these histones were found in an SK-N-AS neuroblastoma cell line, the line with diploid *N-myc* status. An increase in histone H4 acetylation caused by hypoxia in UKF-NB-3 and UKF-NB-4 corresponds to increased levels of *N*-myc transcription factor in these cells.

Introduction

Neuroblastoma is an embryonal cancer of the postganglionic sympathetic nervous system, which most commonly arises in the adrenal gland. It is the most frequent malignant disease of infancy and is a major cause of mortality from neoplasia at this age (1). These tumors are biologically heterogeneous, with cell populations differing in their genetic programs, maturation stage and malignant potential. As neuroblastoma cells seem to have the capacity to differentiate spontaneously *in vivo* and *in vitro* (2), their heterogeneity may affect treatment outcome, in particular the response to apoptosis induced by chemotherapy. Low-risk neuroblastoma is one of the rare human malignancies that are known to demonstrate spontaneous regression in infants from an undifferentiated state to a benign ganglioneuroma, whereas high-risk neuroblastoma grows relentlessly and may be rapidly fatal. Prognosis of the high-risk form of this type of cancer is poor, since drug resistance arises in the majority of the patients initially responding well to chemotherapy (3).

Approximately 40% of patients suffering from neuroblastoma belong to the high-risk group. Unfavorable tumors are characterized by structural chromosomal changes, including deletions of 1p or 11q, unbalanced gain of 17q and/or amplification of the *N-myc* proto-oncogene. Among them, amplification of the *N-myc* is a marker for high-risk neuroblastoma (3). Indeed, *N-myc* overexpression in neuroblastomas with amplified *N-myc* is associated with poor prognosis (3). Among the prognostic indicators of neuroblastoma, *N-myc* amplification is strongly associated with advanced disease stages, rapid tumor progression and the poorest disease outcome. *N-myc* amplification occurs in ~20 to 25% of all neuroblastoma cases and it leads to *N*-myc overexpression at both the mRNA and protein levels (4,5). However, the high *N-myc* expression confers the opposite biological consequence in neuroblastoma, depending on *N-myc* gene status. Indeed, high-level of *N-myc* expression is associated with favorable outcome in neuroblastoma lacking *N-myc* amplification. Forced expression of *N-myc* significantly suppresses growth of neuroblastoma cells lacking *N-myc* amplification by inducing apoptosis and enhancing favorable neuroblastoma gene expression. Hence, it may be postulated that high-level *N-myc* expression in neuroblastoma lacking *N-myc* amplification results in a benign phenotype (4). Whereas *N-myc* overexpression in neuroblastoma cells with *N-myc* amplification induces the malignant phenotype of these neuroblastoma cells (3), overexpression of the other genes of the Myc family

Correspondence to: Professor Marie Stiborová, Department of Biochemistry, Faculty of Science, Charles University, Albertov 2030, 128 40 Prague 2, Czech Republic
E-mail: stiborov@natur.cuni.cz

Key words: hypoxia, neuroblastoma, histone acetylation, *N*-myc expression

induces unrestricted cell proliferation, inhibits differentiation, cell growth, angiogenesis, reduces cell adhesion, metastasis and induces genomic instability (6). In human neuroblastoma cells with inducible *N-myc* expression, the *N-myc* increases apoptosis induced by cytostatics. Furthermore, neuroblastoma cells with *N-myc* amplification can resist treatment only when there is additional dysfunction in the apoptosis pathways (7). Another mechanism of drug resistance in neuroblastoma cells, to which *N-myc* may contribute, is the regulation of ABC transporter genes (8).

A reduction in the normal level of tissue oxygen tension, hypoxia, produces cell death if severe or prolonged (9). In solid tumors it is a consequence of structurally and functionally disturbed microcirculation and the deterioration of diffusion conditions (10). Although hypoxia is toxic to both cancer cells and normal cells, cancer cells undergo genetic and adaptive changes that allow them to survive and even proliferate in the hypoxic environment (9). Therefore, tumor hypoxia appears to be strongly associated with tumor progression and resistance to chemo- and radio-therapy, and has thus become an important issue in tumor physiology and cancer treatment (10). However, the mechanisms explaining how cancer cells can survive hypoxia more efficiently than normal cells remain to be explored.

The epigenetic structure of DNA in chromatin plays a role in the origin of neuroblastomas (11). Dynamic formation of DNA leads not only to transcription of different genes but DNA is also more accessible for DNA-targeted chemotherapeutics. Approximately 75 genes are described as epigenetically affected in neuroblastoma cells (12). DNA hypermethylation and gene silencing is generally associated with the abundance of deacetylated histones, the other essential actors of epigenetic mechanisms (13). Indeed, histones are key players in epigenetics and their status dictates accessibility of chromatin DNA for binding of transcription factors that regulates DNA transcription (14).

The core histones H3, H4, H2A and H2B around which 147 base pairs of DNA are wrapped are predominantly globular except for their *N*-terminal tails, which are unstructured (15). There are at least eight distinct types of modifications. One of the most important histone modifications is acetylation of lysine residues, which regulates various cell processes such as transcription, repair, replication and condensation of DNA (15). Histone acetylation is regulated by the equilibrium of two groups of enzymes: histone acetyltransferases (HATs) and histone deacetylases (HDACs) (13). Watson *et al* showed significant alterations in the global levels of histone acetylation and DNA methylation in response to chronic hypoxic exposure, where cells were permanently maintained at 1% oxygen, i.e., specifically consistent and sustained global increases in H3K9 acetylation and DNA methylation in the absence of hypoxia-inducible factor hypoxia-inducible factor-1α (HIF-1α) (16). Therefore, since acetylation of histones is an important epigenetic mark that may be influenced by hypoxia, investigation of changes in expression levels of acetylated histones H3 and H4 in human neuroblastoma cell lines by hypoxia is one of the aims of the present study. The effect of hypoxia on amounts of HIF-1α protein was also examined. In addition, levels of *N*-myc protein and another member of the Myc family of transcription factors, *c*-Myc, may be influenced by the chromatin structure that is dictated by acetylation of histones H3 and H4 and recruit other co-factors to activate gene expression (17-19). Therefore, the present study also investigated the effect of hypoxia on the relationships between acetylation of histones H3 and H4 and expression of *N*-myc and *c*-Myc in neuroblastoma cells. Since heterogeneity of neuroblastoma cells may affect their responsibility to hypoxia, three neuroblastoma cell lines were tested in the present study: UKF-NB-3, UKF-NB-4 and SK-N-AS cell lines.

Materials and methods

Chemicals and materials. AA mix (acrylamide:bisacrylamide 29:1), natrium butyrate, natrium deoxycholate, natrium dodecyl sulfate (SDS), 1,2-bis(dimethylamino)ethane (TEMED), polyoxyethylene-sorbitan monolaurate (Tween-20), ammonium peroxodisulfate (APS) and glycine were purchased from Sigma-Aldrich (St. Louis, MO, USA). 4-(2-Hydroxyethyl)-1-piperazineethanesulfonic acid (HEPES), dithiothreitol (DTT), phenylmethylsulfonyl fluoride (PMSF) were obtained from Gibco-BRL (Life Technologies, Carlsbad, CA, USA). Phosphate-buffered saline (PBS), trypsin and SeeBlue® Plus2 Pre-Stained Standard were purchased from Invitrogen (Life Technologies, Carlsbad, CA, USA). Natrium hydrogen carbonate, hydrogen chloride and methanol were acquired from Penta (Prague, Czech Republic). Tris [1,1,1-Tris (hydroxymethyl) aminomethane (TRIS)] was obtained from Lachema (Brno, Czech Republic). Blotting Grade Blocker non-fat dry milk was purchased from Bio-Rad (Hercules, CA, USA). All these and other chemicals used in the experiments were of analytical purity or better.

Cell cultures. The human neuroblastoma cells lines UKF-NB-3 and UKF-NB-4 with *N-myc* amplification, established from bone marrow metastases of high-risk neuroblastoma, were a gift from Professor J. Cinatl Jr (J.W., Goethe University, Frankfurt, Germany). SK-N-AS cells with diploid *N-myc* status were purchased from American Type Culture Collection (ATCC, Manassas, VA, USA). Cells were cultivated in Iscove's modified Dulbecco's medium (IMDM) (Lonza, Basel, Switzerland), supplemented with 10% fetal calf serum and 2 mM L-glutamine, (PAA Laboratories, Pasching, Austria) at 37˚C and 5% CO_2. For experiments with hypoxia, a hypoxic chamber purchased from Billups-Rothenberg (Del Mar, CA, USA) was prepared with an atmosphere containing 1% O_2, 5% CO_2 and 94% N_2.

Estimation of contents of acetylated histones H3 and H4 in neuroblastoma cells. Cell pellets were re-suspended in 10 mM HEPES buffer pH 7.9 containing 1.5 mM $MgCl_2$, 10 mM KCl, 0.5 mM dithiothreitol and 1.5 mM PMSF for preparation of acid extraction of proteins as introduced in the anti-H4 antibody datasheet. To each sample, hydrochloric acid was added to a final concentration of 0.2 M. The samples were incubated on ice for 30 min and centrifuged at 11,000 x g for 10 min at 4˚C. The supernatant fraction, which contains the acid soluble proteins, was dialyzed against 0.1 M acetic acid, twice for 1 h each, and against distilled water for 2 h and overnight. Protein concentrations were

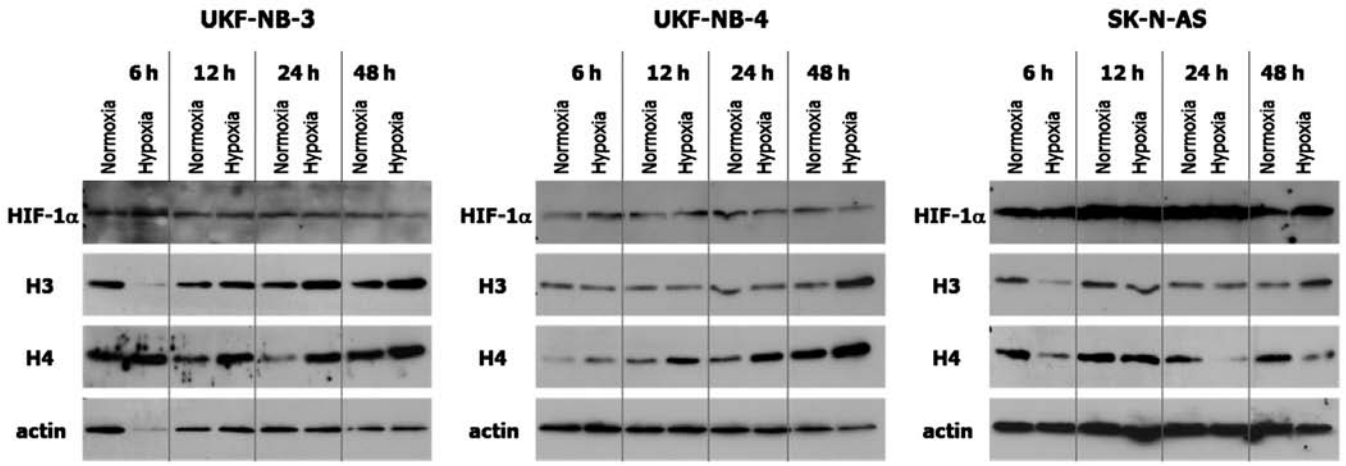

Figure 1. The effect of hypoxia on expression of HIF-1α and acetylated histones H3 and H4 in human neuroblastoma cell lines determined by western blotting. Actin was used as loading control. HIF-1α, hypoxia-inducible factor-1α.

assessed using the DC protein assay (Bio-Rad) with serum albumin as a standard. Five and/or 15 μg of extracted proteins were subjected to SDS-PAGE electrophoresis (20,21) on a 17% gel for analysis of histone H3 and/or H4 acetylation, respectively. After migration, proteins were transferred to a nitrocellulose membrane and incubated with 5% non-fat milk to block non-specific binding. The membranes were then exposed to specific rabbit polyclonal anti-H3 (1:10,000) and anti-H4 (1:20,000) (both from Upstate, Lake Placid, NY, USA), antibodies overnight at 4˚C. Membranes were washed and exposed to peroxidase-conjugated anti-IgG secondary antibodies (1:3,000) and the antigen-antibody complex was visualized by enhanced chemiluminescence detection system according to the manufacturer's instructions (Immun-Star HRP Substrate) (both from Bio-Rad), using X-ray film from MEDIX XBU (Foma, Hradec Králové, Czech Republic). Antibody against actin (1:1,000; Sigma, St. Louis, MO, USA) was used as loading control.

HAT and HDAC activity. Activity of HATs and HDACs was assessed according to the manufacturer's instructions by HAT Activity and HDAC Activity Colorimetric Assay kits (BioVision, Milpitas, CA, USA). Briefly, 68 μl of assay mix containing 40 μl 2X HAT assay buffer, 5 μl HAT substrate, 15 μl HAT substrate II and 8 μl NADH generating enzyme were added to 50 μg of nuclear extract in 40 μl of distilled water. Each well of the 96-well plate was mixed. The plate was incubated at 37˚C for 1 h and then read in a VersaMax™ microplate reader (Molecular Devices, Sunnyvale, CA, USA) at 440 nm. Alternatively, 50-200 μg of nuclear extract were diluted in 85 μl of distilled water. Ten microliters of 10X HDAC assay buffer and 5 μl of an HDAC colorimetric substrate was added to each well. After thorough mixing, plates were incubated at 37˚C for 1 h. The reaction was stopped by adding 10 μl of Lysine developer. After mixing well, the plate was incubated at 37˚C for 30 min. Samples were read in plate reader VersaMax™ microplate reader at 400 nm.

Estimation of contents of HIF-1α, c-Myc and N-myc in neuroblastoma cells. To determine the expression of HIF-1α, c-Myc and N-myc proteins, cell pellets were resuspended in 25 mM Tris-HCl buffer pH 7.6 containing 150 mM NaCl, 1% detergent Igepal® CA-630 (Sigma), 1% sodium deoxycholate and 0.1% SDS and with solution of Complete™ (protease inhibitor cocktail tablet; Roche, Basel, Switzerland) at concentrations described by the provider. The samples were incubated for 60 min on ice and thereafter centrifuged for 20 min at 14,000 x g and 4˚C. Supernatant was used for additional analysis. Protein concentrations were assessed using the DC protein assay (Bio-Rad) with serum albumin as a standard. Then, 50 μg of extracted proteins were subjected to SDS-PAGE electrophoresis on an 11% gel for analysis of HIF-1α, c-Myc and N-myc protein expression. After migration, proteins were transferred to a nitrocellulose membrane and incubated with 5% non-fat milk to block non-specific binding. The membranes were then exposed to specific rabbit polyclonal anti-HIF-1α (1:3,000; Zymed Life Technologies, Carlsbad, CA, USA), rabbit monoclonal anti-c-Myc (1:500) antibodies and to specific mouse monoclonal anti-N-myc (1:1,000) (both from Santa Cruz Biotechnology, Inc., Dallas, TX, USA) antibody overnight at 4˚C. Membranes were washed and exposed to peroxidase-conjugated anti-IgG secondary antibodies (1:3,000; Bio-Rad), and the antigen-antibody complex was visualized by enhanced chemiluminescence detection system according to the manufacturer's instructions (Immun-Star HRP Substrate), using X-ray film from MEDIX XBU. Antibody against actin (1:1,000; Sigma) was used as loading control.

Cell cycle analysis. To determine cell cycle distribution analysis, $5x10^5$ cells were plated in 60 mm dishes and treated under hypoxic conditions for 24 h. After treatment, the cells were collected by trypsinization, stained with DNA PREP reagent kit (Beckmann Coulter, Fullerton, CA, USA), that contains permeabilization reagent and propidium iodide solution with RNase, according to the manufacturer's instructions, and at least 30,000 cells were analyzed by flow cytometry on a FACSCalibur cytometer (BD, San Jose, CA, USA). The data were analyzed using ModFit LT software (Verity Software House, Topsham, ME, USA).

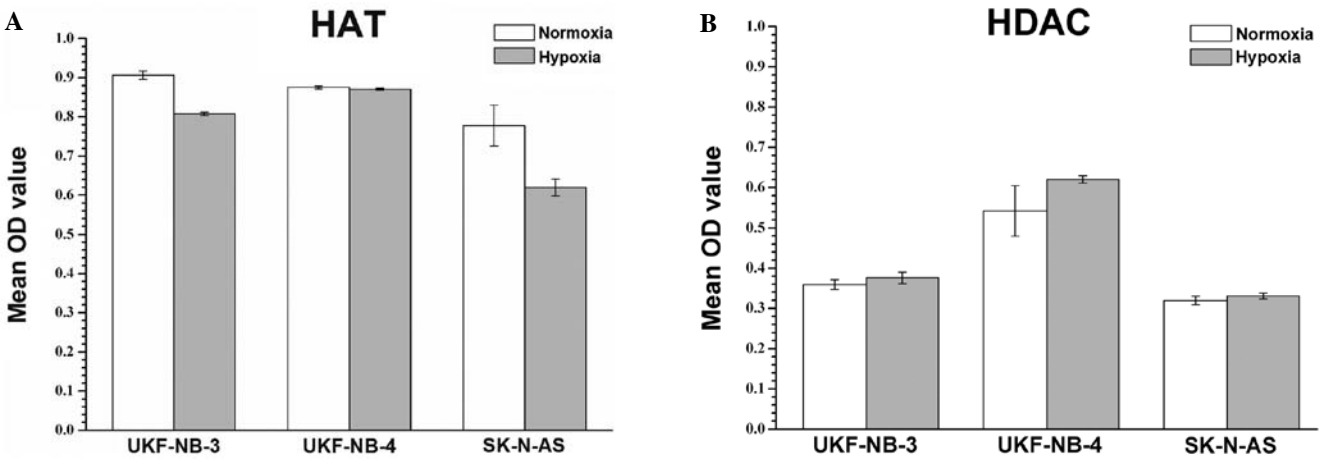

Figure 2. The effect of hypoxia on activities of (A) histone acetyltransferases (HATs) and (B) histone deacetylases (HDACs) in neuroblastoma cells. Hypoxia, 24 h exposure to 1% O_2.

Results and Discussion

The effect of hypoxia on acetylation of histone H3 and H4 in neuroblastoma cells. Epigenetic processes are involved in causation and progression of many types of malignancies, including neuroblastoma. Therefore, we decided to explore how commonly emerging state in neoplasia regions, hypoxia affects chromatin-associated proteins and post-translational modifications of histones regulated transcription. Using western blotting, different levels of acetylated histones H3 and H4 in individual human neuroblastoma cell lines cultivated under normoxic or hypoxic conditions (1% O_2) were found. Cultivation of the tested neuroblastoma cells for 6, 12, 24 or 48 h in hypoxia increased acetylation of histone H4 in UKF-NB-3 and UKF-NB-4 cell lines, the lines derived from high-risk neuroblastomas with *N-myc* amplification. In contrast to these results, decreased levels of histone H4 acetylation after 24 h exposure to hypoxia were detected in an SK-N-AS neuroblastoma cell line having diploid *N-myc* status. Therefore, it may be assumed that an increase in acetylation of histone H4 is related to *N-myc* amplification. Acetylation of the only histone H3 was increased under hypoxic conditions in a UKF-NB-3 cell line. With the exception of 48 h hypoxia, where histone H3 acetylation was increased in UKF-NB-4 and SK-N-AS, almost no changes in histone H3 acetylation were produced by hypoxia in UKF-NB-4 and SK-N-AS cells (Fig. 1).

Activity of HATs and HDACs. Although the activities of HATs were slightly lowered by 24 h hypoxia cultivation of UKF-NB-3 and SK-N-AS cells, no effect of such conditions of cultivation was found on these enzymes in a UKF-NB-4 cell line. In addition, essentially no differences in activities of HDACs were produced by hypoxia in tested neuroblastoma cells (Fig. 2). These findings suggest that increased acetylation of histones H3 and H4 in UKF-NB-3 and UKF-NB-4 neuroblastoma cells and decreased acetylation of the histones in SK-N-AS cells (see Fig. 1) is not directly connected with activities of these enzymes and follows from the other, still unknown, mechanism(s).

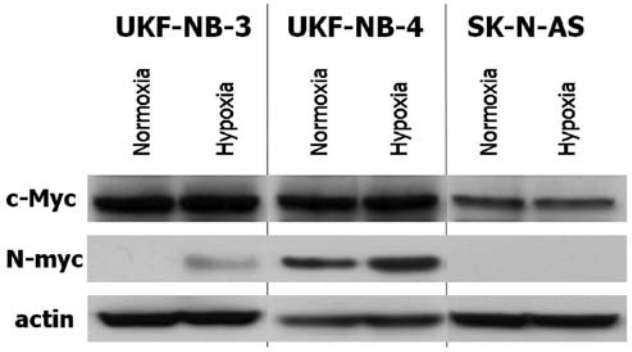

Figure 3. The effect of hypoxia on expression of *c*-Myc and *N*-myc proteins in human neuroblastoma cell lines determined by western blotting. Actin was used as loading control.

Hypoxia influences expression of N-myc but not c-Myc in neuroblastoma cells. Different levels of *N*-myc protein were found in either studied neuroblastoma cell line cultivated both under hypoxic and normoxic (standard) conditions. Of all tested cell lines cultivated under standard conditions, the *N*-myc protein was expressed in detectable amounts only in the UKF-NB-4 cells (Fig. 3). However, hypoxic conditions of cultivation of the neuroblastoma cells (24 h) resulted in increased expression of protein of this transcription factor in these neuroblastoma cells and even in expression of this protein in UKF-NB-3 cells. However, *N*-myc protein was undetectable in the SK-N-AS line, neither in normoxia nor in hypoxia. The increased levels of proto-oncogene *N*-myc protein mediated by hypoxia in UKF-NB-3 and UK-NB-4 neuroblastoma cell lines with *N-myc* amplification were paralleled with an increase in histone H4 acetylation in these cells (compare Figs. 1 and 3). Histone's lysine residue acetylation leads to decreased interactions between distinct chromatin fibres and to a decondensation of chromatin and increased accessibility of DNA to the transcriptional machinery due to the DNA uncoiling (22). These results indicate that hypoxia induces an increase in gene transcription activation in the neuroblastoma cells with *N*-myc amplification. Since *N*-myc

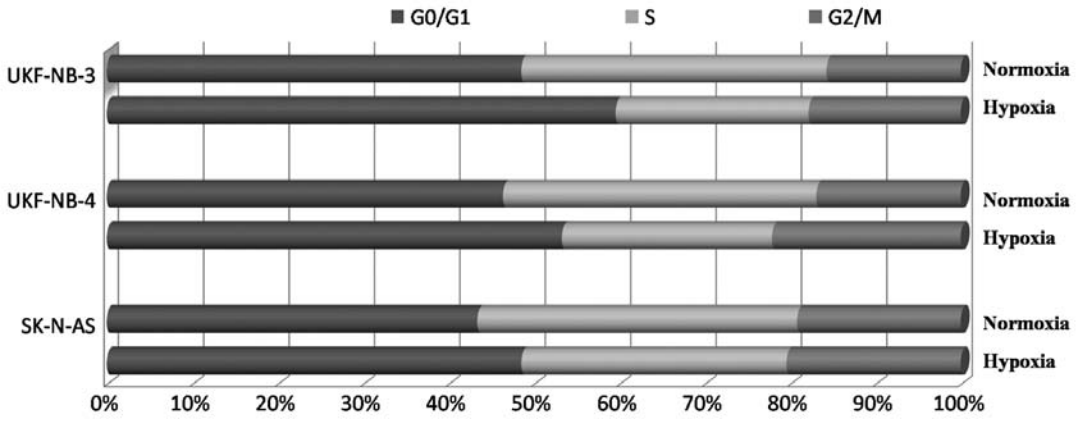

Figure 4. Cell cycle distribution in human neuroblastoma cell lines assessed by flow cytometry; the effect of 24 h hypoxia on cell cycle of these cells in comparison with the standard cultivation conditions.

also both activates and represses the expression of several miRNAs and long non-coding RNAs that play important roles in neuroblastoma progression (23), an increase in its expression may be involved in the higher aggressive property of these neuroblastoma cells. Indeed, regardless of cell cultivation conditions, no *N*-myc expression was detected by western blotting in an SK-N-AS cell line that lacked *N-myc* amplification. It may be speculated that increased acetylation of histone H4 caused by hypoxia is involved in cancer progression of neuroblastoma cells with *N-myc* amplification. Since most tumors contain hypoxic area, *N-myc* overexpression induced by hypoxia may decrease response of neuroblastoma with *N-myc* amplification to chemotherapy.

In contrast to *N*-myc protein, essentially no differences in *c*-Myc protein expression were found in neuroblastoma cells cultivated under normoxic or hypoxic conditions (Fig. 3), which corresponds to the findings of Huang *et al*, who found an inverse relationship between *N-myc* and *c-Myc* expression in various neuroblastoma derived cell lines and that both *N-myc* and *c-Myc* overexpression accelerates tumor cell proliferation and tumorigenesis directly through *BMI1* (polycomb ring finger oncogene) gene transcription (24).

Influence of hypoxia on HIF-1α protein expression in neuroblastoma cells. The transcription factor HIF-1α is a key mediator of the cellular response to hypoxia affecting expression of many genes that may inhibit apoptosis (25). Although HIF-1β is constitutively expressed in the nucleus, HIF-1α is maintained at low levels under normoxic conditions (26). In the presence of oxygen, the HIF-1α subunits undergo hydroxylation by oxygen-dependent prolyl hydroxylases allowing their binding to the von Hippel-Lindau (VHL) protein and targeting for ubiquitination and degradation (27). Overexpression of HIF-1α protein has been described in many different types of human malignancies, but not in benign tumors or normal tissues (28,29). In addition, overexpression of HIF-1α correlates with p53 accumulation, cell proliferation, and direct activation of vascular endothelial growth factor (VEGF) promoter, which suggests important roles for HIF-1α in cancer progression (28,30). As in other tumors, overexpression of HIF-1α protein has been found in all neuroblastoma cell lines tested in this study, with the highest being in an SK-N-AS cell line. Only a slight increase in levels of HIF-1α protein was found after 6 h of cultivation of all tested neuroblastoma cells in hypoxia, but at longer intervals (12, 24 and 48 h), no such increase was observed (Fig. 1).

Hypoxia affects cell cycle distribution of neuroblastoma cells. The cell cycle distribution of tested neuroblastoma cells measured by flow cytometry was slightly altered by oxygen deprivation (1% O_2, for 24 h) in comparison to the cell cycle distribution of cells cultivated under the standard (aerobic) conditions (Fig. 4). An increase in the G0/G1 phase with a concomitant decrease in the S phase of the cell cycle was produced by cultivation of all tested human neuroblastoma cells for 24 h under hypoxic conditions. It is evident that cancer cells cultivated under low levels of oxygen (1% O_2) require more time to be entered into the S phase of the cell cycle. This may be a consequence of a shift of cell metabolism from the oxidative to anaerobic one. It is known that the anaerobic metabolism is less effective in production of energy essential for biosynthesis of components of DNA such as deoxynucleoside triphosphates needed for biosynthesis of DNA in the S phase of the cell cycle. Another mechanism of decreased proliferation in hypoxia is the effect of HIF-1α that inhibits DNA replication and induces cell cycle arrest in various cell types (31).

In conclusion, in the present study, we have demonstrated that hypoxic stress increased levels of acetylated histones H3 and H4 in UKF-NB-3, and histone H4 in UKF-NB-4 neuroblastoma cell lines derived from high-risk neuroblastoma, both cell lines possessing *N-myc* amplification. In contrast, almost no changes in acetylation of these histones were found in an SK-N-AS neuroblastoma cell line with diploid *N-myc* status.

Hypoxia-induced acetylation of histones in tested neuroblastoma cell lines was not associated with expression of the transcription factor HIF-1α in these cells or with changes in HAT and HDAC activities. Although HIF-1α protein was overexpressed in all neuroblastoma cell lines tested in this study, essentially no differences in its expression were produced by hypoxia. Of note, the highest levels of HIF-1α protein were found in SK-N-AS neuroblastoma cells.

The increase in histone H4 acetylation mediated by hypoxia in UKF-NB-3 and UKF-NB-4 neuroblastoma cell lines was paralleled with the increased levels of proto-oncogene *N*-myc protein expression in these neuroblastoma cells with *N-myc* amplification. In addition, expression of this protein was not detectable in an SK-N-AS neuroblastoma cell line, the line with diploid *N-myc* status. These findings suggest that acetylation of histone H4 in neuroblastoma cells with *N-myc* amplification determines expression of transcription factor *N*-myc. The results showing the hypoxia-induced increase in levels of histone acetylation found in this study in UKF-NB-3 and UKF-NB-4 neuroblastoma cells are the opposite of those demonstrated by Li and Costa (19), who examined the effect of hypoxia on human A549 lung carcinoma cells. These authors found that exposure of this cancer cell line to hypoxia caused a decrease in acetylation of histones H3 and H4. Moreover, the authors showed that a decreased level of *c*-Myc expression was consistent with the effect of hypoxia on global histone H4 acetylation in A549 cells (19). These findings, which are different from those found in the present study, may be caused by the different type of cancer cells they used, human A549 lung carcinoma cells, in which *N-myc* amplification is missing. A decrease in acetylation of H3 and H4 by hypoxia in SK-N-AS neuroblastoma cells, a line without *N-myc* amplification, was also observed in the present study.

The results found in the present study indicate that insight into changes in levels of acetylated histones H3 and H4 and *N*-myc protein generated by hypoxic stress in the studied neuroblastoma cell lines may be important for partial explanation of the aggressive property of these cells. This is true predominantly for UKF-NB-4 neuroblastoma cells, the line with *N*-myc amplification and high P-glycoprotein expression that was prepared from chemoresistant recurrence (32,33). The *N*-myc protein is overexpressed in these cells and is even induced by hypoxia in these and UKF-NB-3 cells. An increased acetylation of histones allows *N*-myc to be easily bound to DNA, thereby inducing efficient transcription processes resulting finally in accelerated cell growth and proliferation. Therefore, among the genetic changes which allow high-risk neuroblastoma cells with *N-myc* amplification to survive hypoxia and to efficiently grow and proliferate under these conditions, may be the high expression of *N-myc* proto-oncogene and its induction by hypoxia.

Acknowledgements

The present study was supported by GACR (P301/10/0356), Charles University in Prague (635712/2012, 620612/2012 and UNCE 204025/2012) and MH CZ-DRO, University Hospital Motol, Prague, Czech Republic 00064203.

References

1. Maris JM and Matthay KK: Molecular biology of neuroblastoma. J Clin Oncol 17: 2264-2279, 1999.
2. Morgenstern BZ, Krivoshik AP, Rodriguez V and Anderson PM: Wilms' tumor and neuroblastoma. Acta Paediatr Suppl 93: 78-85, 2004.
3. Brodeur GM: Neuroblastoma: biological insights into a clinical enigma. Nat Rev Cancer 3: 203-216, 2003.
4. Tang XX, Zhao H, Kung B, Kim DY, Hicks SL, Cohn SL, Cheung NK, Seeger RC, Evans AE and Ikegaki N: The *MYCN* enigma: significance of *MYCN* expression in neuroblastoma. Cancer Res 66: 2826-2833, 2006.
5. Lutz W and Schwab M: In vivo regulation of single copy and amplified N-*myc* in human neuroblastoma cells. Oncogene 15: 303-315, 1997.
6. Westermann F, Muth D, Benner A, Bauer T, Henrich KO, Oberthuer A, Brors B, Beissbarth T, Vandesompele J, Pattyn F, Hero B, König R, Fischer M and Schwab M: Distinct transcriptional MYCN/c-MYC activities are associated with spontaneous regression or malignant progression in neuroblastomas. Genome Biol 9: R150, 2008.
7. Fulda S, Lutz W, Schwab M and Debatin KM: MycN sensitizes neuroblastoma cells for drug-induced apoptosis. Oncogene 18: 1479-1486, 1999.
8. Porro A, Haber M, Diolaiti D, Iraci N, Henderson M, Gherardi S, Valli E, Munoz MA, Xue C, Flemming C, Schwab M, Wong JH, Marshall GM, Della Valle G, Norris MD and Perini G: Direct and coordinate regulation of ATP-binding cassette transporter genes by Myc factors generates specific transcription signatures that significantly affect the chemoresistance phenotype of cancer cells. J Biol Chem 285: 19532-19543, 2010.
9. Harris AL: Hypoxia - a key regulatory factor in tumour growth. Nat Rev Cancer 2: 38-47, 2002.
10. Höckel M and Vaupel P: Tumor hypoxia: definitions and current clinical, biologic, and molecular aspects. J Natl Cancer Inst 93: 266-276, 2001.
11. Furchert SE, Lanvers-Kaminsky C, Juürgens H, Jung M, Loidl A and Frühwald MC: Inhibitors of histone deacetylases as potential therapeutic tools for high-risk embryonal tumors of the nervous system of childhood. Int J Cancer 120: 1787-1794, 2007.
12. Decock A, Ongenaert M, Vandesompele J and Speleman F: Neuroblastoma epigenetics: from candidate gene approaches to genome-wide screenings. Epigenetics 6: 962-970, 2011.
13. Santini V, Gozzini A and Ferrari G: Histone deacetylase inhibitors: molecular and biological activity as a premise to clinical application. Curr Drug Metab 8: 383-393, 2007.
14. Portela A and Esteller M: Epigenetic modifications and human disease. Nat Biotechnol 28: 1057-1068, 2010.
15. Kouzarides T: Chromatin modifications and their function. Cell 128: 693-705, 2007.
16. Watson JA, Watson CJ, McCrohan AM, Woodfine K, Tosetto M, McDaid J, Gallagher E, Betts D, Baugh J, O'Sullivan J, Murrell A, Watson RW and McCann A: Generation of an epigenetic signature by chronic hypoxia in prostate cells. Hum Mol Genet 8: 3594-3604, 2009.
17. Frank SR, Schroeder M, Fernandez P, Taubert S and Amati B: Binding of c-Myc to chromatin mediates mitogen-induced acetylation of histone H4 and gene activation. Genes Dev 15: 2069-2082, 2001.
18. Frank SR, Parisi T, Taubert S, Fernandez P, Fuchs M, Chan HM, Livingston DM and Amati B: MYC recruits the TIP60 histone acetyltransferase complex to chromatin. EMBO Rep 4: 575-580, 2003.
19. Li Q and Costa M: c-Myc mediates a hypoxia-induced decrease in acetylated histone H4. Biochimie 91: 1307-1310, 2009.
20. Stiborová M, Martínek V, Rýdlová H, Hodek P and Frei E: Sudan I is a potential carcinogen for humans: evidence for its metabolic activation and detoxication by human recombinant cytochrome P450 1A1 and liver microsomes. Cancer Res 62: 5678-5684, 2002.
21. Poljaková J, Eckschlager T, Kizek R, Frei E and Stiborová M: Electrochemical determination of enzymes metabolizing ellipticine in thyroid cancer cells - a tool to explain the mechanism of ellipticine toxicity to these cells. Int J Electrochem Sci 8: 1573-1585, 2013.
22. Gut P and Verdin E: The nexus of chromatin regulation and intermediary metabolism. Nature 502: 489-498, 2013.
23. Buechner J and Einvik C: N-myc and noncoding RNAs in neuroblastoma. Mol Cancer Res 10: 1243-1253, 2012.
24. Huang R, Cheung NK, Vider J, Cheung IY, Gerald WL, Tickoo SK, Holland EC and Blasberg RG: MYCN and MYC regulate tumor proliferation and tumorigenesis directly through BMI1 in human neuroblastomas. FASEB J 25: 4138-4149, 2011.

25. Liu XH, Yu EZ, Li YY and Kagan E: HIF-1α has an anti-apoptotic effect in human airway epithelium that is mediated via Mcl-1 gene expression. J Cell Biochem 97: 755-765, 2006.
26. Wang GL, Jiang BH, Rue EA and Semenza GL: Hypoxia-inducible factor 1 is a basic-helix-loop-helix-PAS heterodimer regulated by cellular O_2 tension. Proc Natl Acad Sci USA 92: 5510-5514, 1995.
27. Adamski J, Price A, Dive C and Makin G: Hypoxia-induced cytotoxic drug resistance in osteosarcoma is independent of HIF-1Alpha. PloS One 8: e65304, 2013.
28. Zhong H, De Marzo AM, Laughner E, Lim M, Hilton DA, Zagzag D, Buechler P, Isaacs WB, Semenza GL and Simons JW: Overexpression of hypoxia inducible factor 1α in common human cancers and their metastases. Cancer Res 59: 5830-5835, 1999.
29. Talks KL, Turley H, Gatter KC, Maxwell PH, Pugh CW, Ratcliffe PJ and Harris AL: The expression and distribution of the hypoxia-inducible factors HIF-1α and HIF-2α in normal human tissues, cancers, and tumor associated macrophages. Am J Pathol 157: 411-421, 2000.
30. Kwon HJ, Kim MS, Kim MJ, Nakajima H and Kim KW: Histone deacetylase inhibitor FK228 inhibits tumor angiogenesis. Int J Cancer 97: 290-296, 2002.
31. Hubbi ME, Kshitiz, Gilkes DM, Rey S, Wong CC, Luo W, Kim DH, Dang CV, Levchenko A and Semenza GL: A nontranscriptional role for HIF-1α as a direct inhibitor of DNA replication. Sci Signal 6: ra10, 2013.
32. Bedrnicek J, Vicha A, Jarosova M, Holzerova M, Cinatl Jr J, Michaelis M, Cinatl J and Eckschlager T: Characterization of drug-resistant neuroblastoma cell lines by comparative genomic hybridization. Neoplasma 52: 415-419, 2005.
33. Poljakova J, Hrebackova J, Dvorakova M, Moserova M, Eckschlager T, Hrabeta J, Göttlicherova M, Kopejtkova B, Frei E, Kizek R and Stiborova M: Anticancer agent ellipticine combined with histone deacetylase inhibitors, valproic acid and trichostatin A, is an effective DNA damage strategy in human neuroblastoma. Neuro Endocrinol Lett 32 (Suppl 1): 101-116, 2011.

The synergistic effects of DNA-damaging drugs cisplatin and etoposide with a histone deacetylase inhibitor valproate in high-risk neuroblastoma cells

TOMAS GROH[1,2], JAN HRABETA[2], MOHAMMED ASHRAF KHALIL[2], HELENA DOKTOROVA[2], TOMAS ECKSCHLAGER[2] and MARIE STIBOROVA[1]

[1]Department of Biochemistry, Faculty of Science, Charles University, 128 40 Prague 2; [2]Department of Pediatric Hematology and Oncology, 2nd Medical Faculty, Charles University and University Hospital Motol, 150 06 Prague 5, Czech Republic

DOI: 10.3892/ijo_xxxxxxxx

Abstract. High-risk neuroblastoma remains one of the most important therapeutic challenges for pediatric oncologists. New agents or regimens are urgently needed to improve the treatment outcome of this fatal tumor. We examined the effect of histone deacetylase (HDAC) inhibitors in a combination with other chemotherapeutics on a high-risk neuroblastoma UKF-NB-4 cell line. Treatment of UKF-NB-4 cells with DNA-damaging chemotherapeutics cisplatin or etoposide combined with the HDAC inhibitor valproate (VPA) resulted in the synergistic antitumor effect. This was associated with caspase-3-dependent induction of apoptosis. Another HDAC inhibitor trichostatin A and a derivative of VPA that does not exhibit HDAC inhibitory activity, valpromide, lacked this effect. The synergism was only induced when VPA was combined with cytostatics targeted to cellular DNA; VPA does not potentiate the cytotoxicity of the anticancer drug vincristine that acts by a mechanism different from that of DNA damage. The VPA-mediated sensitization of UKF-NB-4 cells to cisplatin or etoposide was dependent on the sequence of drug administration; the potentiating effect was only produced either by simultaneous treatment with these drugs or when the cells were pretreated with cisplatin or etoposide before their exposure to VPA. The synergistic effects of VPA with cisplatin or etoposide were associated with changes in the acetylation status of histones H3 and H4. The results of this study provide a rationale for clinical evaluation of the combination of VPA and cisplatin or etoposide for treating children suffering from high-risk neuroblastoma.

Correspondence to: Professor Marie Stiborova, Department of Biochemistry, Faculty of Science, Charles University, Albertov 2030, 128 40 Prague 2, Czech Republic
E-mail: stiborov@natur.cuni.cz

Key words: neuroblastoma, cisplatin, etoposide, valproate, acetylation of histones, apoptosis

Introduction

Neuroblastoma is the most common extracranial solid tumor of childhood. These tumors are biologically heterogeneous, with cell populations differing in their genetic programs, maturation stage and malignant potential. Neuroblastoma cells seem to have the capacity to differentiate spontaneously *in vivo* and *in vitro*, they may regress spontaneously in infants, mature to benign ganglioneuroma, or grow relentlessly and be rapidly fatal (1,2). This heterogeneity could affect treatment outcome, in particular the response to apoptosis induced by chemotherapy. Even though a great progress has recently been made in pediatric oncology, all accessible approaches have still failed to cure the high-risk neuroblastoma (3). Indeed, little improvement in therapeutic options has been made in the last decade, requiring the development of new therapies.

The chromatin structure plays a role in the origin of neuroblastomas (4). Dynamic formation of chromatin leads not only to transcription of different genes but DNA is also more accessible for DNA-targeted chemotherapeutics. Several genes are described as epigenetically influenced in neuroblastoma cells (5). DNA hypermethylation and gene silencing is usually associated with the abundance of deacetylated histones, the other essential actors of epigenetic mechanisms (6). Therefore, histones are key players in epigenetics, and their status dictates accessibility of transcription factors that regulates DNA transcription (7).

The core histones H3, H4, H2A and H2B around which 147 bp of DNA are wrapped and predominantly globular except for their *N*-terminal tails, which are unstructured (8). There are at least eight distinct types of modifications. One of the most important histone modifications is acetylation of lysine residues, which regulates various cell processes such as transcription, repair, replication and condensation of DNA (8). Histone acetylation is regulated by the equilibrium of two groups of enzymes: histone acetyltransferases (HATs) and histone deacetylases (HDACs) (6). HDACs also play an important role in post-transcriptional modifications in a variety of non-histone proteins such as transcription factors, chaperones or signaling molecules (9).

In the last decades, numerous compounds that act as inhibitors of HDACs have been studied as potential anticancer drugs. Various HDAC inhibitors initiate cancer cell death by different processes, depending on the cell types, because they have a variety of cellular targets. These mechanisms include changed gene expression and alterations of histone and also of non-histone proteins by epigenetic and post-translational modifications (10). The results found in several studies testing the efficiency of HDAC inhibitors alone or in a combination with chemotherapy and/or radiotherapy demonstrated that HDAC inhibitors can have additive and/or even synergistic effects when used with some cytotoxic reagents or ionizing radiation (11-14). Even though various molecular mechanisms were shown to be responsible for the observed higher sensitivity of tumor cells towards therapeutic agents elicited by HDAC inhibitors (reviewed in refs. 10,15-22), these mechanisms need to be further investigated.

In this study, we investigated the combined effects of two HDAC inhibitors, valproate (VPA) and trichostatin A (TSA), with two DNA-damaging drugs, cisplatin and etoposide, on a human high-risk neuroblastoma UKF-NB-4 cell line. Cytotoxicity of cisplatin is based on cisplatin-induced DNA adducts that include protein-DNA cross-links, DNA monoadducts, and interstrand or intrastrand cross-links (23), as well as on the generation of reactive oxygen species (ROS) in cells (24,25). Etoposide acts as a DNA intercalator and an inhibitor of topoisomerase II activity generating the single- and double-strand DNA breaks (26-28). VPA, an inhibitor of class I and IIA HDACs (29), is used as an anti-epileptic drug, but it also exhibits antitumor activity. TSA is a pan-HDAC inhibitor efficient in nanomolar concentrations (30,31) that induces cell cycle arrest and apoptosis in several cell lines, suggesting its potency to be used as an anticancer drug (32).

The combined effects of VPA and TSA with DNA-damaging drugs (cisplatin and etoposide) on UKF-NB-4 neuroblastoma cells were evaluated using the pro-apoptotic effects of these drugs and apoptosis-involved mechanisms underlying the anticancer activity of these drugs. In addition, we also examined the effects of the combination of the HDAC inhibitors with vicristine, the drug that is used to treat neuroblastomas (1), but acts via a different mechanism of anticancer action. The results found in this report suggest that integrating VPA into the DNA-damaging conventional chemotherapy of high-risk neuroblastoma may improve treatment efficacy.

Materials and methods

Cell cultures and chemicals. The UKF-NB-4 cell line, established from bone marrow metastases of recurrent high-risk neuroblastoma, was a gift of Professor J. Cinatl Jr (J.W. Goethe University, Frankfurt, Germany). Valproic acid sodium salt (VPA), valpromide (VPM), trichostatin A (TSA) and etoposide (ETO) were purchased from Sigma Chemical Co. (St. Louis, MO, USA). Vincristine (VCR) sulfate was from Teva Pharmaceuticals, Prague, Czech Republic and cisplatin was Platadiam 50 from PLIVA-Lachema, Brno, Czech Republic. All other chemicals used in experiments were of analytical purity or better. Cells were grown at 37˚C and 5% CO_2, cultivated in Iscove's modified Dulbecco's medium (IMDM) with 10% fetal bovine serum (both Life Technologies, Carlsbad, CA, USA). The cells were cultivated for at least 48 h with tested drugs, because this time period essentially corresponds to the time for two cycles of cell division. Moreover, such a time period is sufficient for the drugs used in this study to enter the tested cells, affect cell cycle and trigger apoptosis (17-20,33,34).

Annexin V/propidium iodide double staining assay. For detection of apoptosis, Annexin V-FITC Apoptosis Detection kit (Biovision, Milpitas, CA, USA) was used according to the manufacturer's instructions and samples were analyzed using flow cytometry (LSR II, BD, Franklin Lakes, CA, USA). Briefly, $0.8x10^6$ UKF-NB-4 cells were plated in 60-mm dishes and treated with individual drugs (VPA dissolved in an IMDM medium), TSA and VPM (dissolved in dimethyl sulfoxide, DMSO), water solution of cisplatin prepared according to the manufacturer's instructions (PLIVA-Lachema, Brno, Czech Republic), etoposide (dissolved in a small volume of DMSO; final volume of DMSO did not exceed 0.5%), vincristine sulfate (Teva Czech Industries, Prague, Czech Republic) or their combinations. After exposure to these compounds for 48 h, cells were washed with cold PBS, trypsinized and collected by centrifugation; cells were further re-suspended in 100 μl of Annexin binding buffer containing 5 μl of FITC Annexin V and 5 μl of PI. Then cells were gently vortexed and incubated for 20 min at room temperature in the dark. Binding buffer (400 μl) was added to each tube and centrifuged. Pellets of cells re-suspended in this buffer were then collected and measured using an LSR II flow cytometer (BD) and analyzed with FlowLogic software.

Detection of active caspase-3. To detect cells with active caspase-3, $0.8x10^6$ neuroblastoma UKF-NB-4 cells were plated in 60-mm dishes and treated with individual drugs or their combinations for 48 h. Percentage of active caspase-3-positive cells was detected using the CaspGLOW™ Flourescein Active Caspase-3 Staining kit (eBioscience, San Diego, CA, USA). The procedure used was as described in the manufacturer's instructions and samples were analyzed using flow cytometry (LSR II, BD, Franklin Lakes, CA, USA). Briefly, after exposure to the compounds, control or treated cells were washed with cold PBS, trypsinized and collected by centrifugation. Cell pellets were washed with PBS and after spinning re-suspended in 300 μl of a complete medium containing 1 μl of FITC labeled DEVD-FMK. Then the cells were incubated for 30 min at 37˚C and 5% CO_2. Cells were collected by spinning and pellet was washed with wash buffer (according to the manufacturer's instructions). Re-suspended washed cells were measured using the LSR II flow cytometer (BD, Franklin Lakes, CA, USA) and analyzed with FlowLogic software.

Real-time monitoring of cell viability. The xCELLigence RTCA DP Instrument (ACEA Bioscience Inc., San Diego, CA, USA) placed in a humidified incubator at 37˚C and 5% CO_2 was used for real-time label-free monitoring of cell-viability (37). UKF-NB-4 cell line (20,000 cells) were seeded into 16-well plates for impedance-based detection. Each condition (control, 1 mM VPA, 4 μM cisplatin and combination of 1 mM VPA with 4 μM cisplatin) was tested in duplicate. Cell index

(CI) was monitored every 30 min for 140 h and data recorded by the supplied RTCA software.

Estimation of contents of acetylated histones H3 and H4. To estimate an acetylation status of histones H3 and H4, $4x10^6$ cells were plated in 100-mm dishes and cultivated and treated with tested drugs. Namely, cells were treated with 1 mM VPA, 40 or 150 nM TSA, or 4 mM VPM for 8 h or with 20 μM cisplatin or 8 μM etoposide for 24 h. Cells were also treated with cisplatin and etoposide in a combination with 1 mM VPA in two different regimens: i) cells were incubated with cisplatin or etoposide for 24 h prior to incubation with VPA for 8 h and ii) cells were incubated with VPA for 8 h prior to incubation with cisplatin or etoposide for 24 h. Cells were harvested and histones were isolated from the cell pellets. The acid extraction followed by precipitation of histones using trichloracetic acid (TCA) method described by Shechter *et al* was used (35). The concentration of proteins was measured using a Lowry method (36) with DC Protein Assay (Bio-Rad, Hercules, CA, USA). Histones (5 μg) were electrophoretically separated using 4-20% TGX precast gels (100 mA). After migration, histones were transferred to a nitrocellulose membrane and incubated with 5% non-fat milk to block non-specific binding. The membranes were then exposed to specific rabbit polyclonal anti-acetyl-histone H3 (1:4,000) and anti-acetyl-histone H4 (1:1,000) antibodies (both from Upstate Biotechnology Inc., Lake Placid, NY, USA) overnight at 4˚C. Membranes were washed and exposed to peroxidase-conjugated anti-IgG secondary antibodies (1:2,000) and the antigen-antibody complex was visualized by enhanced chemiluminescence detection system according to the manufacturer's instructions (Immun-Star HRP Substrate, Bio-Rad), using X-ray film MEDIX XBU (Foma, Hradec Kralove, Czech Republic). The anti-histone H3 antibody (1:10,000; Millipore, San Diego, CA, USA) was used as a loading control.

Histone H2AX phosphorylation status. To determine phosphorylation of histone H2AX, $0.8x10^6$ cells were plated in 60-mm dishes and treated with individual drugs or their combinations. After exposure to the compounds, control or treated cells were washed with cold PBS, trypsinized and collected by centrifugation. Cell pellets were washed with PBS and after spinning the cells were fixed in 2% formaldehyde in PBS for 10 min. After PBS washing, the cells were re-suspended in ice-cold 90% methanol in PBS and incubated for 60 min at -20˚C. Then the cells were washed three times with wash buffer (PBS containing 0.5% BSA and 0.2% Triton X-100). Cells were incubated in 50 μl of wash buffer containing 5 μl of pH2AX antibody [Alexa Fluor® 647 anti-H2A.X-Phosphorylated (Ser139), Biolegend, San Diego, CA, USA] for 60 min at 4˚C. Cells were washed and measured using the LSR II (BD, Franklin Lakes, CA, USA) and analyzed with FlowLogic software.

Statistical analysis. Data are expressed as mean ± SD. Student's t-test was used when comparing two conditions. P-value <0.05 was considered as statistically significant. GraphPad Prism6 software was used for this statistical and graphical processing of data. Two-one-sided-test (TOST) was used to test equivalence, XLSTAT software was used.

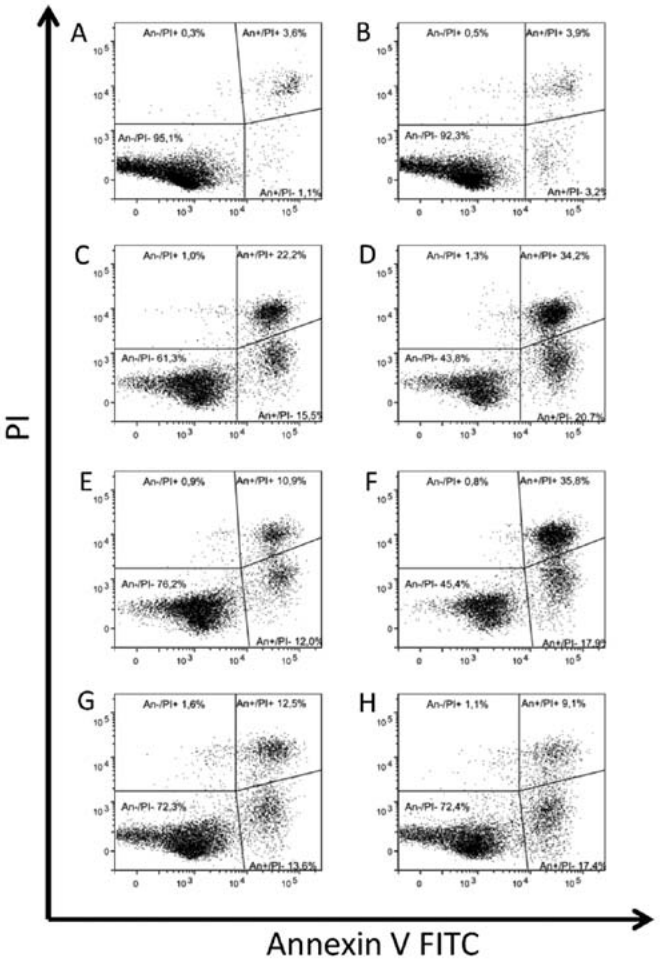

Figure 1. Apoptosis induction in UKF-NB-4 cells by 1 mM VPA (B), 20 μM cisplatin (C), 8 μM etoposide (E), 20 nM vincristine (G) and their combination with 1 mM VPA [(D) VPA + cisplatin, (F) VPA + etoposide, (H) VPA + vincristine)]. (A) Control cells incubated in a medium without drugs. Apoptosis was measured using Annexin V-FITC/PI labeling. Figure shows representative data from one of three independent experiments.

Results

VPA synergizes cytotoxicity of cisplatin on UKF-NB-4 human neuroblastoma cells. The first step of this study was to examine the apoptosis induced in UKF-NB-4 cells treated with individual drugs. As translocation of phosphatidylserine to the external membrane leaflet is one of the earliest features of apoptosis, early apoptotic cells can thus be identified by the Annexin V-FITC/PI double staining assay. Besides, double staining with PI allows differentiation of early apoptotic cells with intact membranes (Annexin V^+/PI^-) from late apoptotic/necrotic cells with leaky membranes (Annexin V^+/PI^+) and normal cells (Annexin V^-/PI^-). As a result, the different groups of these stained cells can be distinguished and quantified by flow cytometry.

As shown in Fig. 1, treatment of UKF-NB-4 neuroblastoma cells with a non-toxic concentration of VPA, 1 mM VPA, for 48 h does not induce apoptosis in these cells (the amount of Annexin V^-/PI^- cells is almost the same as in the control sample, Fig. 1A and B). However, their treatment with cisplatin alone and mainly with this drug simultaneously with

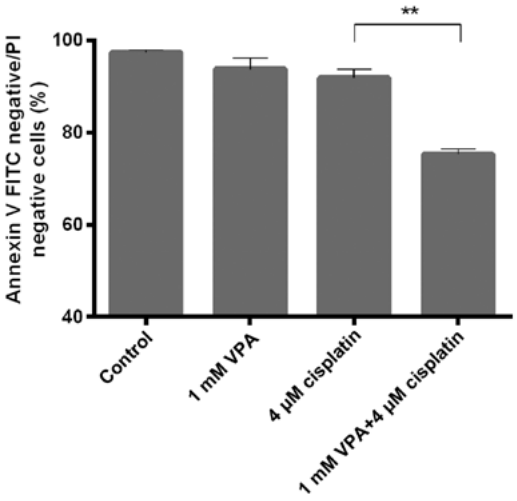

Figure 2. Apoptosis induction in UKF-NB-4 cells by 1 mM VPA, 4 μM cisplatin and their combination. Apoptosis was measured using Annexin V-FITC/PI labeling. Mean and SD from three independent experiments is shown. **P<0.01, a significant difference between cells treated with cisplatin combined with VPA and cisplatin alone (Student's t-test) (n=3).

VPA resulted in induction of apoptosis (Figs. 1C and D and 2). The Annexin V-FITC/PI double staining assay showed that treatment of UKF-NB-4 cells with 20 μM cisplatin for 48 h, decreased the percentage of viable cells to 61.3% (shown in a lower-left panel in Fig. 1C) with a concomitant increase in percentage of early apoptotic cells to 15.5% (shown in a lower-right panel in Fig. 1C), and late apoptotic cells to 22.2% (shown in an upper-right panel in Fig. 1C). These results confirmed that cisplatin plays a critical role in triggering apoptotic cell death in cisplatin-treated UKF-NB-4 cells.

When cells were co-treated with cisplatin and VPA, a higher decrease in the percentage of viable cells than by treatment of cells with cisplatin alone was produced, ≤43.8% (Fig. 1D). This decrease was concomitant with an increase in amounts of early apoptotic cells, to 20.7% and mainly late apoptotic cells, to 34.2% (Fig. 1D). These data indicate that VPA elevates a potency of DNA-damaging agent cisplatin to induce apoptosis in UKF-NB-4 cells. Similar trend in induction of apoptosis in UKF-NB-4 cells was also seen after their treatment with 4 μM cisplatin (the dose exhibiting a low toxicity to the tested cells, Fig. 2) and by this drug combined with VPA (Fig. 2 for a decrease in the percentage of viable UKF-NB-4 cells caused by cell treatment with cisplatin and VPA).

Caspases, a family of cysteine-aspartic proteases, are known to be crucial mediators in the apoptotic-signaling pathways (38). Since caspase-3 is the major executioner caspase essential for activation of one of the primary apoptotic signaling pathways (39) and its activation ultimately leads to cell death (40), it is thus suited as a read-out in an apoptosis assay. Therefore, in further experiments we evaluated whether apoptosis induced by the above-mentioned treatment regimens is associated with changes in caspase-3 activation. A trend similar to that found using Annexin V, the induction of apoptosis caused by a combined effect of VPA and cisplatin was detected by measuring the percentage of cells with active caspase-3 (Fig. 3). Exposure of UKF-NB-4 cells to 1 mM VPA simultaneously with 4 or 20 μM

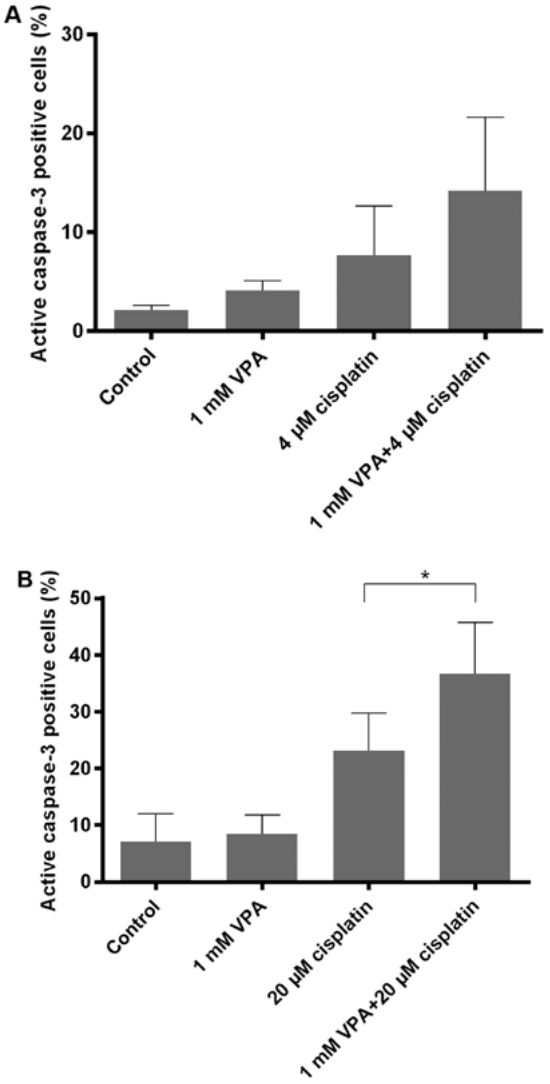

Figure 3. The percentage of UKF-NB-4 cells with active caspase-3 when treated with 1 mM VPA, 4 (A) and 20 μM cisplatin (B) and their combination for 48 h. Mean and SD from three independent experiments is shown. *P<0.05, a significant increase in percentage of cells with active caspase-3 treated with cisplatin combined with VPA, as compared to cells treated with cisplatin alone (Student's t-test) (n=3).

cisplatin increased levels of cells with active caspase-3, by up to 2-times as compared with cells treated with cisplatin alone. These results indicate that apoptosis induced in the UKF-NB-4 neuroblastoma cell line by cisplatin was triggered by the activation of caspase-3 that is potentiated by co-treatment of the tested cell line with VPA.

An increase in a cytotoxic potency of 4 μM cisplatin by 1 mM VPA was also proved by analyzing cell growth with the xCELLigence system (Fig. 4). In this method the relative changes in electrical impedance (expressed as cell index) due to coverage of bottom well by cells, corresponds to cell viability (41). As shown in Fig. 4, the tested cells cultivated with VPA grow slowly up till ~ 90 h of cultivation, while their cell index was not increaed after this time period. UKF-NB-4 cells treated with cisplatin grow exponentially till 50 h of cultivation, but after this time period, cisplatin caused a decrease in their viability. However, after >100 h of cultivation, these cells incubated with 4 μM cisplatin started to grow

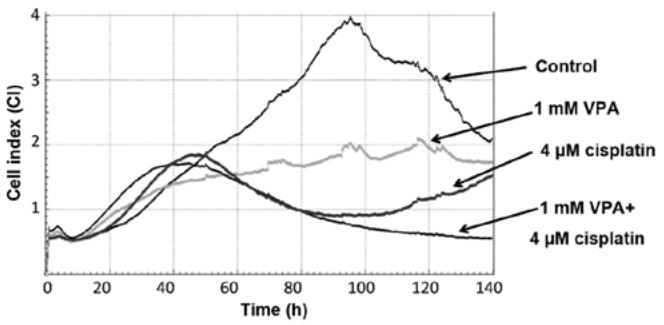

Figure 4. Viability of neuroblastoma UKF-NB-4 cells treated with 1 mM VPA, 4 μM cisplatin, or with both drugs. Viability was measured by the xCELLigence system for real-time label-free monitoring of cells and expressed as cell index. Representative data from one of three independent experiments are shown.

again (Fig. 4). Hence, treatment of cells with 4 μM cisplatin alone is not sufficient to inhibit cell growth totally; after 90-h treatment, a portion of viable cells were able to grow during further cultivation. The most efficient cytotoxic effect on UKF-NB-4 cells was produced by their co-cultivation with VPA and cisplatin; when this combination was used, the value of cell index decreased close to zero (Fig. 4).

Computation analysis of cell survival calculated by Compusyn software (42,43) was used to estimate whether activities of these two drugs are synergistic. Namely, we calculated the value of the combined effect of VPA and cisplatin and expressed it as combination index (CoI). When the values of CoI are <0.90, activities of two drugs are synergistic (the combination index ranging from 0.70 to 0.89 corresponds to a moderate synergism of drugs). However, the values of ≥0.9 indicate that the activities of two drugs are not synergistic (42,43). The value of CoI for the simultaneous effect of 4 μM cisplatin and 1 mM VPA equals 0.70, which corresponds to a moderate synergism of this combination.

Because the effect of the combination of cytostatic drugs with HDAC inhibitors may depend on the treatment regimens, causing either an increase or decrease in cytotoxic effects (17,20,44), we also examined various treatment regimens for a combination of the tested drugs with HDAC inhibitors.

In further experiments, several combinations of treating the UKF-NB-4 cells with VPA and cisplatin were used (Table I). The apoptosis induction in cells cultivated under these treatment regimens is shown in Fig. 5. The most effective drug combination resulting in a decrease in viability of neuroblastoma cells was their exposure to cisplatin and VPA (the cells treated with 20 μM cisplatin for 24 h and then with 1 mM VPA for 48 h) (see a combination cisplatin/VPA in Fig. 5). On the contrary, the opposite sequence of drug application (VPA/cisplatin) led to essentially no changes in viability of cells as compared with cultivation of cells with cisplatin alone (see VPA/cisplatin versus 0/cisplatin regimens in Fig. 5). These results demonstrate that VPA can potentiate the toxic effects of cisplatin only if UKF-NB-4 cells are primarily affected by this DNA-damaging drug.

In contrast to VPA, no effects of TSA, another HDAC inhibitor tested in our study, at a non-toxic concentration for UKF-NB-4 (40 nM), on cytotoxicity of cisplatin to UKF-NB-4 cells was found using Annexin V-FITC/PI double staining assay or active caspase-3 assay (data not shown).

Table I. Combination regimens used for treatment of UKF-NB-4 cells with VPA and cisplatin.[a]

Designation	0-24 h	24-72 h
Control	Medium	Fresh medium
Cisplatin/cisplatin	20 μM cisplatin	20 μM cisplatin
0/cisplatin	Medium	1 mM valproate
Cisplatin/0	20 μM cisplatin	Fresh medium
Cisplatin/VPA	20 μM cisplatin	1 mM valproate
VPA/0	1 mM valproate	Fresh medium
0/cisplatin	Medium	20 μM cisplatin
VPA/cisplatin	1 mM valproate	20 μM cisplatin

[a]0 indicates medium cultivation without any drug added.

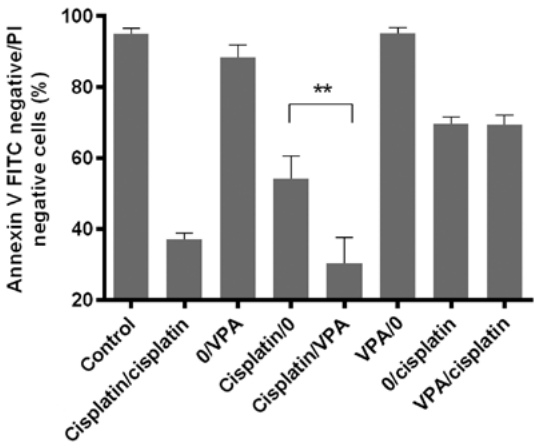

Figure 5. Apoptosis induction in UKF-NB-4 cells by 1 mM VPA, 4 μM cisplatin and their various combinations. Control, cells treated with a medium without any drug. Experimental conditions for combined treatment of cells are described in Table I. Mean and SD from three independent experiments is shown. **P<0.01, a significant decrease in viable cells caused by their pretreatment with cisplatin before incubation with VPA as compared to the cells incubated with cisplatin alone (Student's t-test) (n=3).

VPA synergizes cytotoxicity of etoposide on UKF-NB-4 human neuroblastoma cells. The effect of combined treatment of UKF-NB-4 neuroblastoma cells with VPA and etoposide was also investigated. Treatment of these cells with 8 μM etoposide, and predominantly with this drug together with 1 mM VPA, resulted in induction of apoptosis (Fig. 1E and F). Treatment of UKF-NB-4 cells with etoposide for 48 h induced a decrease in the percentage of viable cells to 76.2% (shown in a lower-left panel in Fig. 1E) with a concomitant increase in percentage of early apoptotic cells, to 12.0% (shown in a lower-right, panel in Fig. 1E) and late apoptotic cells, to 10.9% (shown in an upper-right panel in Fig. 1). These findings confirmed the results found in our previous study (20) that etoposide induces apoptotic cell death in UKF-NB-4 cells.

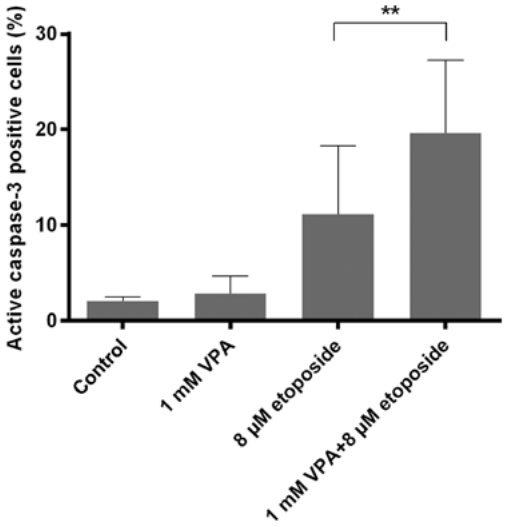

Figure 6. The percentage of UKF-NB-4 cells with active caspase-3 when treated with 1 mM VPA, 8 μM etoposide or their combination for 48 h. Mean and SD from three independent experiments is shown. **P<0.01, a significant increase in percentage of cells with active caspase-3 treated with etoposide combined with VPA, as compared to cells incubated with etoposide alone (Student's t-test) (n=3).

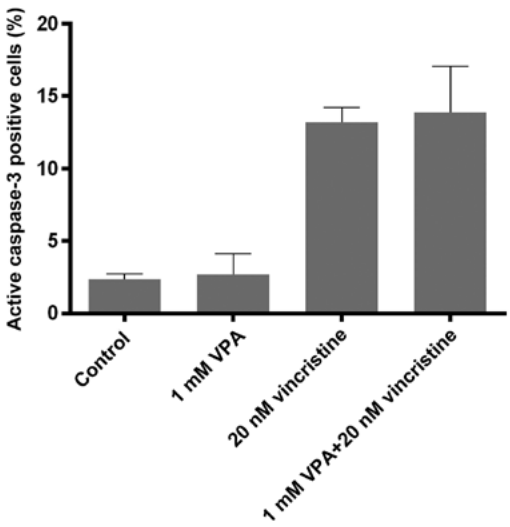

Figure 7. The percentage of UKF-NB-4 cells with active caspase-3 when treated with 1 mM VPA, 20 nM vincristine and their combination for 48 h. Mean and SD from three independent experiments is shown.

Analogously to exposure of the tested neuroblastoma cells to cisplatin combined with VPA, a 1.7-fold decrease in cell viability (expressed as percentage of Annexin V^-/PI^- cells) was generated in these cells by their exposure to VPA combined with etoposide as compared to their exposure to etoposide alone (Fig. 1E and F). This decrease was parallel with an increase in amounts of early apoptotic cells, to 17.9%, and predominantly late apoptotic cells, to 35.8% (Fig. 1F). These data indicate that VPA also elevates the potency of the second tested DNA-damaging drug, etoposide, to induce apoptosis in UKF-NB-4 cells.

Using another method testing the effect of combined treatment of UKF-NB-4 cells, measuring the activation of caspase-3, an increase in the etoposide effect by VPA was also found. Exposure of UKF-NB-4 cells to VPA simultaneously with etoposide increased an amount of cells with the active caspase-3, by ≤1.7-times (Fig. 6). All these results indicate the enhanced effect of the combination of these drugs on induction of apoptosis mediated by caspase-3 activation.

Because several schedules of combined treatment (treatment regimens) of the UKF-NB-4 neuroblastoma cell line with VPA and etoposide have already been carried out in our previous study (20), such experiments were not performed in this study. It should be emphasized that the most effective treatment leading to the highest decrease in viability of neuroblastoma cells was the combined exposure of cells to etoposide followed by their treatment with VPA (cells treated with 8 μM etoposide for 24 h and then with 1 mM VPA for 48 h) (20). Hence, the regimen analogous to that found to be most efficient in treatment of cells with cisplatin combined with VPA. These results demonstrate that VPA can exhibit the potentiation effect only if UKF-NB-4 neuroblastoma cells are primarily influenced either by cisplatin or by etoposide.

Computation analysis (42,43) was again used to estimate whether activities of VPA with etoposide are synergistic. The value of CoI for the simultaneous effect of 8 μM etoposide and 1 mM VPA equals 0.52 that corresponds to a synergism of these drugs.

When TSA at its non-toxic concentration (40 nM) was used, cytotoxicity of etoposide to UKF-NB-4 cells was essentially not influenced by this HDAC inhibitor (data not shown).

VPA does not potentiate cytotoxicity of a mitotic inhibitor vincristine on UKF-NB-4 human neuroblastoma cells. In further experiments, the influence of VPA and TSA on cytotoxicity of vincristine, the anticancer drug acting by a mechanism different from that of DNA damage, was investigated. Vincristine is known to induce cell death in tumor cells including neuroblastoma cells by inhibiting the assembly of microtubule structures and disrupting mitosis in the metaphase (45,46).

As shown in Fig. 1, treatment of UKF-NB-4 neuroblastoma cells with 20 nM vincristine led to induction of apoptosis in these cells. The Annexin V-FITC/PI double staining assay indicated that treatment of UKF-NB-4 cells with vincristine for 48 h induced a decrease in the percentage of viable cells to 72.3% (shown in a lower-left panel in Fig. 1G), with a concomitant increase in percentage of early apoptotic cells to 13.6% (shown in a lower-right panel in Fig. 1G), and late apoptotic cells to 12.5% (shown in an upper-right panel in Fig. 1G). These results confirmed that vincristine is an important drug inducing apoptotic cell death in vincristine-treated UKF-NB-4 cells. However, when the cells were exposed to vincristine combined with VPA, no further changes in cell viability as compared to UKF-NB-4 cells treated with vincristine were found (Fig. 1H). Likewise, in the case of measuring the activation of caspase-3 in the tested cells treated with vincristine simultaneously with VPA, no increase in a toxic potency of vincristine was found (Fig. 7). These findings demonstrate that the sensitizing effect of VPA on the tested cells is produced only when they are affected by the DNA-damaging drugs (cisplatin and etoposide) before their treatment with this HDAC inhibitor. When TSA at a 40 nM concentration was used, cytotoxicity of vincristine to UKF-NB-4 cells was also not influenced by this HDAC inhibitor (data not shown).

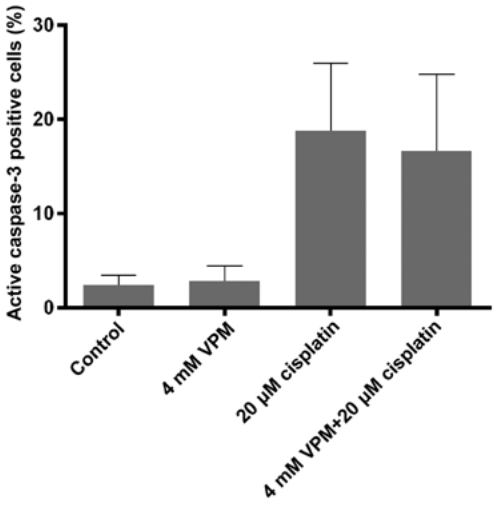

Figure 8. The percentage of UKF-NB-4 cells with active caspase-3 when treated with 4 mM VPM, 20 μM cisplatin and their combination for 48 h. Mean and SD from three independent experiments is shown.

Treatment of UKF-NB-4 human neuroblastoma cells with valpromide has no effect on cisplatin cytotoxicity. In additional experiments, we investigated cytotoxicity of valpromide (VPM), a derivative of VPA which is also used as an antiepileptic drug, but does not exhibit HDAC inhibition activity (47), on UKF-NB-4 neuroblastoma cells. We evaluated the effect of this drug on induction of apoptosis (measured by Annexin V/PI labeling) in these cells. Treatment of UKF-NB-4 neuroblastoma cells with different concentrations of VPM up to concentrations of 4 mM did not induce apoptosis in these cells (data not shown). When UKF-NB-4 cells were treated with this non-toxic concentration of VPM simultaneously with 20 μM cisplatin, no increase in induction of apoptosis caused by cisplatin was produced by VPM (data not shown).

When activation of caspase-3 in cells treated with VPM together with cisplatin was determined, no increase in the potency of cisplatin to activate caspase-3 by VPM was found (Fig. 8). Exposure of UKF-NB-4 cells to 20 μM cisplatin combined with simultaneous treatment with 4 mM VPM does not increase amounts of cells with active caspase-3. These results indicate that the sensitizing effect of VPA on cisplatin toxicity in UKF-NB-4 neuroblastoma cells is related to its HDAC inhibition activity.

Acetylation status of histones H3 and H4 in UKF-NB-4 cells treated with VPA, VPM, TSA, cisplatin, etoposide, and cisplatin and etoposide combined with VPA. Acetylation of histones is an important epigenetic phenomenon that is dictated by HDAC activities. Therefore, here we investigated the changes in acetylation of core histones H3 and H4 in UKF-NB-4 cells treated with VPA and TSA, as well as with VPM. Cultivation of UKF-NB-4 cells with VPA and TSA at their non-toxic concentrations led to the different effects on acetylation of histones H3 and H4. Whereas 1 mM VPA increases acetylation of these histones in UKF-NB-4 cells, confirming its HDAC inhibitory efficiency, a negligible effect of 40 or 50 nM TSA on acetylation of these histones was found (Fig. 9). The concentrations of TSA of 40 or 50 nM are

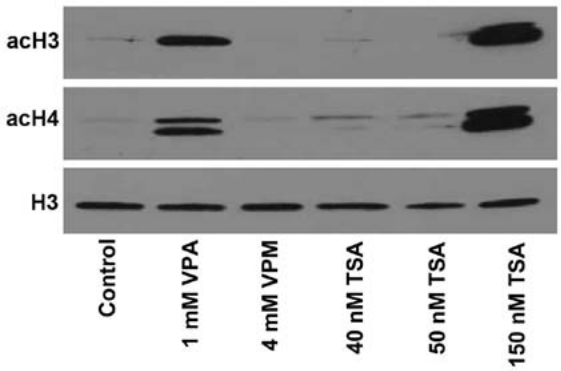

Figure 9. Western blot analysis of acetylated histones H3 and H4 in extracts from cells treated with 1 mM VPA, 4 mM VPM, 40, 50 and 150 nM TSA for 8 h (H3 was used as loading control).

therefore insufficient to inhibit HDAC activities in UKF-NB-4 cells. However, when these cells were cultivated in a medium containing a higher (toxic) concentration of TSA (150 nM), a pronounced increase in acetylation of histones H3 and H4 was detected. In contrast to these results, no increase in acetylation of these histones was caused by VPM (Fig. 9). This confirms the absence of HDAC inhibitory effects of this derivative of VPA.

When UKF-NB-4 neuroblastoma cells were treated with cisplatin or etoposide, a low decrease in acetylation of histone H3 and essentially no effect on acetylation of histone H4 were found (Fig. 10). In further experiments, two combination treatment regimens of the cells with VPA and cisplatin or VPA with etoposide were used to investigate the effects of combined treatment on the histones H3 and H4 acetylation status. Only the regimen, where UKF-NB-4 cells were pretreated with cisplatin or etoposide and then treated with VPA produced an increase in acetylation of histones H3 and H4 (Fig. 10). This increase in histone acetylation paralleled the potentiation of toxic effects of cisplatin (Fig. 5) or etoposide (20). Hence, only if UKF-NB-4 cells were primarily affected by the tested DNA-damaging drugs prior to cultivation with VPA, this HDAC inhibitor increases acetylation of histones (Fig. 10) and potentiated cytotoxicity of both DNA-damaging drugs on UKF-NB-4 cells (Fig. 1).

VPA does not influence etoposide-mediated phosphorylation of histone H2AX. Etoposide is known to be the DNA-damaging drug that acts, beside its intercalation into DNA, as an inhibitor of topoisomerase II activity that leads to formation of double-strand breaks in DNA (26-28). Therefore, we examined the effect of VPA on this mechanism of etoposide-mediated cytotoxic action. Phosphorylation of histone H2A on serine 139, termed γH2AX (pH2AX), by kinases sensing the double-strand DNA break is a sensitive marker of this type of DNA damage (48-51). Therefore, the levels of pH2AX were determined to analyze whether treatment of cells with etoposide is influenced by VPA. After 48-h cultivation of cells in a medium containing 1 mM VPA, 4 μM etoposide or their combination, the levels of pH2AX were examined by flow cytometry. Representative histograms of pH2AX fluorescence found in these experiments are shown in Fig. 11.

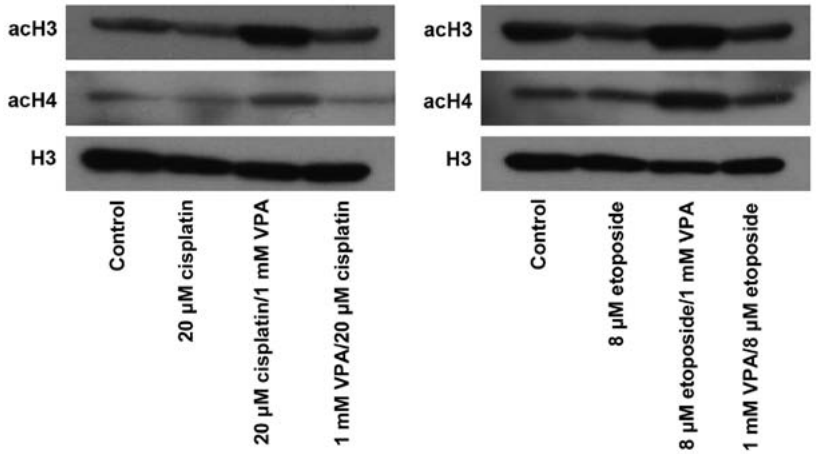

Figure 10. Levels of acetylated histones H3 and H4 in extracts from cells treated with 20 μM cisplatin and 8 μM etoposide, and these drugs combined with 1 mM VPA under different regimens, analyzed by western blotting (H3 was used as loading control).

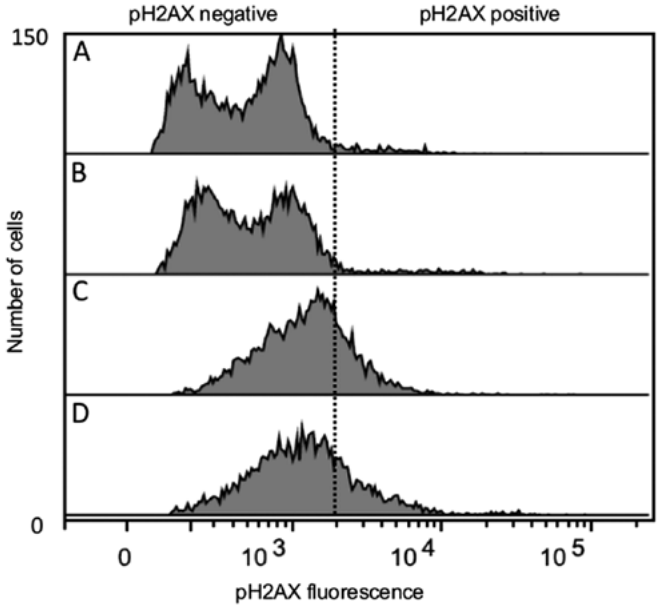

Figure 11. The effects of 1 mM VPA (B), 4 μM etoposide (C) or their combination (D) on generation of pH2AX in UKF-NB-4 cells treated with these drugs for 48 h. (A) Control cells that were incubated without any drug. Representative histogram of pH2AX fluorescence as a marker of double strand breaks is shown.

Whereas essentially no increase in pH2AX was induced by VPA (Fig. 11B), a pronounced enhancement in pH2AX was caused by cell exposure to etoposide (Fig. 11C). Co-cultivation of UKF-NB-4 cells with etoposide and VPA (Fig. 11D) did not change percentage of pH2AX-positive cells as compared with cultivation of UKF-NB-4 cell with etoposide alone (Fig. 11C and D).

Discussion

The poor response of high-risk neuroblastomas to current treatment regimens suggests that novel therapeutic strategies should be developed. The inhibitors of HDACs, used either individually or in the combination with other drugs, were found to be promising anticancer regimens efficient against several cancer cells including neuroblastomas (reviewed in refs. 10,15,17-21).

The results found in this study demonstrate that VPA used at the clinically relevant dose (1 mM) has potentiating effect on cytotoxicity and caspase-3-mediated induction of apoptosis caused by the tested DNA-damaging drugs cisplatin and etoposide. Analyzing the combination index, VPA combined with cisplatin or etoposide was found to act synergistically. However, no sensitizing effect due to VPA was produced with the mitotic inhibitor vincristine. These results indicate that HDAC inhibitor-mediated capability of increasing cytotoxic efficiency of anticancer drugs is connected with the drugs that target cellular DNA. These findings correspond to the results found in the study of dos Santos *et al* (52) that also investigated the effect of a combination of etoposide or vincristine with the HDAC inhibitor (sodium butyrate, an HDAC inhibitor of the same group as VPA) on human lymphoblastic T-cells. The authors demonstrated that from these two drugs, only etoposide, but not vincristine, was sensitized by the used HDAC inhibitor (52). In their study, the sensitizing effect of the HDAC inhibitor on doxorubicin, another DNA-damaging drug, was also proved (52).

The mechanisms of the potentiating effects of HDAC inhibitors on the efficiency of DNA-damaging drugs have not yet been fully elucidated. It was suggested that HDAC inhibitors promote increased lysine acetylation in nucleosomal histones and are thought to relax chromatin, thereby allowing increased access of transcription factors and DNA-damaging agents to DNA (reviewed in refs. 10,15). In our study, the increased toxicity of cisplatin and etoposide was indeed dependent on the acetylation status of core histones H3 and H4 dictated by HDAC inhibitors. VPA increased amounts of acetylated histones H3 and H4 and the elevated levels of these acetylated histones correlated with sensitization of UKF-NB-4 cells to cisplatin and etoposide. TSA, another HDAC inhibitor, at a concentration that essentially did not influence acetylation of these histones (40 nM), was ineffective. Likewise, VPM, a structural analogue of VPA, which however does not increase acetylation of histones

H3 and H4 (Fig. 9), did not enhance cytotoxicity of the tested DNA-damaging drugs (Fig. 8).

It should be, however, emphasized that a sequence of drug application is the crucial feature for sensitizing neuroblastoma cells to cisplatin and etoposide by VPA and the degree of acetylation of histones H3 and H4. Namely, this HDAC inhibitor potentiated the cytotoxic effect of cisplatin or etoposide and acetylation of histones only when added simultaneously, or when cells were preincubated with cisplatin or etoposide before their cultivation with VPA. Only these regimens were appropriate to suppress viability of neuroblastoma cells and to increase acetylation of histones. In contrast, the reversed sequence (pretreatment of cells with VPA before treatment with cisplatin or etoposide) did not give any further increase in cytotoxicity of the DNA-damaging drugs and acetylation of histones. All these findings suggest that DNA damage is crucial for the additional effects of VPA, arguing against the hypothesis based on relaxed chromatin that increases accessibility of DNA-damaging drugs to DNA (10,15). Similarly, the results found by Luchenko *et al* (44) indicated that DNA relaxation is not required for the synergy of two HDAC inhibitors they tested, belinostat and romidepsin, with cisplatin and etoposide. One can speculate that the changes in the structure of DNA caused by cisplatin and etoposide [i.e., formation of DNA adducts or DNA cross-links by cisplatin, intercalation of etoposide into DNA, and/or formation of reactive oxygen species by both drugs (44,53-56)] increase accessibility of nucleosomal core histones to their acetylation, which additionally determines transcription of some genes involved in DNA repair or apoptosis. This suggestion needs, however, to be further investigated.

Despite the observed synergy of the combination where UKF-NB-4 cells were initially treated with etoposide before VPA in cell survival and apoptosis (20), we found no evidence for enhancement of etoposide-mediated H2AX phosphorylation when etoposide was combined with VPA (Fig. 11). Double-strand DNA breaks markedly increased in UKF-NB-4 cells treated with etoposide, but after simultaneous treatment of these cells with etoposide and VPA no further increase in the pH2AX foci formation was detected. Therefore, instead of inhibition of topoisomerase-II activity by etoposide, leading to formation of double-strand-breaks in DNA, the changes in the structure of DNA mediated by intercalation of etoposide into DNA seem to be responsible for the results found in UKF-NB-4 cells.

One of the challenges in conducting a clinical trial when combining an inhibitor of HDACs VPA with DNA damaging agents will be to achieve optimal DNA damage in a given tumor tissue. The results found in the present study demonstrate that treatment of cells with VPA potentiates the cytotoxicity of DNA damaging agents, cisplatin and etoposide, on UKF-NB-4 cells without increasing their access to DNA. The data presented here show that treatment with cisplatin or etoposide prior to addition of VPA is superior to alternative schedules and supports the development of clinical trials using these combinations for neuroblastoma cells. The clinical use of such combined treatment utilizing DNA-damaging drugs with this HDAC inhibitor could reduce frequent problems, such as dose reductions and temporary discontinuation of treatment as a result of toxicity, and thus could improve the treatment itself and the patient's quality of life.

Acknowledgements

This study was supported by the GACR (grant 14-8344S), the Charles University in Prague (grants GAUK 635712/2012, GAUK 620612/2012, UNCE 204025/2012) and by MH CZ-DRO, University Hospital Motol, Prague, Czech Republic 00064203.

References

1. Brodeur GM: Neuroblastoma: Biological insights into a clinical enigma. Nat Rev Cancer 3: 203-216, 2003.
2. Schwab M, Westermann F, Hero B and Berthold F: Neuroblastoma: Biology and molecular and chromosomal pathology. Lancet Oncol 4: 472-480, 2003.
3. Maris JM, Hogarty MD, Bagatell R and Cohn SL: Neuroblastoma. Lancet 369: 2106-2120, 2007.
4. Furchert SE, Lanvers-Kaminsky C, Juürgens H, Jung M, Loidl A and Frühwald MC: Inhibitors of histone deacetylases as potential therapeutic tools for high-risk embryonal tumors of the nervous system of childhood. Int J Cancer 120: 1787-1794, 2007.
5. Decock A, Ongenaert M, Vandesompele J and Speleman F: Neuroblastoma epigenetics: From candidate gene approaches to genome-wide screenings. Epigenetics 6: 962-970, 2011.
6. Santini V, Gozzini A and Ferrari G: Histone deacetylase inhibitors: Molecular and biological activity as a premise to clinical application. Curr Drug Metab 8: 383-393, 2007.
7. Portela A and Esteller M: Epigenetic modifications and human disease. Nat Biotechnol 28: 1057-1068, 2010.
8. Kouzarides T: Chromatin modifications and their function. Cell 128: 693-705, 2007.
9. Glozak MA, Sengupta N, Zhang X and Seto E: Acetylation and deacetylation of non-histone proteins. Gene 363: 15-23, 2005.
10. Stiborová M, Eckschlager T, Poljaková J, Hraběta J, Adam V, Kizek R and Frei E: The synergistic effects of DNA-targeted chemotherapeutics and histone deacetylase inhibitors as therapeutic strategies for cancer treatment. Curr Med Chem 19: 4218-4238, 2012.
11. Atmaca A, Al-Batran SE, Maurer A, Neumann A, Heinzel T, Hentsch B, Schwarz SE, Hövelmann S, Göttlicher M, Knuth A, *et al*: Valproic acid (VPA) in patients with refractory advanced cancer: a dose escalating phase I clinical trial. Br J Cancer 97: 177-182, 2007.
12. Munster P, Marchion D, Bicaku E, Lacevic M, Kim J, Centeno B, Daud A, Neuger A, Minton S and Sullivan D: Clinical and biological effects of valproic acid as a histone deacetylase inhibitor on tumor and surrogate tissues: Phase I/II trial of valproic acid and epirubicin/FEC. Clin Cancer Res 15: 2488-2496, 2009.
13. Rocca A, Minucci S, Tosti G, Croci D, Contegno F, Ballarini M, Nolè F, Munzone E, Salmaggi A, Goldhirsch A, *et al*: A phase I-II study of the histone deacetylase inhibitor valproic acid plus chemoimmunotherapy in patients with advanced melanoma. Br J Cancer 100: 28-36, 2009.
14. Vandermeers F, Hubert P, Delvenne P, Mascaux C, Grigoriu B, Burny A, Scherpereel A and Willems L: Valproate, in combination with pemetrexed and cisplatin, provides additional efficacy to the treatment of malignant mesothelioma. Clin Cancer Res 15: 2818-2828, 2009.
15. Kim MS, Blake M, Baek JH, Kohlhagen G, Pommier Y and Carrier F: Inhibition of histone deacetylase increases cytotoxicity to anticancer drugs targeting DNA. Cancer Res 63: 7291-7300, 2003.
16. Munshi A, Kurland JF, Nishikawa T, Tanaka T, Hobbs ML, Tucker SL, Ismail S, Stevens C and Meyn RE: Histone deacetylase inhibitors radiosensitize human melanoma cells by suppressing DNA repair activity. Clin Cancer Res 11: 4912-4922, 2005.
17. Das CM, Zage PE, Taylor P, Aguilera D, Wolff JE, Lee D and Gopalakrishnan V: Chromatin remodelling at the topoisomerase II-beta promoter is associated with enhanced sensitivity to etoposide in human neuroblastoma cell lines. Eur J Cancer 46: 2771-2780, 2010.
18. Poljakova J, Hrebackova J, Dvorakova M, Moserova M, Eckschlager T, Hrabeta J, Göttlicherova M, Kopejtkova B, Frei E, Kizek R, *et al*: Anticancer agent ellipticine combined with histone deacetylase inhibitors, valproic acid and trichostatin A, is an effective DNA damage strategy in human neuroblastoma. Neuro Endocrinol Lett 32 (Suppl 1): 101-116, 2011.

19. Cipro Š, Hřebačková J, Hraběta J, Poljaková J and Eckschlager T: Valproic acid overcomes hypoxia-induced resistance to apoptosis. Oncol Rep 27: 1219-1226, 2012.
20. Groh T, Hrabeta J, Poljakova J, Eckschlager T and Stiborova M: Impact of histone deacetylase inhibitor valproic acid on the anticancer effect of etoposide on neuroblastoma cells. Neuro Endocrinol Lett 33 (Suppl 3): S16-S24, 2012.
21. Wang G, Edwards H, Caldwell JT, Buck SA, Qing WY, Taub JW, Ge Y and Wang Z: Panobinostat synergistically enhances the cytotoxic effects of cisplatin, doxorubicin or etoposide on high-risk neuroblastoma cells. PLoS One 8: e76662, 2013.
22. Hrabeta J, Stiborova M, Adam V, Kizek R and Eckschlager T: Histone deacetylase inhibitors in cancer therapy. A review. Biomed Pap Med Fac Univ Palacky Olomouc Czech Repub 158: 161-169, 2014.
23. Kartalou M and Essigmann JM: Mechanisms of resistance to cisplatin. Mutat Res 478: 23-43, 2001.
24. Miyajima A, Nakashima J, Yoshioka K, Tachibana M, Tazaki H and Murai M: Role of reactive oxygen species in cis-dichlorodiammineplatinum-induced cytotoxicity on bladder cancer cells. Br J Cancer 76: 206-210, 1997.
25. Huang H-L, Fang L-W, Lu S-P, Chou C-K, Luh T-Y and Lai M-Z: DNA-damaging reagents induce apoptosis through reactive oxygen species-dependent Fas aggregation. Oncogene 22: 8168-8177, 2003.
26. Wozniak AJ and Ross WE: DNA damage as a basis for 4'-demethylepipodophyllotoxin-9-(4,6-O-ethylidene-beta-D-glucopyranoside) (etoposide) cytotoxicity. Cancer Res 43: 120-124, 1983.
27. Hande KR: Etoposide: Four decades of development of a topoisomerase II inhibitor. Eur J Cancer 34: 1514-1521, 1998.
28. Baldwin EL and Osheroff N: Etoposide, topoisomerase II and cancer. Curr Med Chem Anticancer Agents 5: 363-372, 2005.
29. New M, Olzscha H and La Thangue NB: HDAC inhibitor-based therapies: Can we interpret the code? Mol Oncol 6: 637-656, 2012.
30. Yoshida M, Kijima M, Akita M and Beppu T: Potent and specific inhibition of mammalian histone deacetylase both in vivo and in vitro by trichostatin A. J Biol Chem 265: 17174-17179, 1990.
31. Yoon CY, Park MJ, Lee JS, Lee SC, Oh JJ, Park H, Chung CW, Abdullajanov MM, Jeong SJ, Hong SK, *et al*: The histone deacetylase inhibitor trichostatin A synergistically resensitizes a cisplatin resistant human bladder cancer cell line. J Urol 185: 1102-1111, 2011.
32. Meng J, Zhang H-H, Zhou C-X, Li C, Zhang F and Mei Q-B: The histone deacetylase inhibitor trichostatin A induces cell cycle arrest and apoptosis in colorectal cancer cells via p53-dependent and -independent pathways. Oncol Rep 28: 384-388, 2012.
33. Poljaková J, Eckschlager T, Hraběta J, Hrebacková J, Smutný S, Frei E, Martínek V, Kizek R and Stiborová M: The mechanism of cytotoxicity and DNA adduct formation by the anticancer drug ellipticine in human neuroblastoma cells. Biochem Pharmacol 77: 1466-1479, 2009.
34. Poljaková J, Groh T, Gudino ZO, Hraběta J, Bořek-Dohalská L, Kizek R, Doktorová H, Eckschlager T and Stiborová M: Hypoxia-mediated histone acetylation and expression of N-myc transcription factor dictate aggressiveness of neuroblastoma cells. Oncol Rep 31: 1928-1934, 2014.
35. Shechter D, Dormann HL, Allis CD and Hake SB: Extraction, purification and analysis of histones. Nat Protoc 2: 1445-1457, 2007.
36. Lowry OH, Rosebrough NJ, Farr AL and Randall RJ: Protein measurement with the Folin phenol reagent. J Biol Chem 193: 265-275, 1951.
37. Ke N, Wang X, Xu X and Abassi YA: The xCELLigence system for real-time and label-free monitoring of cell viability. Methods Mol Biol 740: 33-43, 2011.
38. Earnshaw WC, Martins LM and Kaufmann SH: Mammalian caspases: Structure, activation, substrates, and functions during apoptosis. Annu Rev Biochem 68: 383-424, 1999.
39. Porter AG and Jänicke RU: Emerging roles of caspase-3 in apoptosis. Cell Death Differ 6: 99-104, 1999.
40. Slee EA, Adrain C and Martin SJ: Executioner caspase-3, -6, and -7 perform distinct, non-redundant roles during the demolition phase of apoptosis. J Biol Chem 276: 7320-7326, 2001.
41. Atienza JM, Yu N, Kirstein SL, Xi B, Wang X, Xu X and Abassi YA: Dynamic and label-free cell-based assays using the real-time cell electronic sensing system. Assay Drug Dev Technol 4: 597-607, 2006.
42. Chou TC and Talalay P: Quantitative analysis of dose-effect relationships: The combined effects of multiple drugs or enzyme inhibitors. Adv Enzyme Regul 22: 27-55, 1984.
43. Chou T-C: Theoretical basis, experimental design, and computerized simulation of synergism and antagonism in drug combination studies. Pharmacol Rev 58: 621-681, 2006.
44. Luchenko VL, Salcido CD, Zhang Y, Agama K, Komlodi-Pasztor E, Murphy RF, Giaccone G, Pommier Y, Bates SE and Varticovski L: Schedule-dependent synergy of histone deacetylase inhibitors with DNA damaging agents in small cell lung cancer. Cell Cycle 10: 3119-3128, 2011.
45. Jordan MA and Wilson L: Microtubules as a target for anticancer drugs. Nat Rev Cancer 4: 253-265, 2004.
46. Tu Y, Cheng S, Zhang S, Sun H and Xu Z: Vincristine induces cell cycle arrest and apoptosis in SH-SY5Y human neuroblastoma cells. Int J Mol Med 31: 113-119, 2013.
47. Phiel CJ, Zhang F, Huang EY, Guenther MG, Lazar MA and Klein PS: Histone deacetylase is a direct target of valproic acid, a potent anticonvulsant, mood stabilizer, and teratogen. J Biol Chem 276: 36734-36741, 2001.
48. Sokolov MV, Dickey JS, Bonner WM and Sedelnikova OA: gamma-H2AX in bystander cells: Not just a radiation-triggered event, a cellular response to stress mediated by intercellular communication. Cell Cycle 6: 2210-2212, 2007.
49. Bonner WM, Redon CE, Dickey JS, Nakamura AJ, Sedelnikova OA, Solier S and Pommier Y: GammaH2AX and cancer. Nat Rev Cancer 8: 957-967, 2008.
50. Nakamura AJ, Rao VA, Pommier Y and Bonner WM: The complexity of phosphorylated H2AX foci formation and DNA repair assembly at DNA double-strand breaks. Cell Cycle 9: 389-397, 2010.
51. Yuan J, Adamski R and Chen J: Focus on histone variant H2AX: To be or not to be. FEBS Lett 584: 3717-3724, 2010.
52. dos Santos MP, Schwartsmann G, Roesler R, Brunetto AL and Abujamra AL: Sodium butyrate enhances the cytotoxic effect of antineoplastic drugs in human lymphoblastic T-cells. Leuk Res 33: 218-221, 2009.
53. Kurz EU, Wilson SE, Leader KB, Sampey BP, Allan WP, Yalowich JC and Kroll DJ: The histone deacetylase inhibitor sodium butyrate induces DNA topoisomerase II alpha expression and confers hypersensitivity to etoposide in human leukemic cell lines. Mol Cancer Ther 1: 121-131, 2001.
54. Bruzzese F, Rocco M, Castelli S, Di Gennaro E, Desideri A and Budillon A: Synergistic antitumor effect between vorinostat and topotecan in small cell lung cancer cells is mediated by generation of reactive oxygen species and DNA damage-induced apoptosis. Mol Cancer Ther 8: 3075-3087, 2009.
55. Itoh T, Terazawa R, Kojima K, Nakane K, Deguchi T, Ando M, Tsukamasa Y, Ito M and Nozawa Y: Cisplatin induces production of reactive oxygen species via NADPH oxidase activation in human prostate cancer cells. Free Radic Res 45: 1033-1039, 2011.
56. Yu C, Friday BB, Lai JP, McCollum A, Atadja P, Roberts LR and Adjei AA: Abrogation of MAPK and Akt signaling by AEE788 synergistically potentiates histone deacetylase inhibitor-induced apoptosis through reactive oxygen species generation. Clin Cancer Res 13: 1140-1148, 2007.

Vacuolar-ATPase-mediated intracellular sequestration of ellipticine contributes to drug resistance in neuroblastoma cells

Jan Hrabeta, [1] Tomas Groh, [1,2] Mohamed Ashraf Khalil, [1] Jitka Poljakova, [2] Vojtech Adam, [3,4] Rene Kizek, [3,4] Jiri Uhlik, [5] Helena Doktorova, [1] Tereza Cerna, [2] Eva Frei, [6] Marie Stiborova [2] and Tomas Eckschlager [1]

[1] Department of Pediatric Hematology and Oncology, 2nd Medical School, Charles University and University Hospital Motol, V Uvalu 84, 150 06 Prague 5, Czech Republic

[2] Department of Biochemistry, Faculty of Science, Charles University, Albertov 2030, 128 40 Prague 2, Czech Republic

[3] Department of Chemistry and Biochemistry, Faculty of Agronomy, Mendel University in Brno, Zemedelska 1, 613 00 Brno, Czech Republic

[4] Central European Institute of Technology, Brno University of Technology, Technicka 3058/10, 616 00 Brno, Czech Republic

[5] Department of Histology and Embryology, 2nd Medical School, Charles University, V Uvalu 84, 150 06 Prague 5, Czech Republic

[6] Division of Preventive Oncology, National Center for Tumor Diseases, German Cancer Research Center (DKFZ), Im Neuenheimer Feld 280, 69 120 Heidelberg, Germany

Correspondence

Marie Stiborova, Department of Biochemistry, Faculty of Science, Charles University, Albertov 2030, 128 40 Prague 2, Czech Republic.

Tel: +420 221951285; Fax.: +420 221951283

E-mail address: stiborov@natur.cuni.cz

Tomas Eckschlager, Department of Pediatric Hematology and Oncology, 2nd Medical School, Charles University and University Hospital Motol, V Uvalu 84, 150 06 Prague 5, Czech Republic.

Tel: +420 224436492; fax.: +420 224436420

E-mail address: tomas.eckschlager@lfmotol.cuni.cz

The manuscript contains 4213 words, 2 Tables and 7 Figures

Exposure to ellipticine induces apoptosis in human neuroblastoma cells and inhibits their growth. However, ellipticine induced resistance in these cells. The up-regulation of a vacuolar *(V)-ATPase* gene is one of the factors associated with resistance development. In accordance with this finding, here we found that levels of V-ATPase protein expression are higher in the ellipticine-resistant UKF-NB-4^{ELLI} line than in the parental ellipticine-sensitive UKF-NB-4 cell line. Treatment of ellipticine-sensitive UKF-NB-4 and ellipticine-resistant UKF-NB-4^{ELLI} cells with ellipticine induced cytoplasmic vacuolization and ellipticine is concentrated in these vacuoles. Confocal microscopy and staining of the cells with a lysosomal marker suggested these vacuoles as lysosomes. Transmission electron microscopy and no effect of an autophagy inhibitor wortmannin ruled out autophagy. Pretreatment with a V-ATPase inhibitor bafilomycin A and/or the lysosomotropic drug chloroquine prior to ellipticine enhanced the ellipticine-mediated apoptosis and decreased ellipticine-resistance in UKF-NB-4^{ELLI} cells. Moreover, pretreatment with these inhibitors increased formation of ellipticine-derived DNA adducts, one of the most important DNA-damaging mechanisms responsible for ellipticine cytotoxicity. In conclusions, resistance to ellipticine in the tested neuroblastoma cells is associated with V-ATPase-mediated vacuolar trapping of this drug, which may be decreased by bafilomycin A and/or chloroquine.

Key words

Neuroblastoma; Resistance to ellipticine; Vacuolation; Drug sequestration; Vacuolar ATPase

Introduction

Neuroblastoma is a malignant tumor consisting of neural crest derived undifferentiated neuroectodermal cells. These tumors are biologically heterogeneous, with cell populations differing in their genetic programs, maturation stage and malignant potential.[1,2] As neuroblastoma cells seem to have the capacity to differentiate spontaneously *in vivo* and *in vitro*,[3] their heterogeneity could affect treatment outcome. Recent studies have provided a link between increased metastatic potential and drug-resistant phenotypes, indicating that in addition to the development of drug resistance, chemotherapy of tumors may cause changes in their biological characteristics.[4,5] Unfortunately, little improvement in therapeutic options in high risk neuroblastoma has been made in the last decade, requiring a need for the development of new therapies.

Recently, we suggested a novel treatment for neuroblastomas, utilizing a drug targeting DNA, the plant alkaloid ellipticine. We found that exposure of human neuroblastoma IMR-32, UKF-NB-3 and UKF-NB-4 cell lines to this agent resulted in strong inhibition of cell growth, followed by induction of apoptosis.[6-11] These effects were associated with formation of two major covalent ellipticine-derived DNA adducts, identical to those formed by the cytochrome P450 (CYP)- and peroxidase-mediated ellipticine metabolites, 13-hydroxy- and 12-hydroxyellipticine.[7,10,12-16]

The levels of covalent ellipticine-derived DNA adducts correlated with ellipticine toxicity in IMR-32 and UKF-NB-4 cell lines. Cells of both lines accumulated in S phase, suggesting that ellipticine-DNA adducts interfere with DNA replication. We therefore concluded that formation of ellipticine-DNA adducts was the predominant DNA-damaging mechanism of ellipticine action, resulting in its high cytotoxicity to these neuroblastoma cells.[6,7,10,11]

Nevertheless, this drug is unfortunately capable of inducing resistance in neuroblastoma cells. Exposure of UKF-NB-4 cells to increasing concentrations of ellipticine resulted in a resistant line assigned as UKF-NB-4^{ELLI}.[6,17] In the UKF-NB-4^{ELLI} cells, lower accumulation of this drug was found in the nuclei after treatment of these cells with ellipticine than in the parental line,[17] which consequently leads to lower levels of DNA adducts and decreased ellipticine toxicity in these cells. Ellipticine resistance in neuroblastoma is caused by a combination of overexpression of Bcl-2, efflux or degradation of the drug, downregulation of topoisomerases and the up-regulation of vacuolar (V)-ATPase.[17] The mechanism of V-ATPase contribution to induction of resistance to ellipticine in the UKF-NB-4^{ELLI} cell line was investigated in this work.

Vacuolar V-ATPase is the multi-subunit membrane protein complex[18] responsible for the acidification of some intracellular compartments such as trans-Golgi network, endosomes, lysosomes, and secretory granules. The V-ATPase-dependent acidification of Golgi complex is essential for the synthesis and delivery of the lysosomal hydrolases from endoplasmic reticulum/Golgi to lysosomes.[19-21] The acidic microenvironment caused by changes in the pH gradient between the intracellular and the extracellular compartments as well as the pH gradient between the cytoplasm and the intracellular organelles can be significantly involved in the mechanism of drug resistance.[22,23] These changes in pH lead to neutralization of weakly basic drugs by the acidic tumor microenvironment or the sequestration of drugs into lysosomal vesicles.[22-26] The questions whether these mechanisms and if so, which of them are responsible for V-ATPase-dependent development of resistance of UKF-NB-4 cells to ellipticine need to be answered. Therefore, this feature was studied in this work.

Materials and methods

Cell lines and cell culture. UKF-NB-4 neuroblastoma cell line, established from recurrent bone marrow metastases of high risk neuroblastoma, was a gift of Prof. J. Cinatl (J. W. Goethe University, Frankfurt, Germany). The ellipticine-resistant cell line, designated UKF-NB-4^{ELLI}, was established by exposing UKF-NB-4 cells to increasing concentrations from 0.2 to 2.5 µM ellipticine over 36 months. The drug resistance of UKF-NB-4^{ELLI} cells to ellipticine was verified using the MTT test.[17] Each cell line was cultivated in Iscove's modified Dulbecco's medium (IMDM) (LifeTechnologies, Carlsbad, CA, USA) supplemented with 10% (v/v) fetal bovine serum (LifeTechnologies, Carlsbad, CA, USA), maintained at 37°C and 5% CO_2. The medium for UKF-NB-4^{ELLI} cells was the same, but contained 2.5 µM ellipticine.[6] Before experiments, UKF-NB-4^{ELLI} cells were cultivated for at least one passage without ellipticine, in order to remove ellipticine from these cells. Ellipticine, chloroquine, wortmannin and bafilomycin A were obtained from Sigma-Aldrich (St. Louis, MO, USA).

Electron microscopy. UKF-NB-4 and UKF-NB-4^{ELLI} cells **(**5 x 10^5 cells**)** were grown on glass 60 mm dishes either untreated or treated with 5 µM ellipticine and 100 nM bafilomycin A as well as combination of 5 µM ellipticine and 100 nM bafilomycin A for 1 h at 37°C. In the case of a combined treatment, bafilomycin A was added to the incubations 20 minutes before adding ellipticine. Cells were mechanically re-suspended, washed, centrifuged and fixed with 2.5% glutaraldehyde in 0.1 M sodium cacodylate buffer pH 7.4 for 90 min. Samples were centrifuged (16,000 g/5 min) and pellets were postfixed for 60 min with 2% OsO_4 in 0.1 M sodium cacodylate buffer pH 7.4, dehydrated in graded series of alcohol and embedded in a Durcupan-Epon mixture. Ultrathin sections were prepared on Leica EM UC6 ultramicrotome (Leica Microsystems, Vienna, Austria), contrasted with uranyl acetate and lead citrate and examined by a JEM 1011 transmission electron microscope (Jeol, Tokyo, Japan).

Fluorescence microscopy. Acidic vesicular organelle staining: UKF-NB-4 cells [5 x 10^5 cells grown on 35 mm glass bottom culture dishes (In Vitro Scientific, Sunnyvale, CA, USA) for 24 h before adding the compounds] were treated either with 5 µM ellipticine alone or in combination with either 100 nM bafilomycin A or 25 µM chloroquine for 1 h at 37°C, then incubated with 75 nM LysoTracker Red (LifeTechnologies, Carlsbad, CA, USA) for 30 min. After washing with Hanks' balanced salt solution (Sigma-Aldrich, St. Louis, MO, USA), cells were observed with a laser-scanning confocal microscope Olympus FV 1000 (Tokyo, Japan).

For excitation of the LysoTracker® red, laser with an excitation wavelength of 559 nm was used; emitted light was collected in the range of 570–670 nm. For excitation of green-ellipticine fluorescence, solid-state laser with an excitation wavelength of 473 nm was used and emmited light was collected in the range of 485–545 nm. All images were recorded with a 40x objective using a zoom factor of 2x and the Olympus FluoView FV1000 system. Each fluorescence channel was scanned individually (sequential scanning). Fluorescent channels were pseudocolored with RGB values corresponding to each of the fluorophore emission spectral profiles.

Western blot analysis of V-ATPase (ATP6V0D1 membrane domain) protein expression. In order to analyze V-ATPase (ATP6V0D1 membrane domain) protein expression, Western blotting was used. UKF-NB-4 and UKF-NB-4^{ELLI} cell (1.5 x 10^6 cells) pellets were re-suspended in 25 mM Tris-HCl buffer pH 7.6 containing 150 mM NaCl, 1% detergent Igepal® CA-630 (Sigma Chemical Co., St. Louis, MO, USA), 1% sodium deoxy-cholate and 0.1% sodium dodecyl sulfate (SDS) and with solution of Complete™ (Roche, Basel, Switzerland) at concentrations described by the provider. The samples were incubated for 30 min on ice and thereafter centrifuged for 20 min at 20,000 x g and 4˚C. Supernatants were used for additional analysis. Protein concentrations were assessed using the DC protein assay (Bio-Rad, Hercules, CA, USA) according to Lowry method. 15 μg of proteins were electrophoretically separated using 4 - 20% TGX precast gel (100 mA). After migration, proteins were transferred to a nitrocellulose membrane and incubated with 5% non-fat milk to block non-specific binding. The membranes were then exposed to specific anti-ATP6V0D1 mouse monoclonal antibody (1:500, Abcam, Cambridge, UK). Membranes were washed and exposed to peroxidase-conjugated anti-IgG secondary antibodies (1:2000; Bio-Rad, Hercules, CA, USA), and the antigen-antibody complex was visualized by enhanced chemiluminescence detection system according to the manufacturer's instructions (Immun-Star HRP Substrate, Bio-Rad, Hercules, CA, USA), using X-ray film (MEDIX XBU, Foma, Hradec Kralove, Czech Republic). Antibody against actin (1:1000; Sigma-Aldrich, St. Louis, MO, USA) was used as loading control.

Determination of apoptosis by Annexin V/DAPI labeling. UKF-NB-4 and UKF-NB-4^{ELLI} cells (5 x 10^5 cells) were seeded in 35-mm culture dishes overnight. Bafilomycin A, chloroquine and/or ellipticine in above mentioned concentrations were added to dishes and the cells were incubated for 24 h. The cells were collected by trypsinization and washed with phosphate buffered saline (PBS). Annexin V staining was accomplished by following

producer´s instructions (Exbio, Vestec, Czech Republic). The cells were re-suspended in Anexin V binding buffer (Exbio, Vestec, Czech Republic), then Annexin V-Dy647 was added and samples were incubated for 15 min in dark at ambient temperature. DAPI (2.5 μg/ml) was added just before analysis. Cells were analyzed using LSR II Flow Cytometer (BD Bioscience, San Jose, CA, USA).

3-(4,5-dimethylthiazol-2-yl)-5-(3-carboxymethoxyphenyl)-2-(4-sulfophe-nyl)-2H-tetrazolium (MTS) assay. The IC_{50} values of ellipticine were determined by CellTiter 96® AQueous One Solution Cell Proliferation Assay (Promega, Fitchburg, WI, USA) in a 96-well plate. For a dose-response curve, cells were seeded in 100 μl of medium with 5 x 10^3 cells per well with 100 nM bafilomycin A, 25 μM chloroquine or 100 nM wortmanin, and 20 minutes later ellipticine in serial dilutions were added. After three days of incubation at 37 ^oC in 5% CO_2, 7 μl of MTS solution per well was added and the plates were incubated for two hours. The absorbance at 490 nm was measured for each well by multiwell ELISA reader Versamax (Molecular Devices, CA, USA). Each value is the mean of 8 wells. The mean absorbance of medium controls was the background and was subtracted. The IC_{50} values were calculated from three independent experiments using the linear regression of the dose-log response curves by SOFTmaxPro software.

Western blot analysis: detection of autophagosomal marker proteins LC3-I and LC3-II. To induce autophagy, UKF-NB-4 and UKF-NB-4^{ELLI} cells were starved in Hanks' balanced salt solution (Sigma-Aldrich, St. Louis, MO, USA) for 4 h at 37°C with or without the inhibitors of autophagy, wortmannin (0.1 μM), chloroquine (25 μM) or bafilomycin A (100 nM). Subsequently cells were collected and lysed in a Laemmli sample buffer (Sigma-Aldrich, St. Louis, MO, USA), and were subjected to immunoanalysis. Protein concentrations were assessed using a DC protein assay kit (Bio-Rad, Hercules, CA, USA) according to manufacturer's instructions. A 50 μg of sample protein was subjected to sodium dodecyl sulfate-polyacrylamide gel electrophoresis. After migration, proteins were transferred to nitrocellulose membranes and incubated with 5% non-fat milk (Bio-Rad, Hercules, CA, USA). The membranes were exposed to anti-LC3 (Microtubule-associated protein 1A/1B-light chain 3) antibody diluted 1:400 (Novus Biologicals, Littleton, CO, USA) overnight at 4°C. Membranes were then washed three times with PBS/Tween and exposed to horseradish peroxidase-conjugated goat anti-rabbit anti-IgG (H+L) secondary antibodies (Bio-Rad,

Hercules, CA, USA). The antigen–antibody complex was visualized using chemiluminescence by Immun-Star HRP Substrate kit (Bio-Rad, Hercules, CA, USA). Antibodies against actin (1:1000, Sigma, St. Louis, MO, USA) were used as loading control.

DNA isolation from neuroblastoma cells and ^{32}P-postlabeling of ellipticine-DNA adducts. Neuroblastoma cell lines were seeded 24 h prior to treatment at a density of 5 x 10^5 cells/ml in two 75 cm^2 culture flasks in a total volume of 20 ml of IMDM. After 24 h incubations with 5 μM ellipticine in IMDM, the cells were harvested after trypsinizing by centrifugation at 2000 x g for three minutes and two washing steps with 5 ml of PBS yielded a cell pellet, which was stored at -80ºC until DNA isolation. An analogous procedure was used to evaluate the effect of treatment of neuroblastoma cells with bafilomycin A or chloroquine before adding ellipticine. Cells were treated with 100 nM bafilomycin A or 25 μM chloroquine for 20 minutes before adding ellipticine. DNA from neuroblastoma cells treated with 5 μM ellipticine in the presence or absence of 100 nM bafilomycin A and/or 25 μM chloroquine for 24 h was isolated by the phenol-chloroform extraction as described.[6,8,13,27,28] The ^{32}P-postlabeling of nucleotides using nuclease P1 enrichment, found previously to be appropriate to detect and quantify ellipticine-derived DNA adducts formed *in vitro* [12,13,27-30] and *in vivo*[7,10,31-33] was used.

Statistical analysis. Data are expressed as mean ± standard deviations (SD). Student's *t*-test (two tailed) was used for statistical analysis. *P* values less than 0.05 were considered statistically significant and are indicated with *; *P* values less than 0.01 are indicated with **, and *P* values less than 0.001 are indicated with ***.

Results

Ellipticine induces cytoplasmic vacuolization in neuroblastoma cells and accumulates in these vacuoles. Treatment of neuroblastoma UKF-NB-4 cells, both sensitive and resistant (UKF-NB-4^{ELLI}) to ellipticine, with ellipticine at concentrations that are toxic to these cells (5 μM) induced extensive cytoplasmic vacuolization in these cells (see vacuoles assigned by arrows in Figure 1B,E). The vacuolar vesicles of a small size were also present in the UKF-NB-4^{ELLI} cell line prepared by cultivation of a UKF-NB-4 cell line with increasing concentrations of ellipticine (from 0.2 to 2.5 μM) over 36 months[17] (see vesicles assigned with arrows in a panel D in Figure 1). The vacuoles were already detectable 30 minutes after adding the ellipticine (data not shown). This ellipticine-mediated cytoplasmic vacuolization seems to be a general phenomenon, because it appears also in two other neuroblastoma cell lines, SK-N-AS and UKF-NB-3 (data not shown). Under the electron microscope, ellipticine-induced vacuoles were found to be electron-lucent and to contain some heterogeneous material. They, however, lacked any detectable content of cytoplasmic material (organelles) and were lined by a single membrane (Fig. 2), ruling out autophagy. In order to characterize the vacuoles further, we used confocal microscopy of cells stained with two specific lysosomal markers, lysosomal-associated membrane protein 1 (LAMP1)[34] and a lysosomal marker selective for acidic compartments, LysoTracker® red.[35] Unfortunately, LAMP1 could not be applied simultaneously with ellipticine, since anti-LAMP1 is used on fixed cells and fixation interferes with ellipticine detection (data not shown). The results found using confocal microscopy of cells stained with LysoTracker® red (Fig. 3) and the finding that the ellipticine-induced vacuoles are single membrane vesicles (Figs. 1 and 2) suggested that these vacuoles are lysosomes.

The green fluorescence of ellipticine (excitation = 440 nm, emission = 520 nm)[10] allowed the detection of its intracellular localization. At physiological pH, ellipticine exists in both protonated (charged) and unprotonated (uncharged) forms.[10] As shown in Figure 3, the UKF-NB-4 cells exposed to ellipticine contained ellipticine-specific green fluorescent vesicles where ellipticine is accumulated. Some of the vesicles where ellipticine was present colocalized with a lysosomal marker LysoTracker® red (Fig. 3). Hence, ellipticine as a protonated chemical is trapped in these vesicles formed in the cells. This might be caused by the pKa value of this compound and the pH gradient between cytoplasm and acidic vacuoles developed by ellipticine. Namely, ellipticine has a pKa of ~6, and can be protonated in a

weakly acidic environment.[6,37] The trapping of ellipticine in these acidic vesicles is followed by osmotic swelling and dilatation (Fig. 1).

A contribution of V-ATPase to ellipticine-induced vacuolation and ellipticine sequestration into these vacuoles was investigated with its specific inhibitor, bafilomycin A[38,39] and the lysosomotropic drug chloroquine, the agent that enters selectively the lysosomes and inhibits enzymes for which the acidic pH is crucial.[40]

Ellipticine-induced vacuolation and intravesicular ellipticine-associated fluorescence were abolished by co-treatment of tested neuroblastoma cells with bafilomycin A and chloroquine (Figs. 1 and 3). These results suggest that ellipticine is responsible for the V-ATPase-mediated formation of cytoplasmic vacuoles (*i.e.* lysosomes) in these neuroblastoma cells, and that is able to be sequestrated into these acidic compartments.

Expression of V-ATPase in the ellipticine sensitive and resistant UKF-NB-4 cells. Because of the suspected role of up-regulation of the *V-ATPase* gene in induction of resistance of UKF-NB-4 cells to ellipticine,[17] we further investigated expression of this enzyme both in the ellipticine sensitive and resistant UKF-NB-4 cells. Using Western blots, expression of a protein product of *ATP6V0D1,* the gene of the V-ATPase membrane domain, which is up-regulated in several drug-resistant cell lines including UKF-NB-4^{ELLI},[17,38-43] was measured in the tested cells. As shown in Figure 4, the V-ATPase (ATP6V0D) protein levels were 2.3-times higher in the resistant UKF-NB-4^{ELLI} cell line than in its parental sensitive line. These results are in agreement with previous finding which demonstrated up-regulation of the *ATP6V0D1* gene in ellipticine-resistant neuroblastoma cells,[17] and point out its importance for acquiring resistance to ellipticine.

Treatment of neuroblastoma cells with bafilomycin A or chloroquine increases the cytotoxic effects of ellipticine and decreases their resistance to ellipticine. The UKF-NB-4 and UKF-NB-4^{ELLI} cell lines were treated with either ellipticine alone or after pretreatment with bafilomycin A or chloroquine. The cytotoxic effects of ellipticine to neuroblastoma cells in the presence or absence of these inhibitors were analyzed by two methods: (i) by detection of apoptosis in the cells using Annexin V/DAPI labeling (Fig. 5), and (ii) by MTS assay (Table 1). Treatment of neuroblastoma cells with bafilomycin A or chloroquine did not induce apoptosis in these cells (Fig. 5). However, pretreatment of the cells with these compounds enhanced markedly the ellipticine-mediated apoptosis induction in both the sensitive and ellipticine-resistant neuroblastoma cells and decreased the resistance of UKF-NB-4^{ELLI} cells to

ellipticine (Fig 5). In addition, pretreatment of cells with bafilomycin A and/or chloroquine was able to reduce the values of IC_{50} both in the ellipticine-sensitive and ellipticine-resistant cell lines to the lower IC_{50} values (Table 1). These results demonstrate that a decrease in sensitivity of neuroblastoma cells to ellipticine is indeed caused by the potency of this drug to induce the formation of acidified vesicles having the lysosomal character in these cells, which additionally trapped the protonated ellipticine, thereby decreasing its cytotoxic effects. They also strongly support the suggestion that these processes participated in ellipticine-induced resistance of UKF-NB-4 cells.

Nevertheless, it should be noted that bafilomycin A and chloroquine act not only as the inhibitors of lysosomal proteases, but that they can also partially prevent maturation of autophagic vacuoles. They, namely, also inhibit fusion between autophagosomes and lysosomes, because they are inhibitors of the late phase of autophagy.[40] Hence, their augmented effects might be caused also by authophagy inhibition. Here, we examined this possibility, namely, whether their potentiating effect on ellipticine-mediated cytotoxicity to neuroblastoma cells is related to autophagy inhibition. For such a study, we used the autophagy inhibitor wortmannin.[44] Wortmannin is an inhibitor of phosphatidylinositol 3-kinase (PI3K)[44,45] that is required for autophagy.[46] In contrast to bafilomycin A and chloroquine, wortmannin had no effect on induction of apoptosis in neuroblastoma cells exposed to ellipticine (Fig. 5). It also did not reduce a value of IC_{50} for ellipticine in these cells (Table 1). These findings demonstrate that the bafilomycin A- and chloroquine-mediated increase in cytotoxicity and induction of apoptosis caused by ellipticine determined in this study are not related to autophagy.

Effectiveness of autophagy inhibitors in tested lines was also investigated by examining the expression of an autophagosomal marker protein LC3-II (Fig. 6), the protein that is highly expressed in both membranes of autophagosomes. Lysosomal turnover of the autophagosomal marker LC3-II namely reflects autophagic activity, and therefore determination of levels of LC3-II is considered as a method suitable to monitor the autophagy process.[47] In our experiments, autophagy in neuroblastoma cells was induced by their starvation and proved by expression of LC3-II in these cells (Fig. 6). High expression of LC-II in these cells were also induced by bafilomycin A and chloroquine (Fig. 6) because both these compounds as inhibitors of proteolytic processes in the lysosomes[38-40] increased lysosomal pH that consequently led to decreased activity of lysosomal proteases. These processes blocked lysosomal degradation and rescued intact LC3-II in neuroblastoma cells (Fig. 6). In contrast, wortmannin as a blocker of autophagosome formation decreased the expression of LC3-II

induced by starvation (Fig. 6). This finding again suggests that the increase in ellipticine-mediated cytotoxicity and induction of apoptosis by ellipticine due to bafilomycin A and chloroquine in neuroblastoma cells are not related to autophagy.

Treatment of neuroblastoma cells with bafilomycin A and chloroquine prior to ellipticine increases the formation of covalent ellipticine-derived DNA adducts. Since formation of covalent DNA adducts of ellipticine is one of the major modes of ellipticine action in several cancer cells including neuroblastoma,[6,7,8,10,11,12,28,29] we investigated whether treatment of UKF-NB-4 and UKF-NB-4^{ELLI} cells with bafilomycin A or chloroquine prior to ellipticine changes DNA adduct levels. Two major and two minor DNA adducts were detected in neuroblastoma cells treated with ellipticine. The levels of the ellipticine-DNA adducts were lower in a resistant cell line (Fig. 7 and Table 2), as it has already been found in our previous work.[6] However, treatment with either bafilomycin A or chloroquine prior to ellipticine significantly increased levels of ellipticine-DNA adducts in both cell lines (Fig. 7 and Table 2). This corresponded to enhanced cytotoxic effects of ellipticine on these cells (Fig. 5). These results indicate that bafilomycin A- and chloroquine-mediated inhibition of ellipticine sequestration into vacuoles led to higher concentrations of ellipticine in cytoplasm and nuclei to be activated to species forming covalent DNA adducts.

Discussion

The results found in this work demonstrate for the first time that sequestration of anticancer drug ellipticine into the subcellular compartments (*i.e.* lysosomes) of UKF-NB-4 neuroblastoma cells is one of the mechanisms contributing to the development of ellipticine-resistance in these cells. Such processes finally result in a decrease in ellipticine cytotoxic effects.[6,17] We demonstrated that this resistance is, among other mechanisms, dependent on up-regulation of the *V-ATPase* gene.[17] Indeed, here we found that the V-ATPase protein expression is enhanced in the ellipticine-resistant UKF-NB-4^{ELLI} cell line.

Since V-ATPase is the major enzyme responsible for the acidification of subcellular compartments, it acidifies newly formed cytoplasmic vacuolar vesicles by pumping protons across the membranes.[19-21] This process is a necessary step for additional sequestration of the protonated form of ellipticine within these organelles. Finally, this sequestration results in lower cytoplasmic concentrations of ellipticine, less nuclear accumulation[17] and lower DNA damage by ellipticine (see Table 2 and Figure 7) and therefore also lower toxic effects to these cells (see Table 1, Figure 5 and our previous work[6]). The formation of covalent ellipticine-derived DNA adducts, which was found to be lower in ellipticine-resistant UKF-NB-4^{ELLI} cells, was increased by an inhibitor of V-ATPase, bafilomycin A, and/or the lysosomotropic drug chloroquine that block formation of lysosomes.[48] In concordance to these results, exposure of the tested cells to bafilomycin A and chloroquine enhanced markedly the cytotoxicity of ellipticine on these cells and decreased resistance of UKF-NB-4^{ELLI} to ellipticine.

Based on these results, we can conclude that the decrease in ellipticine-mediated cytotoxicity on UKF-NB-4 cells as well as in induction of resistance to ellipticine in the ellipticine-resistant UKF-NB-4^{ELLI} cell line is associated with vacuolar trapping of this drug, which may be abolished by bafilomycin A or by chloroquine. Therefore, therapeutic implications could be derived from this study. In principle, the components of the endocytic/lysosomal pathway could be molecular targets for a combination therapy of neuroblastoma with chemotherapeutic drugs and probably also for that of other cancers.

Funding information

This work was supported by GACR (grants P301/10/0356 and 14-8344S), Charles University in Prague (UNCE204025/2012) and by the Ministry of Health of the Czech Republic for conceptual development of research organization 00064203 (University Hospital Motol, Prague, Czech Republic).

Disclosure statement

The authors have no conflict of interest to declare.

References

1 Schwab M, Westermann F, Hero B, Berthold F. Neuroblastoma: biology and molecular and chromosomal pathology. *Lancet Oncol* 2003; **4:** 472-80.

2 Brodeur GM. Neuroblastoma: biological insights into a clinical enigma. *Nat Rev Cancer* 2003; **3:** 203–16.

3 Morgenstern BZ, Krivoshik AP, Rodriguez V, Anderson PM. Wilms' tumor and neuroblastoma. *Acta Paediatr Suppl* 2004; **93:** 78–84, discussion 84–85.

4 Kotchetkov R, Driever PH, Cinatl J, Michaelis M, Karaskova J, Blaheta R, Squire J, Von Deimling A, Moog J, Cinatl J. Increased malignant behavior in neuroblastoma cells with acquired multi-drug resistance does not depend on P-gp expression. Int J Oncol 2005;27: 1029–37.

5 Michaelis M, Klassert D, Barth S *et al.* Chemoresistance acquisition induces a global shift of expression of aniogenesis-associated genes and increased pro-angogenic activity in neuroblastoma cells. *Mol Cancer* 2009; **8:** 80.

6 Poljaková J, Eckschlager T, Hrabeta J *et al.* The mechanism of cytotoxicity and DNA adduct formation by the anticancer drug ellipticine in human neuroblastoma cells. *Biochem Pharmacol* 2009; **77:** 1466–79.

7 Stiborová M, Rupertová M, Frei E. Cytochrome P450- and peroxidase-mediated oxidation of anticancer alkaloid ellipticine dictates its anti-tumor efficiency. *Biochim Biophys Acta* 2011; **1814:** 175–85.

8 Poljakova J, Hrebackova J, Dvorakova M *et al.* Anticancer agent ellipticine combined with histone deacetylase inhibitors, valproic acid and trichostatin A, is an effective DNA damage strategy in human neuroblastoma. *Neuro Endocrinol Lett* 2011; **32 Suppl 1:** 101–116.

9 Stiborová M, Eckschlager T, Poljaková J *et al.* The synergistic effects of DNA-targeted chemotherapeutics and histone deacetylase inhibitors as therapeutic strategies for cancer treatment. *Curr Med Chem* 2012; **19:** 4218–38.

10 Stiborová M, Frei E. Ellipticines as DNA-targeted chemotherapeutics. *Curr Med Chem* 2014; **21:** 575-91.

11 Stiborova M, Poljakova J, Mrizova I *et al.* Expression levels of enzymes metabolizing an anticancer drug ellipticine determined by electromigration assays influence its cytotoxicity to cancer cells - a comparative study. *Int J Electrochem Sci* 2014; **9:** 5675-89.

12 Stiborová M, Bieler CA, Wiessler M, Frei E. The anticancer agent ellipticine on activation by cytochrome P450 forms covalent DNA adducts. *Biochem Pharmacol* 2001; **62:** 1675–84.

13 Stiborová M, Sejbal J, Borek-Dohalská L *et al.* The anticancer drug ellipticine forms covalent DNA adducts, mediated by human cytochromes P450, through metabolism to 13-hydroxyellipticine and ellipticine N^2-oxide. *Cancer Res* 2004; **64:** 8374–80.

14 Stiborova M, Rupertova M, Schmeiser HH, Frei E. Molecular mechanisms of antineoplastic action of an anticancer drug ellipticine. *Biomed Pap Med Fac Univ Palacky Olomouc Czech Repub* 2006; **150:** 13–23.

15 Stiborová M, Poljaková J, Ryslavá H *et al.* Mammalian peroxidases activate anticancer drug ellipticine to intermediates forming deoxyguanosine adducts in DNA identical to those found in vivo and generated from 12-hydroxyellipticine and 13-hydroxyellipticine. *Int J Cancer* 2007; **120:** 243–51.

16 Kizek R, Adam V, Hrabeta J *et al.* Anthracyclines and ellipticines as DNA-damaging anticancer drugs: recent advances. *Pharmacol Ther* 2012; **133:** 26–39.

17 Procházka P, Libra A, Zemanová Z *et al.* Mechanisms of ellipticine-mediated resistance in UKF-NB-4 neuroblastoma cells. *Cancer Sci* 2012; **103:** 334–41.

18 Marshansky V, Rubinstein JL, Grüber G. Eukaryotic V-ATPase: novel structural findings and functional insights. *Biochim Biophys Acta* 2014; **1837:** 857–79.

19 Maxfield FR, McGraw TE. Endocytic recycling. *Nat Rev Mol Cell Biol* 2004; **5:** 121–32.

20 Goldman SDB, Funk RS, Rajewski RA, Krise JP. Mechanisms of amine accumulation in, and egress from, lysosomes. *Bioanalysis* 2009; **1:** 1445–59.

21 Coutinho MF, Prata MJ, Alves S. Mannose-6-phosphate pathway: a review on its role in lysosomal function and dysfunction. *Mol Genet Metab* 2012; **105:** 542–50.

22 Simon S, Roy D, Schindler M. Intracellular pH and the control of multidrug resistance. *Proc Natl Acad Sci USA* 2004; **91:** 1128–32.

23 Mahoney BP, Raghunand N, Baggett B, Gillies RJ. Tumor acidity, ion trapping and chemotherapeutics. I. Acid pH affects the distribution of chemotherapeutic agents *in vitro*. *Biochem Pharmacol* 2003; **66:** 1207–18.

24 Chapuy B, Koch R, Radunski U *et al.* Intracellular ABC transporter A3 confers multidrug resistance in leukemia cells by lysosomal drug sequestration. *Leukemia* 2008; **22:** 1576–86.

25 Spugnini EP, Citro G, Fais S. Proton pump inhibitors as anti vacuolar-ATPases drugs: a novel anticancer strategy. *J Exp Clin Cancer Res* 2010; **29:** 44.

26 Yamagishi T, Sahni S, Sharp DM *et al.* P-glycoprotein mediates drug resistance *via* a novel mechanism involving lysosomal sequestration. *J Biol Chem* 2013; **288:** 31761–71.

27 Frei E, Bieler CA, Arlt VM, Wiessler M, Stiborová M. Covalent binding of the anticancer drug ellipticine to DNA in V79 cells transfected with human cytochrome P450 enzymes. *Biochem Pharmacol* 2002; **64:** 289–95.

28 Poljaková J, Frei E, Gomez JE *et al.* DNA adduct formation by the anticancer drug ellipticine in human leukemia HL-60 and CCRF-CEM cells. *Cancer Lett* 2007; **252:** 270–9.

29 Martinkova E, Dontenwill M, Frei E, Stiborova M. Cytotoxicity of and DNA adduct formation by ellipticine in human U87MG glioblastoma cancer cells. *Neuro Endocrinol Lett* 2009; **30 Suppl 1:** 60–6.

30 Martinkova E, Maglott A, Leger DY *et al.* alpha5beta1 integrin antagonists reduce chemotherapy-induced premature senescence and facilitate apoptosis in human glioblastoma cells. *Int J Cancer* 2010; **127:** 1240–8.

31 Stiborová M, Breuer A, Aimová D *et al.* DNA adduct formation by the anticancer drug ellipticine in rats determined by ^{32}P postlabeling. *Int J Cancer* 2003; **107:** 885–90.

32 Stiborová M, Rupertová M, Aimová D, Ryslavá H, Frei E. Formation and persistence of DNA adducts of anticancer drug ellipticine in rats. *Toxicology* 2007; **236:** 50-60.

33 Stiborová M, Arlt VM, Henderson CJ *et al.* Role of hepatic cytochromes P450 in bioactivation of the anticancer drug ellipticine: studies with the hepatic NADPH:cytochrome P450 reductase null mouse. *Toxicol Appl Pharmacol* 2008; **226:** 318–27.

34 Hunziker W, Geuze HJ. Intracellular trafficking of lysosomal membrane proteins. *Bioessays* 1996; **18:** 379-89.

35 Oeste CL, Seco E, Patton WF, Boya P, Pérez-Sala D. Interactions between autophagic and endo-lysosomal markers in endothelial cells. *Histochem Cell Biol* 2013; **139:** 659-70.

36 Garbett NC, Graves DE. Extending nature's leads: the anticancer agent ellipticine. *Curr Med Chem Anti-Cancer Agents* 2004; **4:** 149–72.

37 Wu Y, Sadatmousavi P, Wang R *et al.* Self-assembling peptide-based nanoparticles enhance anticancer effect of ellipticine *in vitro* and *in vivo*. *Int J Nanomedicine* 2012; **7:** 3221–33.

38 Bowman EJ, Siebers A, Altendorf K. Bafilomycins: a class of inhibitors of membrane ATPases from microorganisms, animal cells, and plant cells. *Proc Natl Acad Sci USA* 1988; **85:** 7972–6.

39 Huss M, Wieczorek H. Inhibitors of V-ATPases: old and new players. *J Exp Biol* 2009; **212:** 341–6.

40 Shacka JJ, Klocke BJ, Shibata M *et al.* Bafilomycin A1 inhibits chloroquine-induced death of cerebellar granule neurons. *Mol Pharmacol* 2006; **69:** 1125–36.

41 Martínez-Zaguilán R, Raghunand N, Lynch RM *et al.* pH and drug resistance. I. Functional expression of plasmalemmal V-type H+-ATPase in drug-resistant human breast carcinoma cell lines. *Biochem Pharmacol* 1999; **57:** 1037–46.

42 Murakami T, Shibuya I, Ise T *et al.* Elevated expression of vacuolar proton pump genes and cellular PH in cisplatin resistance. *Int J Cancer* 2001; **93:** 869–74.

43 Huang L, Lu Q, Han Y *et al.* ABCG2/V-ATPase was associated with the drug resistance and tumor metastasis of esophageal squamous cancer cells. *Diagn Pathol* 2012; **7:** 180.

44 Wymann MP, Bulgarelli-Leva G, Zvelebil MJ *et al.* Wortmannin inactivates phosphoinositide 3-kinase by covalent modification of Lys-802, a residue involved in the phosphate transfer reaction. *Mol Cell Biol* 1996; **16:** 1722–33.

45 Arcaro A, Wymann MP. Wortmannin is a potent phosphatidylinositol 3-kinase inhibitor: the role of phosphatidylinositol 3,4,5-trisphosphate in neutrophil responses. *Biochem J* 1993; **296:** 297-301.

46 Blommaart EF, Krause U, Schellens JP, Vreeling-Sindelárová H, Meijer AJ. The phosphatidylinositol 3-kinase inhibitors wortmannin and LY294002 inhibit autophagy in isolated rat hepatocytes. Eur J Biochem 1997; **243:** 240-6.

47 Tanida I, Ueno T, Kominami E. LC3 and Autophagy. *Methods Mol Biol* 2008; **445:** 77–88.

48 Solomon VR, Lee H. Chloroquine and its analogs: a new promise of an old drug for effective and safe cancer therapies. *Eur J Pharmacol* 2009; **625:** 220–33.

Table 1. The effect of bafilomycin A, chloroquine and wortmannin on the IC_{50} values for ellipticine in ellipticine-sensitive UKF-NB-4 and ellipticine-resistant UKF-NB-4^{ELLI} neuroblastoma cell lines

Compound	UKF-NB-4 cells	UKF-NB-4^{ELLI} cells
	IC_{50} for ellipticine (μM)	
ellipticine	0.86 ± 0.007	1.42 ± 0.004$^{\Delta\Delta\Delta}$
ellipticine + 100 nM bafilomycin A	0.21 ± 0.006***	0.69 ± 0.014$^{***\Delta\Delta\Delta}$
ellipticine + 25 μM chloroquine	0.19 ± 0.010***	0.35 ± 0.012$^{***\Delta\Delta\Delta}$
ellipticine + 100 nM wortmannin	1.02 ± 0.005**	1.39 ± 0.014$^{\Delta\Delta\Delta}$

IC_{50} values determined by the MTS test (see Materials and Methods) were calculated from the linear regression of the dose-log response curves. Values are mean ± S.D. of three experiments. The data were analyzed statistically by Student's *t*-test. Values significantly different from individual cell lines (UKF-NB-4 or UKF-NB-4^{ELLI}) cultivated with ellipticine alone: $^{**}P<0.01$, $^{***}P<0.001$. Values significantly different from UKF-NB-4 cells: $^{\Delta\Delta\Delta}P<0.001$.

Table 2. DNA adduct formation by ellipticine in UKF-NB-4 and UKF-NB-4^{ELLI} cell lines

Cells	RAL (mean ± SD/10^7 nucleotides)[a]				
	Adduct 1[b]	Adduct 2[b]	Adduct 6[b]	Adduct 7[b]	Total
UKF-NB-4					
ELLI	2.92 ± 0.85	1.75 ± 0.78	0.55 ± 0.03	0.51 ± 0.005	5.73 ± 1.51
BAF + ELLI	4.3 ± 0.67**	2.03 ± 0.12*	0.69 ± 0.03**	0.60 ± 0.03**	7.62 ± 0.41**
CQ + ELLI	4.08 ± 0.72**	2.64 ± 0.14***	0.91 ± 0.04***	0.77 ± 0.4***	8.4 ± 0.53**
UKF-NB-4^{ELLI}					
ELLI	1.02 ± 0.01 $^{\Delta\Delta\Delta}$	0.89 ± 0.01 $^{\Delta\Delta\Delta}$	0.5 ± .0.01	0.03 ± .0.01 $^{\Delta\Delta\Delta}$	1.99 ±.0.06 $^{\Delta\Delta\Delta}$
BAF + ELLI	1.69 ±.0.21** $^{\Delta\Delta\Delta}$	1.65 ±.0.07*** $^{\Delta\Delta}$	0.6 ± 0.03**	0.22 ±.0.01*** $^{\Delta\Delta\Delta}$	4.16 ± 0.36*** $^{\Delta\Delta}$
CQ + ELLI	1.78 ± 0.1*** $^{\Delta\Delta\Delta}$	1.82 ± 0.11*** $^{\Delta\Delta}$	0.51 ± 0.03$^{\Delta\Delta}$	0.41 ± 0.02*** $^{\Delta\Delta\Delta}$	4.52 ± 0.33*** $^{\Delta\Delta\Delta}$

BAF – bafilomycin A, 100 nM; CQ – chloroquine, 25 μM; ELLI – 5 μM ellipticine.

[a]Values of relative adduct labeling (RAL) are expressed as adducts per 10^7 normal nucleotides. Values are mean ± S.D. of three experiments. Asterisks represent statistical significance of differences between the levels of RALs determined in DNA of the cells cultivated with ellipticine and those with ellipticine and bafilomycin A or chloroquine (*$P<0.05$; **$P<0.01$;***$P<0.001$) and $^{\Delta}$ statistical differences between the levels of RALs determined in DNA of the UKF-NB-4 and UKF-NB-4^{ELLI} cell lines ($^{\Delta\Delta}P<0.01$ and $^{\Delta\Delta\Delta}P<0.001$) as calculated by Student's *t*-test.

[b] See Figure 7 insert.

Legends to Figures

Fig 1. Transmission electron microscope images show a significant vacuolization of cytoplasm in the UKF-NB-4 ellipticine-sensitive (images A – C) and UKF-NB-4^{ELLI} ellipticine resistant (images D – F) cell lines after exposure to ellipticine. UKF-NB-4 cell line A: control; B: 1 h incubation with 5 μM ellipticine; C: 1 h incubation with 100 nM bafilomycin A and 5 μM ellipticine; UKF-NB-4^{ELLI} cell line D: control; E: 1 h incubation with 5 μM ellipticine; F: 1 h incubation with 100 nM bafilomycin A and 5 μM ellipticine**.** Images C and F demonstrate disapperance of cytoplasmic vacuolization after co-incubation with V-ATPase inhibitor bafilomycin A and ellipticine in both cell lines. Locations of vacuoles are indicated by arrows. Figure shows representative data from one of three independent experiments.

Fig. 2. Transmission electron microscope image shows a detail of one vacuole (formed in **a** UKF-NB-4 cell line by treating with 5 μM ellipticine) located close to mitochondria. The vacuole is lined by a single membrane that ruled out autophagy. Figure shows representative data from one of three independent experiments.

Fig. 3. Confocal microscope images demonstrate colocalization (yellow/orange color in "MERGE" or yellow in "Colocalization") of ellipticine (green "ELLI", 5 μM) and LysoTracker (red "LT", 75 nM), a marker of the acidic lysosomal compartment, in UKF-NB-4 cells. Cells were incubated with 5 μM ellipticine (dissolved in "DMSO") without or with 100 nM bafilomycin A (Baf A) or 25 μM chloroquine (CQ) as described in the Materials and methods section 2.3., and examined by confocal microscopy. See the text for further details. Figure shows representative data from one of three independent experiments.

Fig. 4. Expression of V-ATPase (ATP6V0D1) protein detected by Western blotting in UKF-NB-4 ellipticine-sensitive and UKF-NB-4 ellipticine-resistant cell lines. Actin was used as loading control. (A) Representative Western blot. (B) V-ATPase expressed relative to levels of actin. Figure B shows averages and standard deviations (S.D.) from three independent experiments. Values significantly different from individual cell lines (UKF-NB-4 or UKF-NB-4^{ELLI}): $*P<0.05$ (Student's *t*-test).

Fig. 5. Detection of apoptosis induced in UKF-NB-4 and UKF-NB-4^{ELLI} neuroblastoma cells using the AnnexinV/DAPI labeling after 24 h incubation with 5 μM ellipticine (ELLI) and inhibitors bafilomycin A (BAF, 100 nM), chloroquine (CQ, 25 μM), or wortmannin (W, 100 nM). Bafilomycin A and chloroquine, but not an autophagy inhibitor wortmannin, potentiate the anticancer effect of ellipticine. Figure shows averages and standard deviations (S.D.) from three independent experiments. Values significantly different from individual cell lines (UKF-NB-4 or UKF-NB-4^{ELLI}) cultivated with ellipticine alone: ***$P<0.001$ (Student's *t*-test).

Fig. 6. Expression of LC3‑I and LC3‑II proteins determined by Western blotting in UKF-NB-4 cells after treatment with different autophagy inhibitors. Control (Ctrl) cells were cultivated for 4 h in Hanks' balanced salt solution to induce autophagy. Actin was used as loading control. (A) Representative Western blot. (B) LC3-II expressed relative to levels of actin. Wortmannin (W, 100 nM), an inhibitor of autophagosome formation, decreased LC3-II expression (compare lanes Ctrl and W). Chloroquine (CQ, 25 μM) and bafilomycin A (BAF, 100 nM) increased lysosomal pH, and consequently decreased activity of lysosomal proteases and degradation of LC3-II (LC3-II expression is increased, see lanes CQ and BAF). Experiments verified that the concentrations of inhibitors used are able to inhibit proteolytic processes in the lysosomes (bafilomycin A and chloroquine) or autophagosome formation (wortmannin). Figure B shows averages and standard deviations (S.D.) from three independent experiments. Values significantly different from control UKF-NB-4 cells: ***$P<0.001$ (Student's *t*-test).

Fig. 7. Levels of covalent DNA adducts (sum of adducts 1, 2, 6 and 7 shown in insert) formed in UKF-NB-4 (grey columns) and UKF-NB-4^{ELLI} (black columns) neuroblastoma cells after their 24 h treatment with ellipticine (ELLI, 5 μM) either without pretreatment or with pretreatment with bafilomycin A (BAF, 100 nM) or chloroquine (CQ, 25 μM) (the cells were pre-treated with bafilomycin A and/or chloroquine for 20 minutes before adding ellipticine and further incubated 24 h). The data represent means of total levels of ellipticine-DNA adducts and standard deviations determined from three independent experiments. Values of relative adduct labeling (RAL) are expressed as adducts per 10^7 normal nucleotides. Asterisks represent statistical significance as calculated by Student's *t*-test (*$P<0.05$; **$P<0.01$; ***$P<0.001$). Insert: an

autoradiographic profile of ellipticine-DNA adducts formed in UKF-NB-4 cells determined by ^{32}P-postlabeling. The adduct spots 1 and 2 are formed in deoxyguanosine residues of DNA by the ellipticine metabolites, 13-hydroxy- and 12-hydroxyellipticine.[7,10,13,15]

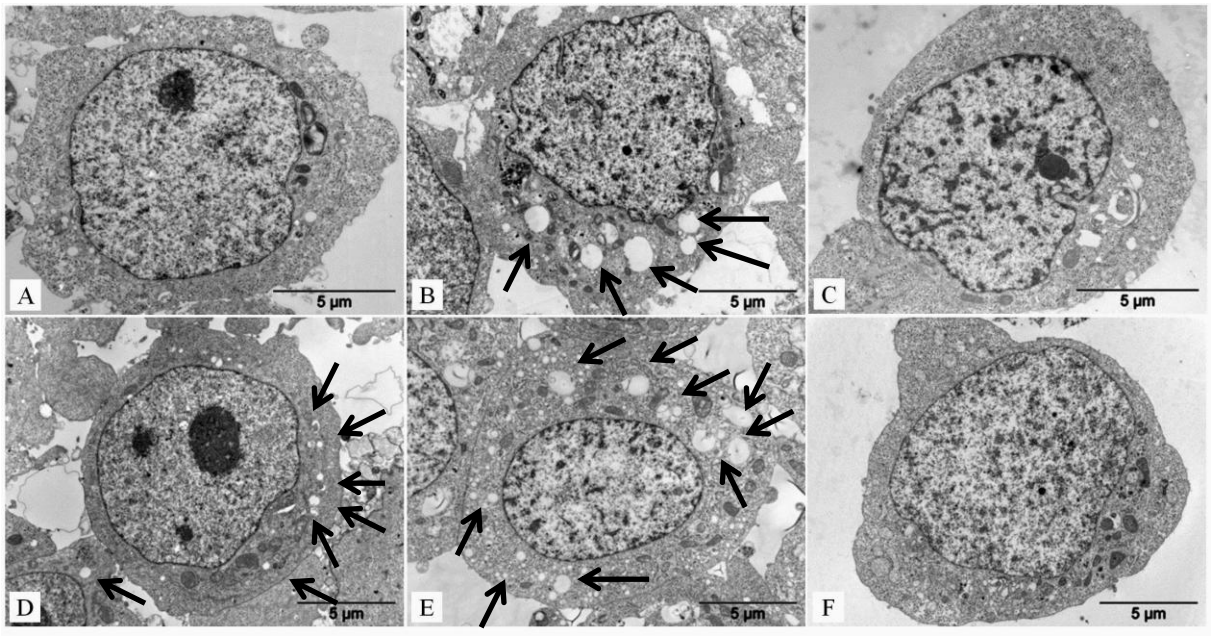

Fig. 1.

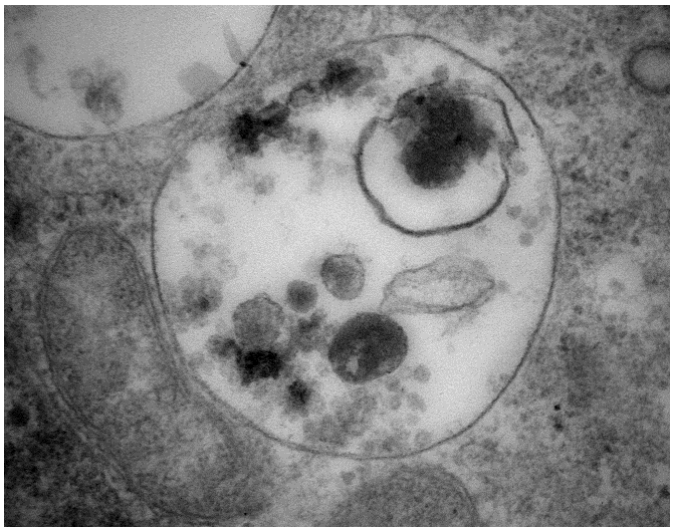

Fig 2.

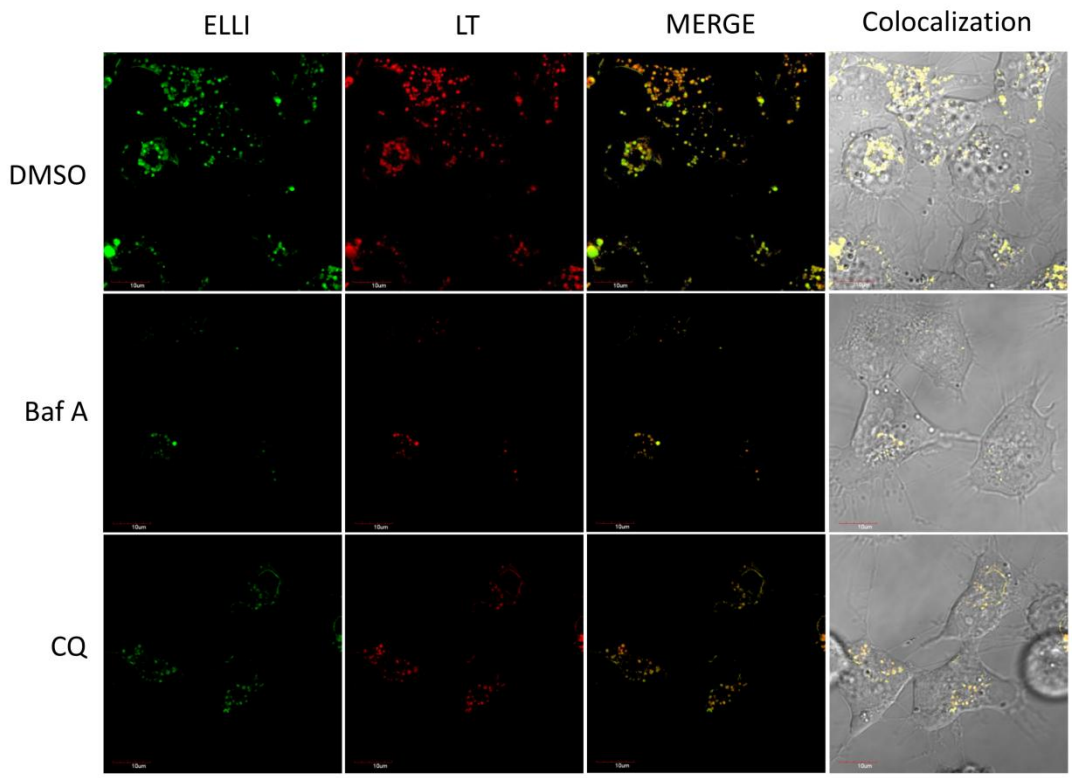

Fig. 3.

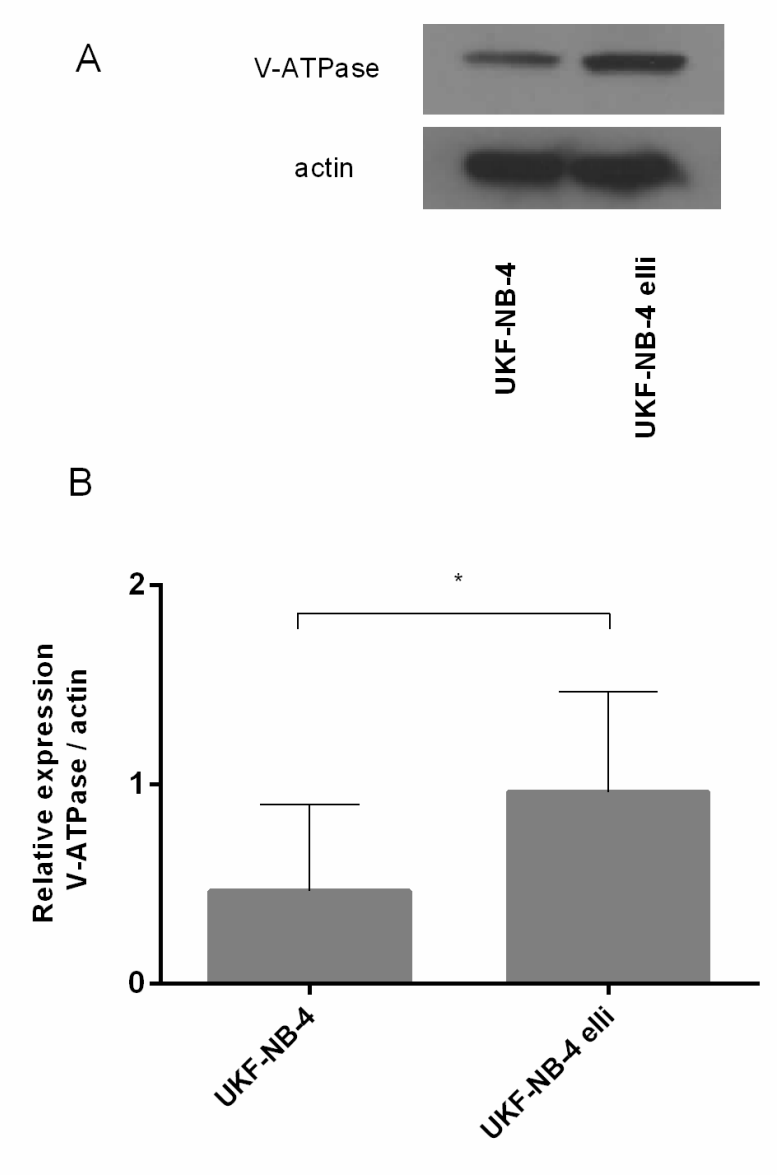
A
V-ATPase
actin
UKF-NB-4
UKF-NB-4 elli
B
Relative expression
V-ATPase / actin
2
1
0
*
UKF-NB-4
UKF-NB-4 elli

Fig. 4.

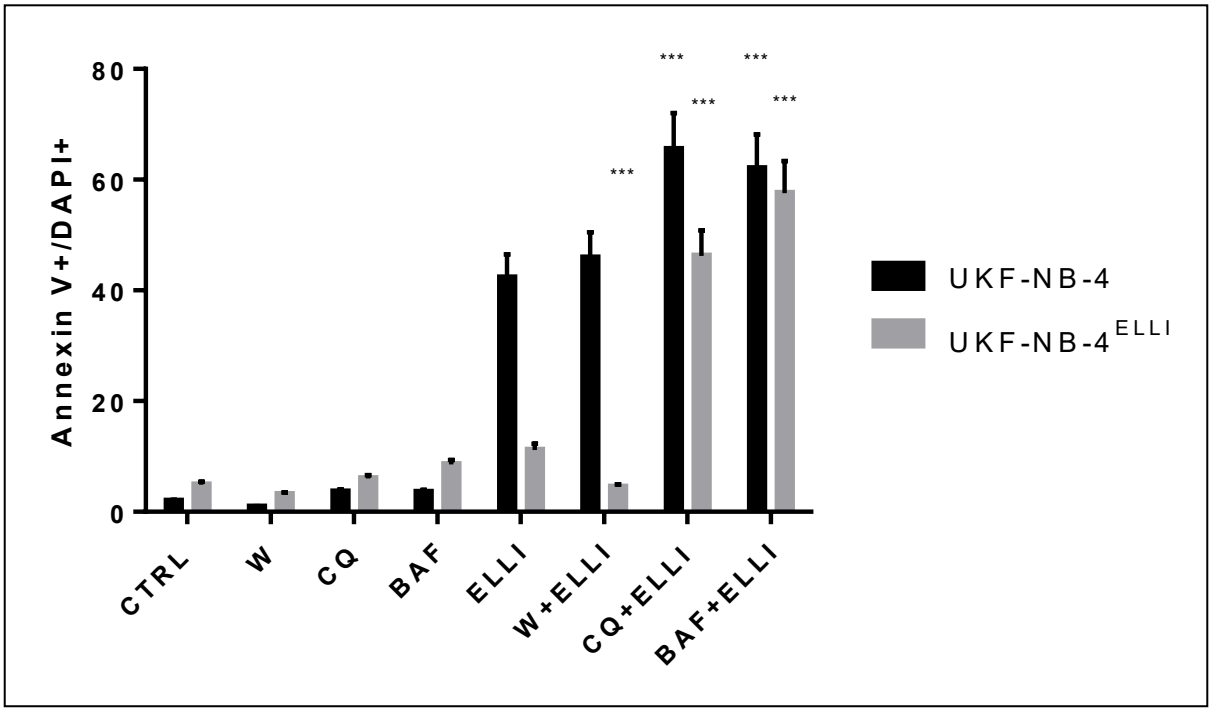
Annexin V+/DAPI+
80
60
40
20
0
***
***
***
***
***
CTRL
W
CQ
BAF
ELLI
W+ELLI
CQ+ELLI
BAF+ELLI
UKF-NB-4
UKF-NB-4ELLI

Fig. 5.

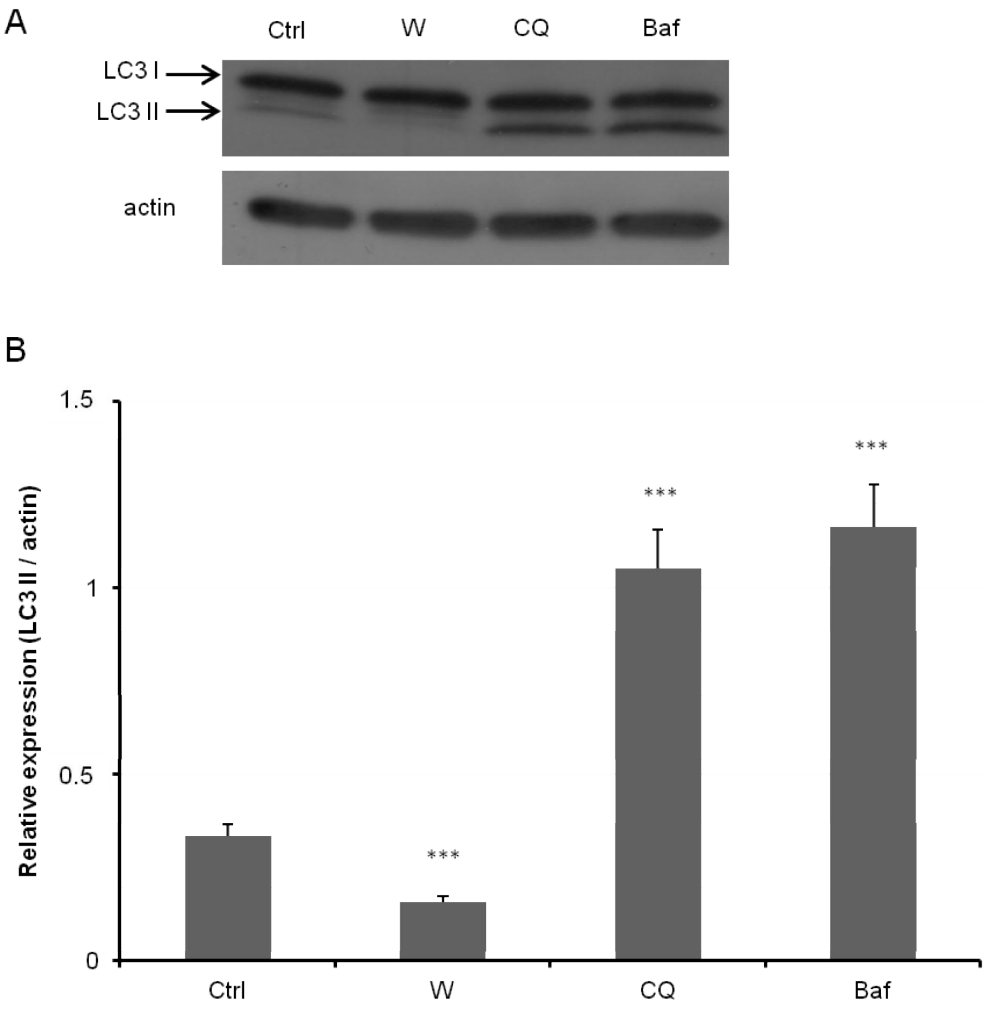
A
Ctrl
W
CQ
Baf
LC3 I
LC3 II
actin
B
Relative expression (LC3 II / actin)
1.5
1
0.5
0
***
***
***
Ctrl
W
CQ
Baf

Fig. 6.

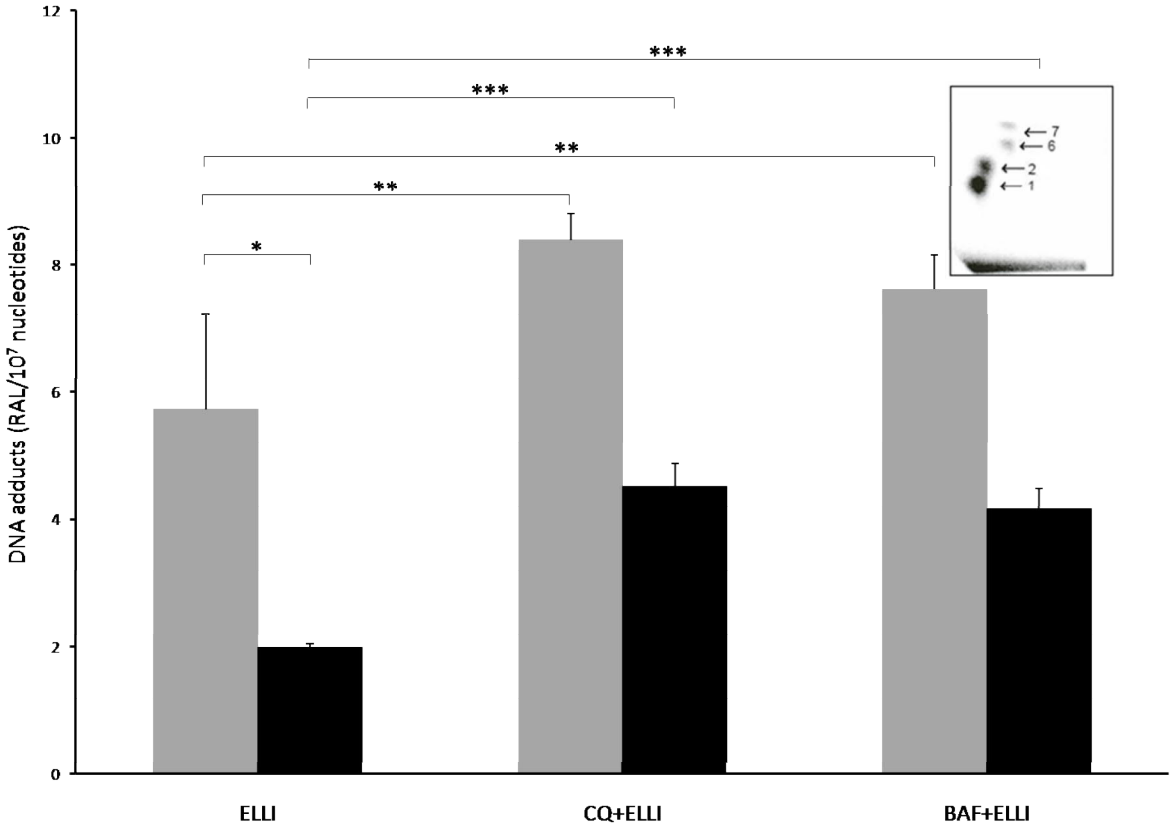
12
10
8
6
4
2
0
DNA adducts (RAL/10^7 nucleotides)
***
***
**
**
*
7
6
2
1
ELLI
CQ+ELLI
BAF+ELLI

Fig. 7.